STUDIES ON STABILIZATION OF PHOTOINDUCED RADICAL IONS IN POLYMER SYSTEMS(Dissertation_全文)

AUTHOR(S):

Tsujii, Yoshinobu

STUDIES ON STABILIZATION OF PHOTOINDUCED RADICAL IONS IN POLYMER SYSTEMS

YOSHINOBU TSUJII

1990

CONTENTS

CHAPTER 1

GENERAL INTRODUCTION

Polymers having photosensitive and/or photoresponsive groups have potential applications as photo-functional polymers.[1] Photo-functional polymers were first developed in the field of photolithography. In 1959, Minsk et al.[2] suggested the applicability of poly(vinyl cinnamate) as a negative-type photoresist, which utilized polymer-crosslinking by the photodimerization of cinnamoyl groups. Since then, various types of photoresists based on the use of photocrosslinking, photodissociation and photopolymerization have been studied. On the other hand, Hoegel[3] discovered the photoconductivity of poly(N-vinylcarbazole) (PVCz) in 1962. PVCz was put in practical use as an organic photoconductor. The mechanism of a carrier generation and a carrier transport has been investigated extensively.[4] Recently, from the viewpoint of recording of information by light, photochromism[5] and photochemical hole burning[6] have been studied, though they have not been in practical use as yet.

Photo-functional polymers utilize the chemical and physical characteristics of photosensitive groups (chromophores) attached to the polymer chain. The molecular design of advanced photo-functional polymers requires basic research on the photochemistry and photophysics in polymer systems having chromophores. From this viewpoint, in recent years, polymers

having aromatic chromophores as pendant groups have been extensively studied.[7-11] Aromatic compounds are typical photosensitive chromophores. Their excited states and deactivation processes have been investigated in detail.[12] The photochemical and photophysical properties of polymers are different from those of low molecular-weight compounds. This is due to a high local concentration of chromophores along the polymer chain, which is preserved even in dilute solution. In a polymer system, the interaction between neighboring chromophores (the neighboring chromophore interaction) is known to play an important role. In the excited states of chromophores on a polymer chain, the neighboring chromophore interaction induces a highly efficient intramolecular excimer formation and energy migration along the polymer chain.[12-16]

On the other hand, the photoinduced electron transfer is an important relaxation process of the excited state. By the photoinduced electron transfer, radical ions or excited donor-acceptor complexes (exciplexes) are formed, which are intermediates of photochemical reactions. Charge-transfer intermediates such as radical ions and exciplexes can interact with a neutral chromophore to form dimer radical ions and excited triple complexes (exterplexes). In polymer systems having pendant aromatic chromophores, the interaction of the charge-transfer intermediates with the neighboring neutral chromophores is expected to be significant owing to the high local concentration of chromophores. However, the neighboring chromophore interaction in the charge-transfer intermediates in a polymer system has not yet been fully understood. The aim of this thesis is to elucidate how radical ions and exterplexes in a polymer system are stabilized by the neighboring chromophore interaction. Main experimental tools to be used

are laser photolysis and fluorescence techniques.

I-1. A Short Survey on Interaction of Radical Cations

(A) Formation of Intermolecular Dimer Radical Cations

The formation of intermolecular dimer radical cations in aromatic hydrocarbon systems has been studied by means of ESR, γ-ray irradiated rigid matrix method, and pulse radiolysis. Lewis et al.[17] and Howarth et al.[18] measured the ESR spectra of the radical cations prepared by the oxidation of aromatic hydrocarbons such as naphthalene, anthracene and pyrene with $SbCl_5$ in dichloromethane. An analysis of the ESR hyperfine structure suggested that the formed radical cation has a sandwich and symmetrical dimer structure, where two chromophores lie in parallel. Willigen et al.[19] studied the dimer radical cation of coronene by ESR and indicated the possible existence of a trimer radical cation.

Many dimer radical cations of aromatic hydrocarbons give a charge-resonance (CR) band in a near-infrared region. As will be described in detail in Appendix, the CR band is one of the most important characteristics of the dimer radical cation; this band is associated with the transition between two energy levels of the highest occupied molecular orbital (HOMO) splitted by charge resonance.[20] By slightly warming a γ-ray irradiated rigid matrix, Badger et al.[21,22] observed CR bands of dimer radical cations of aromatic hydrocarbons such as naphthalene, benzene derivatives, anthracene derivatives and pyrene in the near-infrared region.

Kira et al.[23] studied the optical properties of the radical cations of many aromatic hydrocarbons in γ-ray

irradiated glassy solutions at 77 K. A new band and a band shift caused by warming the glassy matrices have been reported. The absorption bands of the dimer radical cation and higher-order aggregates such as trimer and tetramer radical cations have been assigned. The results indicate that the CR band energy decreases with increasing molecular size, viz, in the order of naphthalene, phenanthrene, anthracene, benz[a]anthracene and chrysene. This was explained in terms of a repulsion between filled orbitals of chromophore.[24)]

The stability of dimer radical cations is also an important subject to study. The formation of intermolecular dimer radical cations by aromatic hydrocarbons has been discussed on the basis of thermodynamic considerations. Badger and Brocklehurst[25)] estimated the stabilization energies of the dimer radical cations of benzene derivatives, naphthalene derivatives and pyrene by using "half of the CR band energy", and compared them with those of the excimer. By pulse radiolysis in benzonitrile, Kira et al.[26)] and Rodgers[27)] measured, for some aromatic hydrocarbons, the equilibrium constants between dimer and monomer radical cations, and estimated the free energy and enthalpy changes associated with the formation of a dimer radical cation. The result shows that the interaction of the dimer radical cation is comparable to or larger than that of the excimer.

(B) Structure of Dimer Radical Cations

It is generally difficult to determine the structure of the dimer radical cation. ESR data as described previously merely indicate a possibility of a symmetrical arrangement.[17,18)] The stability or the degree of interaction of the dimer radical cation would depend on the extent of overlapping of two

chromophores. Badger and Brocklehurst[24)] searched for a stable conformation of the naphthalene dimer radical cation by Hückel molecular orbital (MO) calculations. Their results suggest that, in the case of the intermolecular naphthalene dimer radical cation, the most stable arrangement is not a perfect sandwich conformation but the conformation in which the molecular axes of naphthalenes have some angle each other. In order to obtain experimental information on the structure of dimer radical cations, bichromophoric model compounds which have two chromophores linked by a methylene chain were used in the same way as in the studies of excimers.[28-36)] In these compounds, the relative conformation of the chromophores is restricted by the methylene-chain bridge. Thus, different degrees of overlapping of chromophores can be modeled according to the substitution position of the chromophore or the configuration of the bridge.

Irie et al.[37)] measured the absorption spectra of the radical cations of 1,3-, 1,6-, and 1,12-di(2-naphthyl)alkanes in the glassy matrix at 77 K and in solution at room temperature. They made the assignment of the absorption bands and suggested a possible existence of fully-overlapped and partially-overlapped dimer radical cations of 1,3-di(2-naphthyl)propane. By laser photolysis, Masuhara et al.[38)] measured the transient absorption spectra in the visible region for meso- and rac-2,4-di(N-carbazolyl)pentanes (m- and r-DCzPe) in the presence of an electron acceptor, 1,2-dicyanobenzene. They assigned the absorption bands for meso and racemic isomers to a fully-overlapped and a partially-overlapped dimer radical cation, respectively.

(C) Stability of Radical Cation in Polymer Systems

In polymers with pendant aromatic chromophores, radical

cations of dimer or higher-ordered aggregates would be easily formed because of the high local concentration of chromophores. Irie et al.[37] studied the transient absorption spectra of the radical cation formed in polystyrene and poly(2-vinylnaphthalene) in a γ-ray irradiated glassy matrix at 77 K. These radical cations showed CR bands in the near-infrared region even without warming the matrix. The CR bands were observed to shift to shorter wavelengths after annealing. As for the radical cation formed in PVCz,[39,40] a transient absorption band was observed around 750 nm by laser photolysis. This band was very broad as compared with that of the monomer radical cation, very likely due to the neighboring chromophore interaction. Washio et al.[41] studied the scavenging reaction of the radical cation formed in PVCz by pulse radiolysis and demonstrated the stabilization of the radical cation by the neighboring chromophore interaction. However, no systematic, detailed investigation on polymer systems has been carried out yet.

1-2. A Short Survey on Interaction of Radical Anions

Sprague et al.[42] detected, by ESR, the dimer radical anion of acetonitrile in an upper crystalline phase, produced by γ-ray irradiation at 77 K. Arai et al.[43] observed absorption bands, ascribable to dimer radical anions, in the near-infrared region by γ-ray irradiation of tetramethylfuran solutions which contain various electron-accepting olefins. In contrast to the dimer radical cations, there is little information about the dimer radical anions of aromatic hydrocarbons except for a few pieces of information obtained under special conditions; Shida et al.[44] detected the anthracene dimer radical anion in the γ-ray

irradiated rigid matrix of dianthracene at 77 K. The formation mechanism of the dimer radical anion was considered to be as follows; ionization of dianthracene by γ-ray irradiation causes its decomposition to a pair of anthracene and anthracene anion. Then, they interact with each other to form a dimer radical anion. A doublet CR band ascribable to the anthracene dimer radical anion was observed in the near-infrared region. The possibility of the stabilization of radical anions by the interaction with neutral chromophores and of the formation of dimer radical anions are still under controversy.

1-3. A Short Survey of Excited Triple Complex

The photoinduced electron transfer in a non-polar solvent leads to the formation of an excited complex (exciplex), because in a non-polar solvent, the stabilization of free ions by solvation cannot be attained. The exciplex plays an important role as an intermediate in many photochemical reactions, and its photochemical and photophysical properties have been investigated extensively. Since the exciplex is formed by a partial electron-transfer from an electron donor (D) to an electron acceptor (A), it is a charge-transfer intermediate of ionic character and is mainly stabilized by a charge-transfer interaction. Like dimer radical ions, this charge-transfer intermediate is expected to interact with a neutral electron donor or acceptor, forming an exterplex stabilized by charge-delocalization.[45]

In 1968, Beens and Weller,[46] reported that, for a naphthalene - 1,4-dicyanobenzene (p-DCNB) system, the exciplex emission decreases, accompanying a new emission in a longer wavelength region, when the naphthalene concentration is

increased. They ascribed this new emission to a DDA type exterplex with an asymmetrical polar structure, which consisted of two naphthalenes and p-DCNB. Since then, there have been many studies on the DDA type exterplexes.[47-54] Masuhara et al.,[53] who investigated the fluorescent properties of m- and r-DCzPe in the presence of 1,3-dicyanobenzene, reported that these diastereomers form a different DDA type exterplex; r-DCzPe forms a exterplex in which two carbazolyl (Cz) chromophores overlap partially (partially-overlapped exterplex), while m-DCzPe forms one in which two Cz chromophores overlap completely with each other (fully-overlapped exterplex).

Polymers having pendant aromatic chromophores are expected to show efficient exterplex formation or a high tendency of aggregation due to the high local chromophore concentration along the chain. Hoyle and Guillet[52] investigated a PVCz - dimethyl terephthalate system and a poly(1-vinylnaphthalene) (P1VN) - p-DCNB system by a time-resolved fluorescence spectroscopy; the PVCz and P1VN systems showed a broad emission around 520 nm and around 480 nm. These emissions were assigned to DDA type exterplexes. Thus, the neighboring chromophore interaction contributes to the stabilization of the charge-transfer state in polymer systems and hence plays an important role in polymer photochemistry and photophysics.

On the contrary, there are only a few reports on DAA type exterplexes in which a negative charge is delocalized between two electron acceptors.[54,56] The situation is similar to that of dimer radical anions. This has been considered to be due to the small stabilization energy gained by delocalization of a negative charge. However, the reason has not been fully understood. Hirata et al.[55] reported, for a benzonitrile - amine system, the formation of a new type of

higher-order aggregate in the excited state at a high benzonitrile concentration, and suggested the possibility of the formation of a DAA exterplex with two benzonitrile molecules.

1-4. Outline of This Thesis

The aim of this thesis is to investigate the stability of radical ions and exterplexes in polymer systems having pendant chromophores and to elucidate the degree of charge delocalization by the neighboring chromophore interaction. The degree of charge delocalization should depend on the relative arrangement of the chromophores or the degree of overlapping of the chromophores. In this regard, the bichromophoric model compounds in which two chromophores are linked by a methylene chain are useful models. In this thesis, the relationship between the dimer structure and the stability of radical ions and exterplexes is studied by using such bichromophoric model compounds. On the basis of the result to be obtained, the charge delocalization by the neighboring chromophore interaction in polymer systems is discussed. By use of carbazolyl and naphthyl chromophores as electron-donating groups, and terephthalate chromophore as an electron-accepting group, the neighboring chromophore interactions of the charge-transfer intermediates formed in PVCz, poly(vinylnaphthalene) (PVN), and poly(vinyl methyl terephthalate) (PVMTP) are studied.

This thesis consists of two parts; Part I (Chapter 2 - 5) describes the stability of carbazole radical cation in polymer and dimeric model compound systems, and Part II (Chapter 6 - 8) deals with radical ions of various chromophores.

In Chapter 2, the stability of the carbazole dimer radical cations is studied for the diastereoisomers, m- and r-DCzPe as

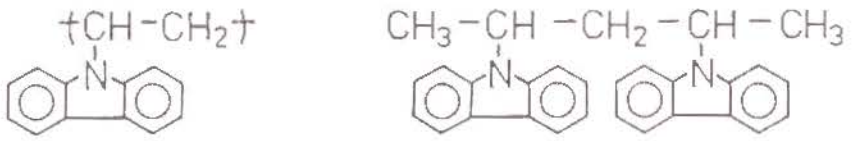

PVCz DCzPe

Figure 1-1. Molecular structures of PVCz and DCzPe

model systems of PVCz (Figure 1-1). The CR band is measured by laser photolysis and the stabilization energy is estimated by the radical cation transfer method. The stability of the dimer radical cation is discussed in connection with the dimer structure, viz, the degree of overlapping of carbazole chromophores. Figure 1-2 shows the conformations of m- and r-DCzPe. They can take a fully-overlapped and a partially-overlapped conformation, respectively, because of their different configurations.

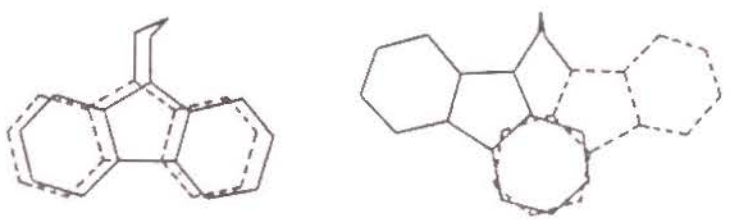

m-DCzPe r-DCzPe

Figure 1-2. Fully-overlapped conformation of m-DCzPe and partially-overlapped conformation of r-DCzPe.

In Chapter 3, the CR band and the estimation of the stabilization energy for the carbazole radical cation formed in PVCz are described. The stability of the radical cation and the

degree of charge delocalization are discussed in comparison with those of the dimeric model compounds and the copolymers of N-vinylcarbazole.

In Chapter 4, the fluorescence properties of the DDA exterplex of PVCz and its dimeric model compounds (Figure 1-1) with dimethyl terephthalate are examined. The formation dynamics and the structure of the exterplexes are described.

In Chapter 5, steric effects on the formation of dimer radical cations and exterplexes are investigated by using poly(3,6-di-tert-butyl-N-vinylcarbazole) and its dimeric model compounds (Figure 1-3). The transient absorption spectra of radical cations are measured in a polar solvent and the fluorescence properties of exterplexes are measured in a non-

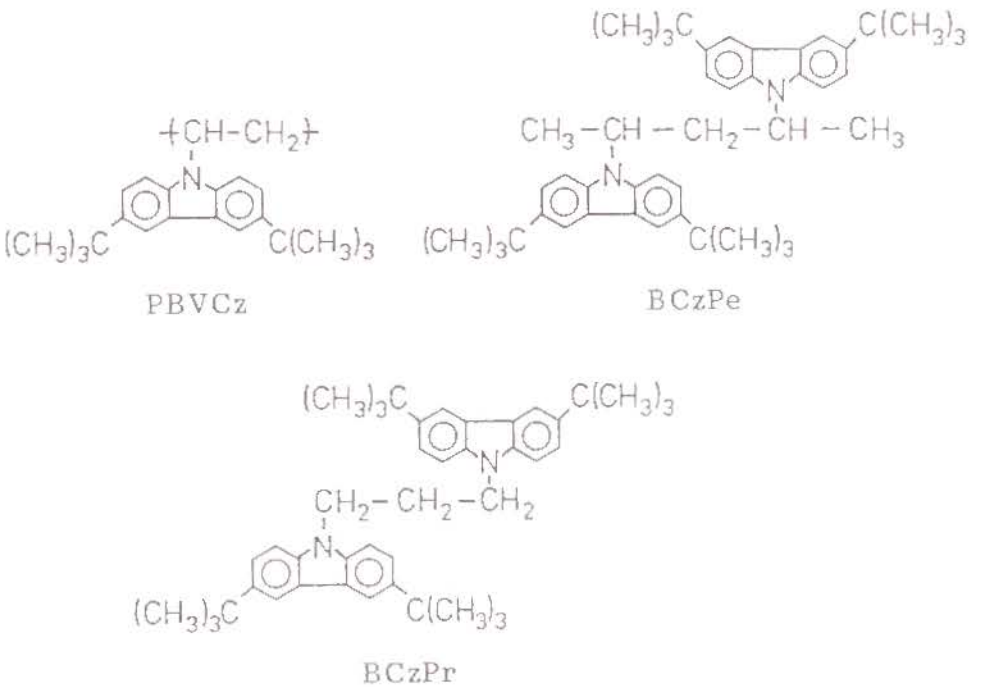

PBVCz BCzPe

BCzPr

Figure 1-3. Molecular structures of PBVCz and its dimeric model compounds.

polar solvent. The steric effects on the magnitude of interaction in these charge-transfer states are compared with those in the excimer state.

In Chapter 6, the structure and the stability of naphthalene dimer radical cations are studied for PVN and their dimeric model compounds (Figure 1-4). The relationship between the degree of overlapping of naphthyl chromophores and the stability of dimer radical cations is discussed in comparison with the carbazole systems. As shown in Figure 1-5, each dimeric model compound can take two types of overlapping of naphthyl rings; 11DNP and 22DNP take a fully-overlapped and a

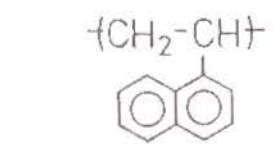

P1VN

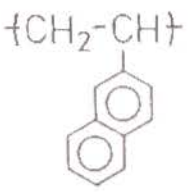

P2VN

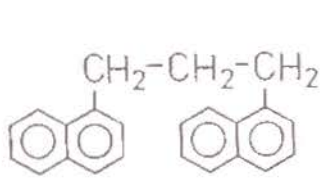

11DNP

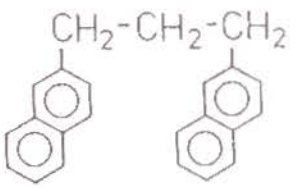

22DNP

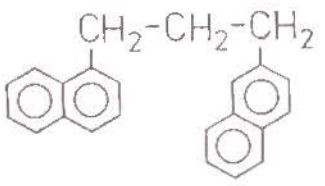

12DNP

Figure 1-4. Molecular structures of PVN and their dimeric model compounds.

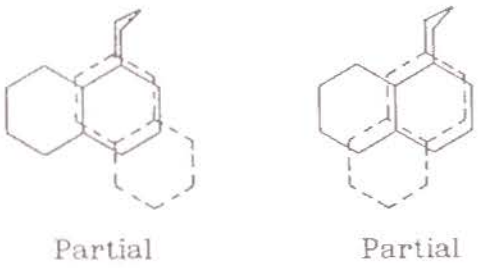

Partial Partial

(a) 12DNP

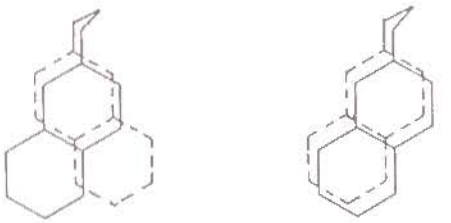

Partial Full

(b) 22DNP

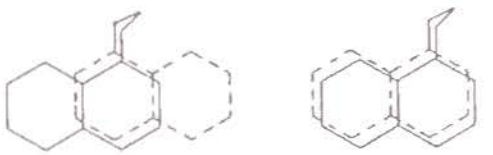

Partial Full

(c) 11DNP

Figure 1-5. Overlapped conformations of dinaphthylpropanes.

partially-overlapped conformation, while 12DNP takes two types of partially-overlapped conformations.

In Chapter 7, theoretical considerations on the formation of carbazole and naphthalene dimer radical cations are given by MO calculations. First, by the Austin Model 1 (AM1) MO method, stable conformations of the fully-overlapped and partially-overlapped dimer radical cations are determined. Next, the CR band energy of the dimer radical cations in the stable conformation is calculated by CNDO/S and compared with

experimental results. Finally, the interaction energy is analyzed by Ab Initio calculations, and the difference between carbazole and naphthalene dimer radical cations is discussed.

In Chapter 8, the stabilization of the terephthalate radical anion in PVMTP (Figure 1-6) is demonstrated by the radical anion transfer method. In addition, the quenching of carbazole - terephthalate exciplex by the neighboring terephthalate chromophore in PVMTP is studied. The characteristics of the stabilization of a negative charge by the neighboring chromophore interaction is discussed in comparison with the case of a positive charge.

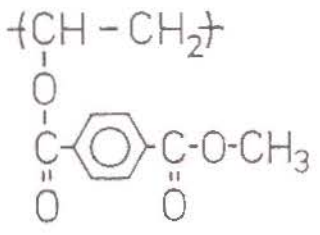

PVMTP

Figure 1-6. Molecular structure of PVMTP.

In Appendix, two methods for estimating the stability of radical cations are described; one is based on the relationship between the CR band energy and the stability of radical cations, and the other is the radical cation transfer method to evaluate the stabilization energy. Furthermore, a laser photolysis apparatus for transient absorption measurements is introduced.

References

1) K. Yoshino, ed., Denshi-Hikari-Kinosei Kobunshi, Kodansya, Tokyo, 1989.

2) L. M. Minsk, J. G. Smith, W. P. Van Deusen and J. F. Wright, J. Appl. Polym. Sci. 1959, 2, 302.

3) H. Hoegel, U.S.Pat., 3037861 (1962).

4) H. Mikawa and S. Kusabayashi, eds., Kobunshi Handotai, Kodansya, Tokyo, 1977.

5) G. H. Brown ed., Techniques of Chemistry Vol. III Photochromism, John Wiley Interscience, New York, 1970.

6) A. R. Gutierrez, J. Friedrich, D. Hadrer and H. Wolfrum, IHM J. Res. Develop. 1982, 26, 198.

7) J. Guillet, Polymer Photophysics and Photochemistry, Cambridge University Press, London, 1985.

8) M. Winnik, Photophysical and Photochemical Tools in Polymer Science, D. Reidel Pub. Co., Dordrecht, 1986.

9) D. Phillips and G. Rumbles, in Photochemistry and Photophysics in Polymers, N. S. Allen and W. Schnabel, eds., Elsevier Appl. Sci. Pub., London, 1984, p.153.

10) W. Schnabel, in Developments in Polymer Photochemistry-3, N. S. Allen, ed., Elsevier Appl. Sci. Pub., London, 1982, p.237.

11) V. Balzani ed., Supramolecular Photochemistry, D. Reidel, Dordrecht, 1987.

12) J. B. Birks, ed., Organic Molecular Photophysics, John Wiley & Sons, Inc., New York, 1973.

13) S. N. Semerak and C. W. Frank, Adv. Polym. Sci. 1983, 54, 31.

14) W. Klöpffer, Ann. N. Y. Acad. Sci. 1981, 366, 373.

15) (a) A. M. North and M. F. Treadaway, Eur. Polym. J. 1973, 9, 609. (b) A. M. North and D. A. Ross, J. Polym. Sci. Symposium 1976, 55, 259.

16) (a) S. Ito, M. Yamamoto and Y. Nishijima, Polym. J. 1981, 13, 791. (b) S. Ito, K. Yamashita, M. Yamamoto and Y. Nishijima, Chem. Phys. Lett. 1985, 117, 171.

17) I. C. Lewis and L. S. Singer, J. Chem. Phys. 1965, 43, 2712.

18) (a) O. W. Howarth and G. K. Fraenkel, J. Am. Chem. Soc. 1966, 88, 4514. (b) O. W. Howarth and G. K. Fraenkel, J. Chem. Phys. 1970, 52, 6258.

19) H. van Willigen, E. de Boer, J. T. Cooper and W. F. Forbes, J. Chem. Phys. 1968, 49, 1190.

20) M. Itoh, in Kagakuhanno no Denshiron, S. Nagakura ed., Kyoritsu Shuppan, Tokyo, Japan, 1986, Chapter 7.

21) B. Badger, B. Brocklehurst and R. D. Russell, Chem. Phys. Lett. 1967, 1, 122.

22) (a) B. Badger, and B. Brocklehurst, Trans. Faraday Soc. 1969, 65, 2576. (b) B. Badger, and B. Brocklehurst, ibid. 1969, 65, 2582. (c) B. Badger and B. Brocklehurst, ibid. 1969, 65, 2588.

23) (a) A. Kira, M. Imamura and T. Shida, J. Phys. Chem. 1976, 80, 1445. (b) A. Kira, T. Nakamura and M. Imamura, ibid. 1977, 81, 511. (c) A. Kira and M. Imamura, ibid. 1979, 83, 2267.

24) B. Badger, and B. Brocklehurst, Trans. Faraday Soc. 1970, 66, 2939.

25) B. Badger, and B. Brocklehurst, Nature 1968, 219, 263.

26) (a) A. Kira, S. Arai, and M. Imamura, J. Chem. Phys. 1971, 54, 4890. (b) A. Kira, S. Arai and M. Imamura, J. Phys. Chem. 1972, 76, 1119. (c) S. Arai, A. Kira and M. Imamura, J. Chem. Phys. 1972, 56, 1777.

27) (a) M. A. J. Rodgers, Chem. Phys. Lett. 1971, 9, 107. (b) M. A. J. Rodgers, J. Chem. Soc., Faraday Trans. 1 1972, 68, 1278.

28) (a) F. C. De Schryver, P. Collart, J. Vandendriessche, R. Goedeweeck, A. M. Swinnen and M. Van der Auweraer, Acc. Chem. Res. 1987, 20, 159. (b) F. C. De Schryver, L. Moens, M. Van der Auweraer, N. Boens, L. Monnerie and L. Bokobza, Macromolecules 1982, 15, 64. (c) P. Collart, S. Toppet, Q. F. Zhou, N. Boens and F. C. De Schryver, ibid. 1985, 18, 1026. (d) P. Collart, S. Toppet and F. C. De Schryver, ibid. 1987, 20, 1266. (e) F. C. De Schryver, J. Vandendriessche, S. Toppet, K. Demeyer and N. Boens, ibid. 1982, 15, 406. (f) J. Vandendriessche, P. Palmans, S. Toppet, N. Boens, F. C. De Schryver and H. Masuhara, J. Am. Chem. Soc. 1984, 106, 8057.

29) F. Hirayama, J. Chem. Phys., 1965 42, 3163.

30) E. A. Chandross and C. J. Dempster, J. Am. Chem. Soc. 1970, 92, 3586.

31) (a) S. Ito, M. Yamamoto and Y. Nishijima, Bull. Chem. Soc. Jpn. 1981, 54, 35. (b) S. Ito, M. Yamamoto and Y. Nishijima, Ibid. 1982, 55, 353.

32) H. Itagaki, N. Obukata, A. Okamoto, K. Horie and I. Mita, J. Am. Chem. Soc. 1982, 104, 4469.

33) (a) K. A. Zachariasse and W. Kühnle, Z. Phys. Chem. (Wiesbaden) 1976, 101, 267. (b) K. A. Zachariasse, G. Duveneck and R. Busse, J. Am. Chem. Soc. 1984, 106, 1045. (c) P. Reynders, H. Droeskamp, W. Kühnle and K. A. Zachariasse, J. Phys. Chem. 1987, 91, 3982. (d) K. A. Zachariasse, R. Busse, U. Schrader and W. Kühnle, Chem. Phys. Lett. 1982, 89, 303.

34) W. Klöpffer, Chem. Phys. Lett. 1969, 4, 193.

35) (a) G. E. Johnson, J. Chem. Phys. 1974, 61, 3002. (b) G. E. Johnson, ibid. 1975, 63, 4047.

36) F. Evers, K. Kobs, R. Memming and D. R. Terrell, J. Am. Chem. Soc. 1983, 105, 5988.

37) (a) S. Irie, H. Horii and M. Irie, Macromolecules 1980, 13, 1355. (b) S. Irie and M. Irie, ibid. 1986, 19, 2182.

38) (a) H. Masuhara, N. Tamai, N. Mataga, F. C. De Schryver and J. Vandendriessche, J. Am. Chem. Soc. 1983, 105, 7256. (b) H.

Masuhara, K. Yamamoto, N. Tamai, K. Inoue and N. Mataga, J. Phys. Chem. 1984, 88, 3971.

39) (a) U. Lachish, D. J. Williams and R. W. Anderson, Chem. Phys. Lett. 1979, 65, 574. (b) U. Lachish, R. W. Anderson, D. J. Williams, Macromolecules 1980, 13, 1143.

40) H. Masuhara, S. Ohwada, N. Mataga, A. Itaya, K. Okamoto and S. Kusabayashi, J. Phys. Chem. 1980, 84, 2363.

41) M. Washio, S. Tagawa and Y. Tabata, Polm. J. 1981, 13, 935.

42) E. D. Sprague, K. Takeda and F. Williams, Chem. Phys. Lett. 1971, 10, 299.

43) S. Arai, A. Kira and M. Imamura, J. Phys. Chem. 1977, 81, 110.

44) T. Shida and S. Iwata, J. Chem. Phys., 1972, 56, 2858.

45) N. Tsujino, H. Masuhara and N. Mataga, Chem. Phys. Lett. 1973, 21, 301.

46) H. Beens and A. Weller, Chem. Phys. Lett. 1968, 2, 140.

47) G. N. Taylor, E. A. Chandross and A. H. Schiebel, J. Am. Chem. Soc. 1974, 95, 2693.

48) (a) R. A. Caldwell and L. Smith, J. Am. Chem. Soc. 1974, 96, 2994. (b) D. Creed and R. A. Caldwell, ibid. 1974, 96, 7369. (c) H. Ohta, D. Creed, P. H. Wine, R. A. Caldwell and L. A. Melton, ibid. 1976, 98, 2002.

49) J. Saltiel, D. E. Townsend, B. D. Watson and P. Shannon, J. Am. Chem. Soc. 1975, 97, 5688.

50) K. H. Grellmann and U. Suckow, Chem. Phys. Lett. 1975, 32, 250.

51) (a) T. Mimura and M. Itoh, J. Am. Chem. Soc. 1976, 98, 1095. (b) T. Mimura and M. Itoh, Bull. Chem. Soc. Jpn. 1977, 50, 1739.

52) (a) C. E. Hoyle and J. E. Guillet, Macromolecules 1978, 11, 221. (b) C. E. Hoyle and J. E. Guillet, ibid. 1979, 12, 956.

53) H. Masuhara, J. Vandendriessche, K. Demeyer, N. Boens and F. C. De Schryver, Macromolecules 1982, 15, 1471.

54) G. F. M. Hendrik, J. van Ramesdonk and J. W. Verhoeven, J. Am. Chem. Soc. 1984, 106, 1335.

55) Y. Hirata, M. Takimoto, N. Mataga, Y. Sakata and S. Misumi, Chem. Phys. Lett. 1982, 92, 76.

56) A. M. Swinnen, F. Ruttens, M. Van der Auweraer and F. C. De Schryver, Chem. Phys. Lett. 1985, 116, 217.

PART I

STABILITY OF CARBAZOLE RADICAL CATION IN POLYMER AND BICHROMOPHORIC MODEL COMPOUNDS

CHAPTER 2

STABILIZATION ENERGY OF CARBAZOLE DIMER RADICAL CATIONS

2-1. Introduction

The radical cations of some aromatic chromophores form dimer radical cations intramolecularly[1-3] or intermolecularly[4-12] by neighboring chromophore interaction. The characteristic of the dimer radical cation depends on the overlapping of chromophores.[9,13] The structures of dimer radical cations have been studied for several bichromophoric compounds whose preferable conformations have been proposed.[1-3]

meso- and rac-2,4-Di(N-carbazolyl)pentane (m- and r-DCzPe) are used as dimeric model compounds of an isotactic and a syndiotactic dyads of poly(N-vinylcarbazole) (PVCz), respectively. m-DCzPe can take a sandwich conformation in which two carbazole chromophores overlap completely, whereas r-DCzPe hardly takes such a sandwich conformation because of the steric hindrance of methyl groups. In fact, m-DCzPe forms a sandwich excimer with a fully-overlapped conformation, and r-DCzPe forms a second excimer with a partially-overlapped conformation.[14-17] DCzPr also forms the same sandwich excimer as m-DCzPe.[18,19] In the case of the radical cations, the change of transient absorption spectra corresponding to the excimer conformation was observed.[3] DCzPr and m-DCzPe form a dimer radical cation[18] with a fully-overlapped conformation (fully-overlapped

dimer radical cation), and their absorption bands appear around 760 nm for DCzPr and 770 nm for m-DCzPe. r-DCzPe forms a dimer radical cation with a partially-overlapped conformation (partially-overlapped dimer radical cation) and has a broad absorption band around 710 nm.

In this chapter, the stability of the radical cations for the dimeric model compounds was estimated by a charge-resonance (CR) band measurement and by the radical cation transfer method. The stabilization energy was discussed in connection with the conformations of two carbazole chromophores, i.e., the overlapping between two carbazole chromophores.

2-2. Experimental Section

2-2-1. Chemicals

(A) Electron Donors (D_1)

N-Ethylcarbazole (EtCz) was synthesized by N-alkylation of carbazole and was purified by silica-gel column chromatography and recrystallization. DCzPr was prepared from 1,3-dibromopropane (Wako Pure Chem. Ind.) and sodium carbazole,[20] and was purified by recrystallization from a mixture of dichloromethane and hexane. The diastereoisomers, r- and m-DCzPe, were synthesized from 2,4-di(tosyloxy)pentane,[16] which was prepared from 2,4-pentanediol (Tokyo Kasei Kogyo Co.).[21] These diastereoisomers of DCzPe were separated by silica-gel column chromatography and by liquid chromatography (Japan Spectroscopic Co.) with the eluent of a mixture of hexane and ethyl acetate (7:1) and were purified by recrystallization from ethanol.

(B) Electron Acceptors (A)

Dimethylterephthalate (DMTP, Wako Pure Chem. Ind.), 1,2-dicyanobenzene (o-DCNB, Tokyo Kasei Kogyo Co.) and 1,4-Dicyanobenzene (p-DCNB, Wako Pure Chem. Ind.) were purified several times by recrystallization.

(C) Radical Cation Acceptors (D_2)

Similar amine compounds were used as a radical cation acceptor. 4-Dimethylaminostyrene (DMASt) was prepared from 4-dimethylaminobenzaldehyde (Nakarai Chem.)[22] and was purified by distillation under a reduced pressure. N,N-Dimethyl-1,4-toluidine (DMT, Wako Pure Chem. Ind.) and N,N-dimethylaniline (DMA, Wako Pure Chem. Ind.) were purified by distillation under a reduced pressure. N,N,N',N'-Tetramethyl-1,4-phenylenediamine (TMPD, Tokyo Kasei Kogyo Co.), diphenylamine (DPA, Tokyo Kasei Kogyo Co.), triphenylamine (TPA, Tokyo Kasei Kogyo Co.), and 1,2-dimethylindole (DMI, Aldrich Chem. Co.) were purified by recrystallization.

(D) Solvents

Acetonitrile (MeCN, Wako Pure Chem. Ind.) was refluxed over P_2O_5 several times and was fractionally distilled. Spectroscopic grade of N,N-dimethylformamide (DMF, Dotite Spectrosol) was used without further purification.

2-2-2. Measurements

(A) Transient Absorption Spectra

The transient absorption spectra of radical ions were measured by the excimer laser photolysis system. The carbazole chromophore was excited by a 308 nm-laser pulse of a XeCl excimer laser (Lambda Physik EMG101). As a detector, a

photomultiplier and an InAs photodiode were used for the measurements in the visible region (350 - 850 nm) and in the near-infrared region (600 to 2200 nm), respectively. For the concentration of carbazole chromophores, the absorbance at 308 nm was adjusted to about 1.8. p-DCNB (8.0×10^{-2} M) was used as an electron acceptor. The samples were degassed by the freeze-pump-thaw method in a 1-cm quartz cell. The measurements were made in DMF at 298 K.

(B) Radical Cation Transfer

The radical cation transfer was measured by the ruby laser photolysis system. As a detector, the photomultiplier tube (Hamamatsu, R928) having the faster response time (ca. 5 ns) was used. The measurements were made in degassed MeCN at 298 K. The sets of D_1-D_2-A systems measured in this study are listed in Table 2-I and 2-II. D_1, D_2 and A denote an electron donor, a radical cation acceptor and an electron acceptor, respectively. The detail of the radical cation transfer method will be described in Appendix. As for the concentration of electron donors (D_1), the absorbance at 347 nm was adjusted to about unity. The concentration conditions of D_2 and A were shown in Table 2-I and Table 2-II. The rate constants of the recombination (k_{r1}, k_{r2}) and the molar extinction coefficients of individual ion radicals were determined by the laser photolysis for two-component systems (D_1-A and D_2-A systems). The transient absorption spectra of radical cations, $TMPD^{+\cdot}$, $DMASt^{+\cdot}$, $DMT^{+\cdot}$, $DMA^{+\cdot}$, $DPA^{+\cdot}$ and $TPA^{+\cdot}$, have the absorption peaks at 620, 640, 470, 680, 670 and 670 nm, respectively. The transient absorption spectrum of $DMI^{+\cdot}$ could not be detected by the present nanosecond laser photolysis. This may be due to the small molar extinction coefficient of $DMI^{+\cdot}$. However, DMI under

Table 2-I. Rate constants and free energy change of radical cation transfer in EtCz-D_2-A systems.

No.	$[D_2]/10^{-4}$M		[A]/10^{-2}M		$k_{tr}/10^9 M^{-1}s^{-1}$	ΔG^0/eV
1	TMPD	2.5	o-DCNB	2.0	13.1	-1.04
2	DMASt	2.8	DMTP	1.0	11.0	-0.54
3	DMT	3.6	o-DCNB	1.9	8.9	-0.46
4	DMA	4.0	o-DCNB	1.9	9.7	-0.41
5	DPA	2.0	DMTP	2.0	7.8	-0.23
6	TPA	2.5	DMTP	2.0	7.8	-0.19
7	DMI	4.0	DMTP	2.0	6.6	-0.12

Table 2-II. Rate constants of radical cation transfer in D_1-DMASt-DMTP systems.

No.	$[D_1]$	$[D_2]/10^{-4}$M		[A]/10^{-2}M		$k_{tr}/10^9 M^{-1}s^{-1}$
8[1)]	EtCz	DMASt	2.8	DMTP	1.0	11.0
9	r-DCzPe	DMASt	2.8	DMTP	1.0	9.8
10	m-DCzPe	DMASt	2.8	DMTP	1.0	8.2
11	DCzPr	DMASt	3.3	DMTP	2.0	6.8

1) This system is the same as system No. 2 in Table 2-I.

γ-ray irradiation in the rigid matrix of sec-butyl chloride at 77 K gave an absorption band around 540 - 600 nm, which was ascribed to $DMI^{+\cdot}$. The absorption peaks of $DMTP^{-\cdot}$ and $o\text{-}DCNB^{-\cdot}$ appear at 530 nm and 375 nm, respectively. The absorption spectra of these radical cations and radical anions were

confirmed by γ-ray irradiation in rigid matrices of sec-butyl chloride and of 2-methyltetrahydrofuran at 77 K, respectively.[23]

(C) Oxidation Potentials

The oxidation potentials of EtCz and the radical cation acceptors were measured by cyclic voltammetry. The reference electrode, Ag/0.01 N Ag^+ in MeCN, was employed. The potentials were converted to the ones vs. SCE ($E_{1/2}$): $E_{1/2}$ = 1.18 V for EtCz, 1.06 V for DMI, 0.99 V for TPA, 0.95 V for DPA, 0.77 V for DMA, 0.72 V for DMT, 0.64 V for DMASt, and 0.14 V for TMPD.

2-3. Results

2-3-1. Transient Absorption Spectra

Figure 2-1 shows the transient absorption spectrum of the EtCz - p-DCNB system in DMF at 1.5 μs after excitation in the visible and near-infrared region. Transient absorption bands at ca. 430 nm and 790 nm were assigned to a radical anion of p-DCNB (p-DCNB$^{\cdot-}$) and a radical cation of EtCz (EtCz$^{\cdot+}$), respectively.[24] No absorption was observed in the near-infrared region (1000 - 2000 nm). At this concentration of EtCz (1.4×10^{-3} M), an intermolecular dimer radical cation does not exist.

As for the dimeric model compounds, the absorption band of carbazole radical cation (Cz$^{\cdot+}$) in the visible region (visible dimer band) is broader than that of the monomer radical cation, EtCz$^{\cdot+}$ and a new CR band appears in the near-infrared region where EtCz$^{\cdot+}$ has no absorption. Figure 2-2 shows the transient absorption spectrum of the m-DCzPe - p-DCNB system in DMF at 1.5 μs after excitation. The absorption bands of Cz$^{\cdot+}$ appear at ca. 780 nm[3] and at ca. 1600 nm. The former band is shifted to a wavelength slightly shorter than that of EtCz$^{\cdot+}$ and is similar

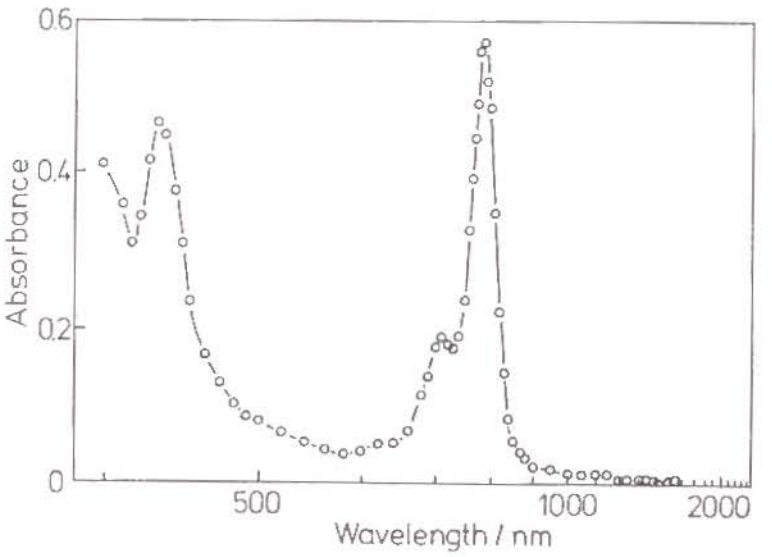

Figure 2-1. Transient absorption spectrum of EtCz - p-DCNB in DMF at 1.5 μs after excitation: [EtCz]=1.4×10^{-3}M, [p-DCNB]=8.0×10^{-2}M.

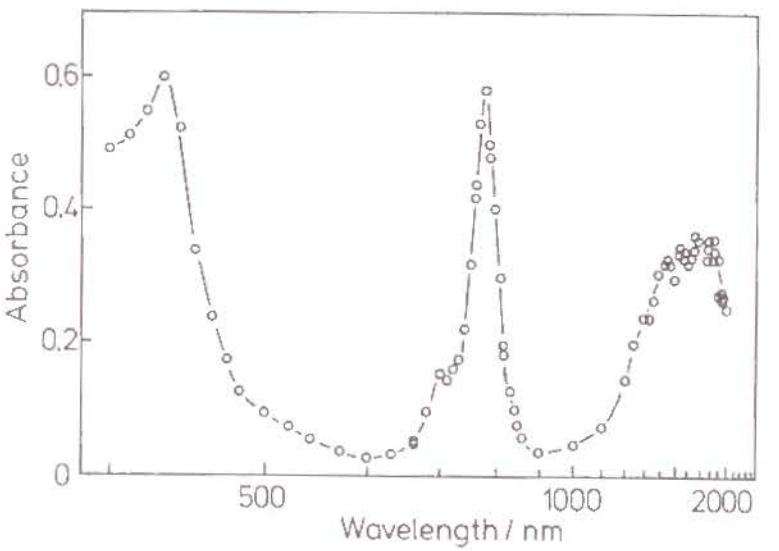

Figure 2-2. Transient absorption spectrum of m-DCzPe - p-DCNB in DMF at 1.5 μs after excitation: [m-DCzPe]=6.7×10^{-4}M, [p-DCNB]=8.0×10^{-2}M.

in shape to that of $EtCz^{+\cdot}$. The latter band was ascribed to the CR band. Figure 2-3 shows the transient absorption spectrum of the DCzPr - p-DCNB system in DMF at 1.5 μs after excitation. The spectrum of the dimer radical cation is the same as that for m-DCzPe. A visible dimer band and a CR band appear at ca. 770 nm and at 1600 nm, respectively. Figure 2-4 shows the transient absorption spectrum of the r-DCzPe - p-DCNB system at 1.5 μs after excitation: an absorption band of $Cz^{+\cdot}$ around 710 nm[3] was very broad and a CR band was observed at ca. 1800 nm. Rise times of the CR bands for all samples are within a time resolution of the apparatus (<500 ns) and a much higher resolution is necessary to investigate the formation process of dimer radical cations.

2-3-2. Relationship between k_{tr} and ΔG

At first a standard relationship between the transfer rate constant (k_{tr}) and the free energy change (ΔG^0) of the radical cation transfer for low molecular-weight compounds was measured as a reference. The rate constant k_{tr} from $EtCz^{+\cdot}$ to D_2 was measured by laser photolysis. Figure 2-5 shows the oscillograms of the transient absorption decay for the EtCz (D_1) systems at 780 nm (the peak wavelength of the absorption band of $EtCz^{+\cdot}$). The oscillogram (a) shows the decay of $EtCz^{+\cdot}$ for the EtCz-DMTP system at 780 nm: the absorption scarcely decays by the recombination of $EtCz^{+\cdot}$ ($D_1^{+\cdot}$) with $DMTP^{-\cdot}$ ($A^{-\cdot}$) in this time region. The oscillogram (b) shows the decay of $EtCz^{+\cdot}$ for the EtCz-DMASt-DMTP system (No.2 in Table 2-1) at the same wavelength: the decay is accelerated. The rate constant k_{tr} from $EtCz^{+\cdot}$ to DMASt was determined to be 11.0×10^9 $M^{-1}s^{-1}$ by eq. 7 in Appendix, since the rate of the radical cation transfer from $EtCz^{+\cdot}$ to DMASt is much faster than that of the

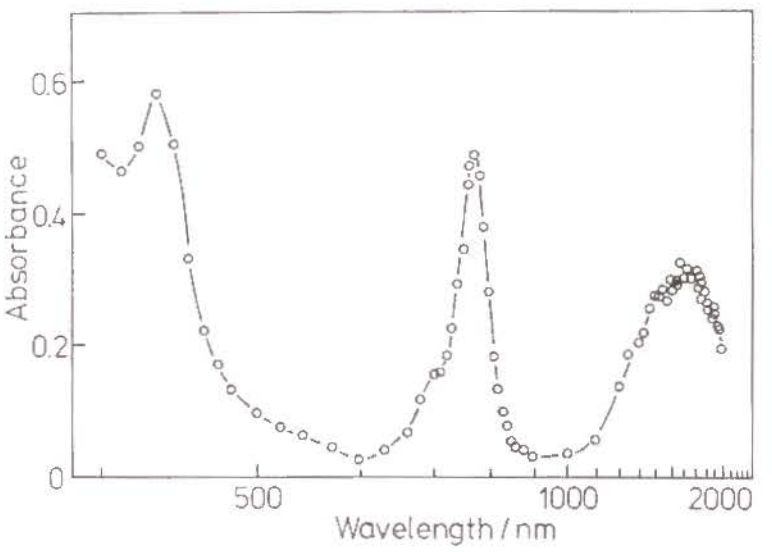

Figure 2-3. Transient absorption spectrum of DCzPr - p-DCNB in DMF at 1.5 μs after excitation: [DCzPr]=7.2×10^{-4}M, [p-DCNB]=8.0×10^{-2}M.

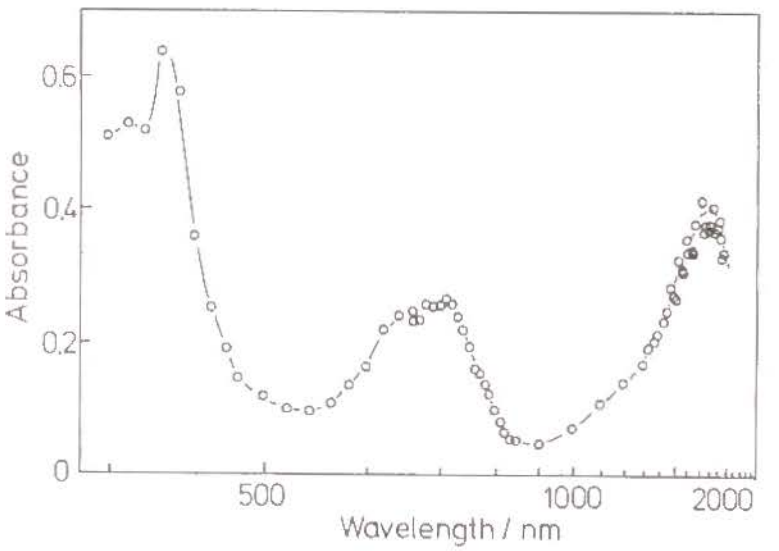

Figure 2-4. Transient absorption spectrum of r-DCzPe - p-DCNB in DMF at 1.5 μs after excitation: [r-DCzPe]=6.9×10^{-4}M, [p-DCNB]=8.0×10^{-2}M.

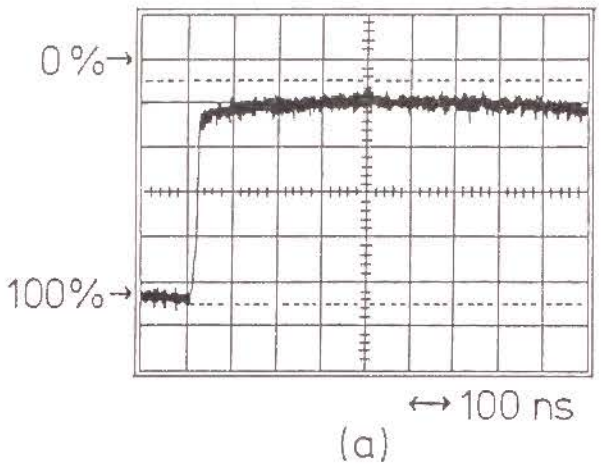

Figure 2-5. Oscillograms of transient absorption decay of $EtCz^{\cdot+}$ at its peak wavelength (780 nm) in radical cation transfer systems in MeCN. (a): EtCz-DMTP, (b): EtCz-DMASt-DMTP. For the concentration, see Table 2-I.

recombination of $EtCz^{\cdot+}$ with $DMTP^{\cdot-}$. The rate constant k_{tr} for other systems was also determined in the same way. Table 2-I shows the results. These k_{tr}'s were confirmed by simulating the rise of $D_2^{\cdot+}$ except the EtCz-DMI-DMTP system in which no absorption of $DMI^{\cdot+}$ could be observed.

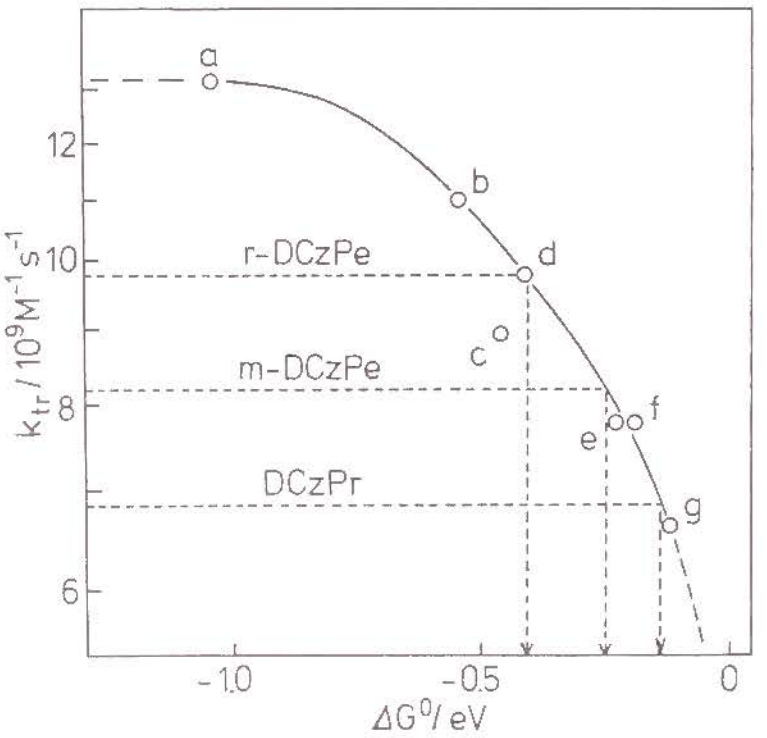

Figure 2-6. Relation between k_{tr} and ΔG^0 in the radical cation transfer process from $EtCz^{\cdot+}$ to D_2.
(a): $EtCz^{\cdot+}$ --> TMPD (system No. 1), (b): $EtCz^{\cdot+}$ --> DMASt (system No. 2), (c): $EtCz^{\cdot+}$ --> DMT (system No. 3), (d): $EtCz^{\cdot+}$ --> DMA (system No. 4), (e): $EtCz^{\cdot+}$ --> DPA (system No. 5), (f): $EtCz^{\cdot+}$ --> TPA (system No. 6), (g): $EtCz^{\cdot+}$ --> DMI (system No. 7). In the case of the dimeric model compounds, ΔG^0 of the radical cation transfer to DMASt was evaluated from k_{tr} as shown by the dotted lines (see text).

The free energy change (ΔG^0) of the radical cation transfer from $D_1^{+\cdot}$ to D_2 is obtained by the difference between the oxidation potentials of D_1 and of D_2.

$$\Delta G^0 = E_{1/2}(D_2/D_2^{+\cdot}) - E_{1/2}(D_1/D_1^{+\cdot}) \qquad (2\text{-}1)$$

where $E_{1/2}(D_2/D_2^{+\cdot})$ and $E_{1/2}(D_1/D_1^{+\cdot})$ are the oxidation potentials of D_2 and D_1, respectively.

Figure 2-6 shows the relationship between k_{tr} and ΔG^0. In the region, $\Delta G^0 < -0.9$ eV, the rate constant k_{tr} is diffusion-controlled and in the region, $\Delta G^0 > -0.9$ eV, k_{tr} decreases with increasing ΔG^0. Experimental values give a smooth curve which is expected for the electron-transfer reaction, though point C slightly deviates from the curve. On the basis of this standard relationship, ΔG^0 for the stabilized systems is estimated by measuring the transfer rate constant k_{tr}.

2-3-3. Radical Cation Transfer

The radical cation transfer rate from the radical cation of various compounds having carbazole chromophores to DMASt was measured by the laser photolysis method. The rate constants k_{tr}'s are listed in the last column of Table 2-II. In this study only the single radical cation acceptor DMASt was used for each system since this makes the evaluation of the stabilization much easier. The rate constant k_{tr} decreases in the following order, 9.8×10^9 $M^{-1}s^{-1}$ for r-DCzPe, 8.2×10^9 $M^{-1}s^{-1}$ for m-DCzPe and 6.8×10^9 $M^{-1}s^{-1}$ for DCzPr, whereas k_{tr} from $EtCz^{+\cdot}$ to DMASt is 11.0×10^9 $M^{-1}s^{-1}$.

2-4. Discussion

2-4-1. Stabilization of Dimer Radical Cation

DCzPr and m-DCzPe are known to form the fully-overlapped dimer radical cations, while r-DCzPe forms the partially-overlapped dimer radical cation. In these dimeric model compounds, the peak wavelengths of the CR band are in the following order; 1800 nm for r-DCzPe and 1600 nm for m-DCzPe and DCzPr. As will be described in Appendix, the CR band reflects directly the degree of chromophore interaction, and the stronger the interaction, the shorter the peak wavelength of the CR band. The shift of the CR band suggests that the fully-overlapped dimer radical cation for m-DCzPe and DCzPr has stronger interaction than the partially-overlapped dimer radical cation for r-DCzPe. This was confirmed by the radical cation transfer method. As shown in Table 2-II, the rate constants k_{tr}'s decrease in the order, $EtCz^{+\cdot}$ (11.0×10^9 $M^{-1}s^{-1}$), r-DCzPe$^{+\cdot}$ (9.8×10^9 $M^{-1}s^{-1}$), m-DCzPe$^{+\cdot}$ (8.2×10^9 $M^{-1}s^{-1}$) and DCzPr$^{+\cdot}$ (6.8×10^9 $M^{-1}s^{-1}$). This means that the partially-overlapped dimer radical cation causes the radical cation transfer to DMASt more easily than the fully-overlapped one. This is due to the stabilization of $Cz^{+\cdot}$ by the neighboring chromophore interaction. Therefore, the order for k_{tr}'s indicates that the fully-overlapped dimer radical cation is stabler than the partially-overlapped dimer radical cation.

2-4-2. Thermodynamic Consideration of Stabilization Energy

In the ground state, dimeric model compounds have such conformations that the steric hindrance is minimized: m-DCzPe and r-DCzPe have mainly TG and TT conformation, respectively,[14] and DCzPr has the conformation such as two carbazole

chromophores are farthest apart. These conformations will be called "open form" hereafter. When a radical cation of carbazole chromophore is photochemically produced, it is stabilized by the interaction with the neighboring chromophore to form the dimer radical cation, in which two carbazole chromophores overlap with each other. Such a conformation of the dimer radical cation will be called "closed form". For DCzPr and m-DCzPe, it corresponds to the completely overlapping conformation. For r-DCzPe, it corresponds to the partially overlapping conformation in which two carbazole chromophores approach a little more closely each other than those in TT conformation of the ground state. Figure 2-7 shows a scheme to consider the stabilization of dimer radical cations as described

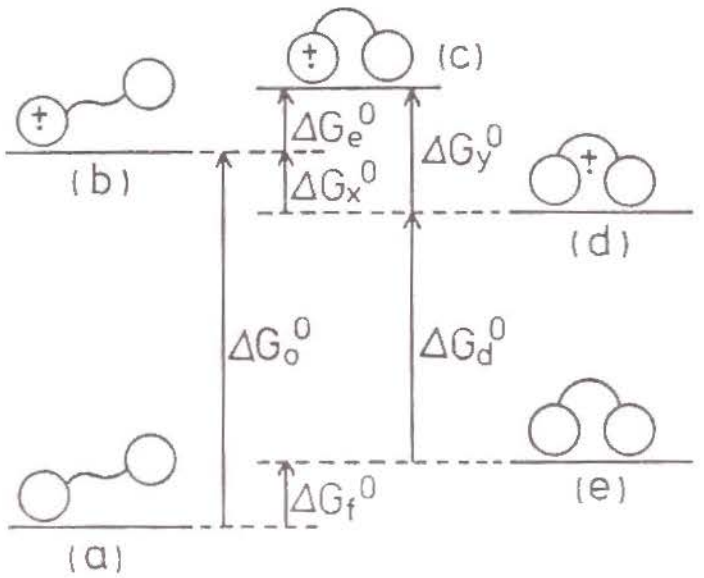

Figure 2-7. Scheme of formation of dimer radical cation. (a): ground state of open form, (b): localized radical cation of open form, (c): localized radical cation of closed form, (d): dimer radical cation, (e): ground state of closed form.

above. State (a) is in a ground state with an open form. State (b) is a localized radical cation with an open form: a radical cation which is free from the neighboring interaction will be called "localized radical cation" and distinguished from the dimer radical cation. State (d) is a dimer radical cation, which can be observed by the nanosecond laser photolysis. State (e) is a ground state dimer (a closed form) formed immediately after the radical cation transfer from (d) to D_2. A localized radical cation with a closed form (c) is assumed as a transition state in the course of formation of (d) from (b). In this manner, it is supposed that first the conformation changes, and then, a dimer radical cation is formed by the neighboring interaction. The arrows in Figure 2-7 show the free energy change (ΔG^0) between individual states. ΔG_e^0 is a free energy change when the state (b) goes to the state (c) by the conformational change and is considered to be mainly caused by an entropy term. ΔG_y^0 corresponds to an enthalpy term of the charge delocalization since the conformation is held. Therefore, ΔG_x^0 is a free energy change when a dimeric model compound forms state (d) from state (b), and its entropy term and enthalpy term are considered to correspond to ΔG_e^0 and ΔG_y^0, respectively.

The radical cation transfer from the dimer radical cation (d) to D_2 is considered to be much faster than the conformational change from the closed form (e) to the open form (a). Then the rate constants of the radical cation transfer are considered to depend on ΔG_d^0 and not to depend on ΔG_f^0. Therefore, the stabilization energy of the dimer radical cation corresponds to the difference between ΔG_o^0 and ΔG_d^0. When the oxidation potentials of the open form (eq. 2-2) and the closed form (eq. 2-3) are measured, ΔG_o^0 and ΔG_d^0 can be calculated from these oxidation potentials.

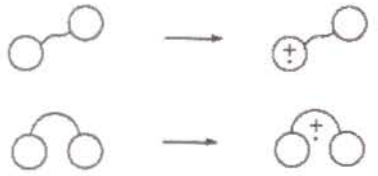

$E_{1/2}$(open) (2-2)

$E_{1/2}$(closed) (2-3)

The oxidation potential of the open form is taken to be equal to that of EtCz since the neighboring interaction can be neglected. Then, the stabilization energy (ΔE) can be estimated by the difference between the oxidation potential of EtCz and that of the closed form (eq. 2-4).

$$\begin{aligned}\Delta E &= -(\Delta G_o^0 - \Delta G_d^0) \\ &= E_{1/2}(\text{open}) - E_{1/2}(\text{closed}) \\ &= E_{1/2}(\text{EtCz/EtCz}^{+\cdot}) - E_{1/2}(\text{closed}) \qquad (2\text{-}4)\end{aligned}$$

On the other hand, ΔG_f^0 is assumed to be equal to ΔG_e^0 since both are the conformational energies between the open form and the closed form, though their states are different: one is the state of the radical cation and the other is the neutral state. Therefore, from another viewpoint the stabilization energy $-(\Delta G_o^0 - \Delta G_d^0)$ is considered to be equal to $-(\Delta G_x^0 + \Delta G_e^0)$ (= $-\Delta G_y^0$), which corresponds to the enthalpy term in the process from the localized radical cation to the dimer radical cation.

2-4-3. Stabilization Energy of Dimeric Model Compounds

(A) Oxidation Potentials in the Closed Form

Eq. 2-4 shows that the stabilization energy of dimer radical cations can be estimated if the oxidation potential of the closed form of the dimeric model compounds is obtained. The oxidation potential measured by cyclic voltammetry, however,

corresponds to that of the open form ($E_{1/2}$(open)) and not to $E_{1/2}$(closed). Therefore, direct evaluation of $E_{1/2}$(closed) is impossible. The free energy change (ΔG^0) of the radical cation transfer is related to the difference between the oxidation potential of a dimeric model compound and that of DMASt by eq. 2-1. Thus, the oxidation potential ($E_{1/2}$(closed)) of a dimeric model compound in the closed form can be estimated from ΔG^0 using the following equation,

$$\begin{aligned}E_{1/2}(\text{closed}) &= E_{1/2}(\text{DMASt/DMASt}^{+\cdot}) - \Delta G^0 \\ &= 0.64 - \Delta G^0 \qquad (2\text{-}5)\end{aligned}$$

In this study, ΔG^0 was estimated by using the relation between ΔG^0 and k_{tr} for low molecular weight compounds (Figure 2-6). In Figure 2-6, ΔG^0 was obtained from the transfer rate constant k_{tr} in the ordinate as shown by the dotted lines. The values of ΔG^0 and of $E_{1/2}$(closed) are shown in the second and third columns in Table 2-III, respectively.

Table 2-III. Oxidation potential and stabilization energy of dimeric model compounds.

compound	ΔG^0/eV	$E_{1/2}$(closed)/V	ΔE/eV
EtCz	-0.54[1)]	1.18	-
r-DCzPe	-0.41	1.05	0.13
m-DCzPe	-0.24	0.88	0.30
DCzPr	-0.13	0.77	0.41

1) This value was calculated from the oxidation potentials of EtCz and DMASt.

The oxidation potential $E_{1/2}$(closed) decreases in the order, r-DCzPe (1.05 V vs. SCE), m-DCzPe (0.88 V vs. SCE) and DCzPr (0.77 V vs. SCE), whereas that of EtCz is 1.18 V vs. SCE. This shows that the oxidation potential decreases with the increase of the stabilization by the neighboring interaction.

Beens and Weller[25] investigated the oxidation potential of dimers by the emission spectra of D-D-A exterplex. They estimated the oxidation potential of the naphthalene dimer using eq. 2-6.

$$E_{1/2}(D/D^+) - E_{1/2}(DD/DD^+) = \nu'_{max} - \nu''_{max} \quad (2\text{-}6)$$

where $E_{1/2}(D/D^+)$ and $E_{1/2}(DD/DD^+)$ are the oxidation potentials of monomer and dimer, respectively, and ν'_{max} and ν''_{max} are the wavenumbers of the peaks of D-A exciplex emission and D-D-A exterplex emission, respectively. Later, Masuhara et al. applied this method to the DCzPe - o-DCNB system.[26] In the present study, the oxidation potential of the dimeric model compounds was estimated by applying this equation to the dimeric model compound - DMTP systems in benzene. The values $E_{1/2}(D/D^+)$ and ν'_{max} are taken from the oxidation potential of EtCz and the wavenumber of the peak of exciplex emission in the EtCz - DMTP system, respectively. The peak wavelength of the exterplex emission in the dimeric model compound - DMTP systems is about 520 nm for r-DCzPe, 560 nm for m-DCzPe and 550 nm for DCzPr, whereas the exciplex in the EtCz - DMTP system appears at ca. 480 nm. Then, the oxidation potentials of the dimeric model compounds are estimated to be ca. 0.99 V for r-DCzPe, 0.81 V for m-DCzPe and 0.85 V for DCzPr. These values agree within ±0.1 V to those estimated by the rate constants of the radical cation transfer mentioned above.

(B) Estimate of Stabilization Energy

Eq. 2-4 shows that the stabilization energy (ΔE) corresponds to the difference between the oxidation potential (1.18 V) of EtCz measured by cyclic voltammetry and that ($E_{1/2}$(closed)) of the dimeric model compounds in the closed form listed in Table 2-III. Thus, by using the values $E_{1/2}$(closed) in Table 2-III, ΔE can be calculated. The obtained values ΔE's are listed in the last column in Table 2-III: ca. 0.1 eV for r-DCzPe, 0.3 eV for m-DCzPe and 0.4 eV for DCzPr. This means that the stabilization of the dimer radical cations is closely related to the overlapping of the two carbazole rings and that the stabilization energies are 0.3 - 0.4 eV and 0.1 eV for the fully-overlapped dimer radical cation and the partially-overlapped dimer radical cation, respectively.

2-5. Conclusion

The CR band of the carbazole dimer radical cations was measured by the nanosecond laser photolysis. The fully-overlapped dimer radical cation for m-DCzPe and DCzPr shows the CR band around ca. 1600 nm, while the partially-overlapped one for r-DCzPe shows the CR band around ca. 1800 nm. This suggests that the former is stabler than the latter. This was confirmed quantitatively by the radical cation transfer method. The dimer radical cations of the dimeric model compounds were stabilized by the neighboring chromophore interaction in the order, r-DCzPe, m-DCzPe and DCzPr, and their stabilization energies were estimated to be ca. 0.1 eV, 0.3 eV and 0.4 eV, respectively.

References

1) H. Yoshimi and K. Kuwata, Mol. Phys. 1972, 23, 297.

2) (a) S. Irie, H. Horii and M. Irie, Macromolecules 1980, 13, 1355. (b) S. Irie and M. Irie, ibid. 1986, 19, 2182.

3) (a) H. Masuhara, N. Tamai, N. Mataga, F. C. De Schryver and J. Vandendriessche, J. Am. Chem. Soc. 1983, 105, 7256. (b) H. Masuhara, K. Yamamoto, N. Tamai, K. Inoue and N. Mataga, N. J. Phys. Chem. 1984, 88, 3971.

4) I. C. Lewis and L. S. Singer, J. Chem. Phys. 1965, 43, 2712.

5) O. W. Howarth and G. K. Fraenkel, J. Am. Chem. Soc. 1966, 88, 4514.

6) T. C. Chiang and A. H. Reddoch, J. Chem. Phys. 1970, 52, 1371.

7) R. E. Büehler and W. Funk, J. Phys. Chem. 1975, 79, 2098.

8) (a) B. Badger, B. Brocklehurst and R. D. Russell, Chem. Phys. Lett. 1967, 1, 122. (b) B. Badger, and B. Brocklehurst, Trans. Faraday Soc. 1969, 65, 2576. (c) B. Badger, and B. Brocklehurst, ibid. 1969, 65, 2582.

9) B. Badger and B. Brocklehurst, ibid. 1969, 65, 2588.

10) A. Kira, S. Arai, and M. Imamura, J. Chem. Phys. 1971, 54, 4890. (b) A. Kira, S. Arai and M. Imamura, J. Phys. Chem. 1972, 76, 1119. (c) A. Kira and M. Imamura, ibid. 1979, 83, 2267.

11) M. A. J. Rodgers, J. Chem. Soc., Faraday Trans. 1 1972, 68, 1278.

12) J. R. Grover, E. A. Walters and E. T. Hui, J. Chem. Phys. 1987, 91, 3233.

13) (a) M. S. El-Shall, S .A. Kafafi, M. Meot- Ner(Mautner) and M. Kertesz, J. Am. Chem. Soc. 1986, 108, 4391. (b) M. S. El-Shall and M. Meot- Ner(Mautner), J. Phys. Chem. 1987, 91, 1088.

14) F. C. De Schryver, J. Vandendriessche, S. Toppet, K. Demeyer and N. Boens, Macromolecules 1982, 15, 406.

15) J. Vandendriessche, P. Palmans, S. Toppet, N. Boens, F. C. De Schryver and H. Masuhara, J. Am. Chem. Soc. 1984, 106, 8057.

16) F. Evers, K. Kobs, R. Memming and D. R. Terrell, J. Am. Chem. Soc. 1983, 105, 5988.

17) F. C. De Schryver, P. Collart, J. Vandendriessche, R. Goedeweeck, A. Swinnen and M. Van der Auweraer, Acc. Chem. Res. 1987, 20, 159.

18) W. Klöpffer, Chem. Phys. Lett. 1969, 4, 193.

19) (a) G. E. Johnson, J. Chem. Phys. 1974, 61, 3002. (b) G. E. Johnson, ibid. 1975, 63, 4047.

20) I. K. Lewis, G. B. Russell, R. D. Topsom, and J. Vaughan, J. Org. Chem. 1964, 29, 1186.

21) E. L. Eliel and R. O. Hutchins, J. Am. Chem. Soc. 1969, 91, 2703.

22) C. S. Marrel, C. G. Overberger, R. E. Allen, and J. H. Saunders, J. Am. Chem. Soc. 1946, 68, 736.

23) W. H. Hamill, in Radical Ions, E. T. Kaiser and L. Kevan eds., Interscience, New York, 1968, Chapter 9.

24) A. Tsuchida, M. Yamamoto and Y. Nishijima, J. Phys. Chem. 1984, 88, 5062.

25) H. Beens and A. Weller, Chem. Phys. Lett. 1968, 2, 140.

26) H. Masuhara, J. Vandendriessche, K. Demeyer, N. Boens, F. C. De Schryver, Macromolecules 1982, 15, 1471.

CHAPTER 3

STABILITY OF CARBAZOLE RADICAL CATION FORMED IN POLY(N-VINYLCARBAZOLE) BY CHARGE DELOCALIZATION

3-1. Introduction

Carbazole radical cation ($Cz^{\cdot+}$) formed in poly(N-vinylcarbazole) (PVCz) is stabilized by the neighboring chromophore interaction. Washio et al.[1] studied the formation process of $Cz^{\cdot+}$ in PVCz and its reactivity by a pulse radiolysis method and found that the recombination and scavenging reactions are suppressed by the stabilization.

Masuhara et al.[2] suggested that the dimeric model compounds, meso- and rac-2,4-di(N-carbazolyl)pentane (m- and r-DCzPe), form the sandwich dimer radical cation having the fully-overlapped conformation of carbazole chromophore and the second dimer radical cation having the partially-overlapped one, respectively. Furthermore, in comparison with the absorption spectra for dimeric model compounds, they concluded that the transient absorption spectrum of $Cz^{\cdot+}$ in PVCz is a superposition of absorption bands of three kinds of dimer radical cations.[3]

In the previous chapter, the stability of carbazole dimer radical cations was studied for dimeric model compounds of PVCz in a solution by the radical cation transfer method and by the charge-resonance (CR) band measurement to understand the neighboring chromophore interaction of the radical cation. The

stabilization energy was estimated to be 0.3 - 0.4 eV for the fully-overlapped dimer radical cation and ca. 0.1 eV for the partially-overlapped one.

In this chapter, transient absorption spectra (CR band) of $Cz^{+\cdot}$ were measured by laser photolysis for PVCz and the copolymers of N-vinylcarbazole (VCz) with methyl methacrylate (MMA) and vinyl acetate (VAc). In the copolymers, the neighboring chromophore interaction on $Cz^{+\cdot}$ is interrupted by the inert comonomer, MMA or VAc. By investigating the relation between the CR band and the fraction of VCz in the copolymer, the degree of the charge delocalization in PVCz was estimated. By the radical cation transfer method, the stabilization energy of $Cz^{+\cdot}$ in PVCz was estimated quantitatively and compared with that of the dimer radical cation.

3-2. Experimental Section

3-2-1. Materials

(A). Electron Donors (D_1)

VCz (Tokyo Kasei Kogyo Co.) was recrystallized from methanol and hexane several times. PVCz was prepared by a radical polymerization initiated by AIBN in degassed benzene at 60 ^{o}C. The molecular weight ($\bar{M}w$) was determined to be 8×10^5 by GPC (Toyo Soda HLC 802 UR) with a G4000H and a GMH columns. MMA (Wako Pure Chem. Ind.) was washed with aqueous Na_2SO_3, aqueous NaOH and aqueous NaCl, and then dried on Na_2SO_4, and finally distilled under reduced pressure. VAc (Wako Pure Chem. Ind.) was purified by distillation. The copolymers of VCz with MMA and of VCz with VAc were obtained by a radical copolymerization initiated by AIBN in degassed benzene at 60 ^{o}C and was purified by precipitation three times.[4,5] The

Table 3-1. Monomer feed ratio (F), $\bar{M}w$, the fraction of VCz (f_{VCz}), sequential distributions of VCz (F_1, F_2, F_3, see the text) for the copolymers of VCz with MMA (A series) and of VCz with VAc (B series).

Copolymer	F[a]	$\bar{M}w/10^5$	f_{VCz}	F_1	F_2	F_3
A1	0.18	1.3	0.07	0.93	0.06	0.01
A2	0.69	1.6	0.22	0.77	0.19	0.04
A3	1.6	3.0	0.37	0.58	0.28	0.14
B1	0.11	0.45	0.38	0.59	0.27	0.14
B2	0.25	0.56	0.62	0.36	0.29	0.35
B3	0.67	1.2	0.79	0.13	0.17	0.70
B4	1.5	2.4	0.83	0.04	0.06	0.90

[a] F=[VCz]/[Comonomer]

conversion of the copolymerization was suppressed to below 30 mol%. The molecular weight ($\bar{M}w$) was measured by GPC, and the fraction (f_{VCz}) of VCz unit in the copolymer was determined by UV absorption spectra in dichloromethane with a Shimadzu UV-200S spectrophotometer. Three samples of the copolymer of VCz with MMA and four samples of the copolymer of VCz with VAc were prepared. These copolymers were designated as A1, A2, and A3 for the former and B1, B2, B3, and B4 for the latter in the order of increasing f_{VCz}. The molecular weight ($\bar{M}w$) and the fraction (f_{VCz}) are summarized in Table 3-1 with the sequential distribution (F_1, F_2, F_3) calculated from the monomer reactivity ratios, r_1 and r_2, according to the terminal model.[6] F_1 is the fraction of isolated VCz. F_2 is the probability that a VCz unit

is found in a dyad sequence of VCz. F_3 is the probability that a VCz unit is found in the sequence whose sequential length is more than two. N-Ethylcarbazole (EtCz) was synthesized by the reaction of sodium carbazole with ethylbromide and purified by recrystallization.

(B) Electron Acceptor (A)

1,4-Dicyanobenzene (p-DCNB, Wako Pure Chem. Ind.) was purified by recrystallization from ethanol three times.

(C) Radical Cation Acceptors (D_2)

N,N,N',N'-Tetramethyl-1,4-phenylenediamine (TMPD, Tokyo Kasei Kogyo Co.), 2,5-dimethoxyaniline (DMOA, Wako Pure Chem. Ind.), diphenylamine (DPA, Tokyo Kasei Kogyo Co.), triphenylamine (TPA, Tokyo Kasei Kogyo Co.), and 1,2-dimethylindole (DMI, Wako Pure Chem. Ind.) were purified by recrystallization. N,N-Dimethyl-1,4-toluidine (DMT, Wako Pure Chem. Ind.) and N,N-dimethylaniline (DMA, Wako Pure Chem. Ind.) were purified by distillation under reduced pressure.

(D) Solvents

Spectroscopic grade of N,N-dimethylformamide (DMF, Dotite Spectrosol) and dichloromethane (Dotite Spectrosol) were used without further purification. Acetonitrile (MeCN, Wako Pure Chem. Ind.) was fractionally distilled after reflux over P_2O_5.

3-2-2. Measurements

(A) Transient Absorption Spectra

The transient absorption spectrum of $Cz^{+\cdot}$ was measured in the presence of an electron acceptor, p-DCNB, by the excimer laser photolysis system. The photoexcitation was made by a 308-

nm laser pulse of a XeCl excimer laser. The pulse intensity was attenuated properly by filters. As the monitoring system for the measurements of transient absorption spectra, a photovoltaic indium arsenide (InAs) diode detector (Hamamatsu, P838) was used. For the measurements of transient absorption spectra, the absorbance of carbazole chromophore at 308 nm was adjusted to be ca. 1.8, and p-DCNB (8.0×10^{-2}M) was added to the system. The measurements were carried out in a 1-cm quartz cell in DMF solvent at 298 K. The samples were degassed by the freeze-pump-thaw method.

(B) Radical Cation Transfer

In this chapter, the radical cation transfer was measured from $EtCz^{+\cdot}$ and $Cz^{+\cdot}$ in the copolymer A1 and in PVCz to amine compounds (D_2). For the radical cation transfer measurements, the detection system equipped with a photomultiplier tube (Hamamatsu, R928) was used since it has a fast response time of ca. 5 ns. To avoid excitation of D_2, carbazole chromophore was photoexcited by an attenuated 351-nm laser pulse of XeF excimer laser. For the radical cation transfer measurements, the absorbance of carbazole chromophore at 351 nm was adjusted to ca. 0.7 for A1 system and ca. 1 for EtCz system and PVCz system. D_2 was added to the EtCz and A1 systems in the following concentration; [TMPD]=2.0×10^{-4}M, [DMOA]=6.0×10^{-4}M, [DMT]=7.0×10^{-4}M, [DMA]=7.0×10^{-4}M, [DPA]=7.0×10^{-4}M, [TPA]=7.0×10^{-4}M, and [DMI]=1.0×10^{-3}M. The concentration of D_2 (DMOA, DMA, and DPA) in the PVCz system was adjusted to 1.0×10^{-2} M. The samples contain 6.4×10^{-2} M p-DCNB as the electron acceptor. The measurements were made in degassed DMF solvent at 298 K.

(C) Oxidation Potentials

The oxidation potentials of EtCz and D_2 were measured by cyclic voltammetry using Ag/0.01 N Ag^+ in MeCN as a reference electrode. The potentials were converted to the ones relative to SCE($E_{1/2}$): $E_{1/2}$=1.18 V for EtCz, 1.06 V for DMI, 0.99 V for TPA, 0.95 V for DPA, 0.77 V for DMA, 0.72 V for DMT, 0.64 V for DMOA, and 0.14 V for TMPD.

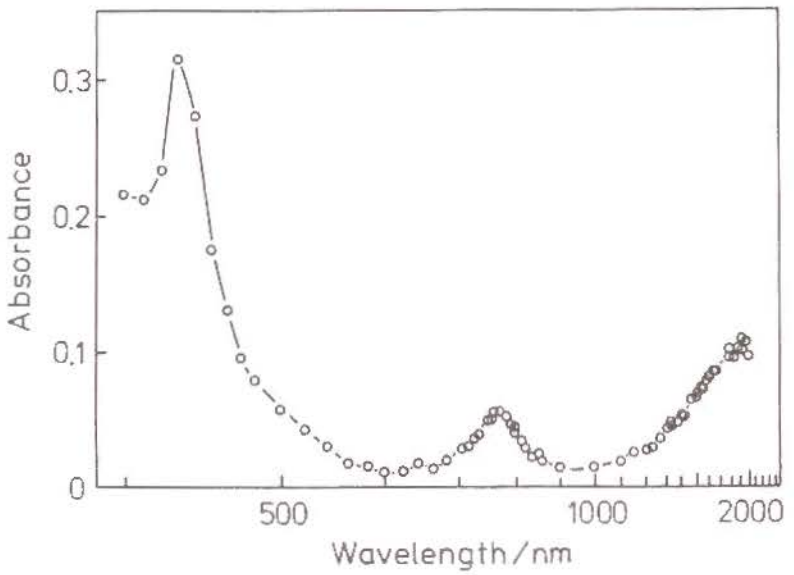

Figure 3-1. Transient absorption spectrum of PVCz - p-DCNB(8.0×10^{-2}M) system in DMF at 298 K at 2 μs after excitation. The concentration of carbazole chromophore was adjusted to be 3.0×10^{-3}M.

3-3. Results and Discussion

3-3-1. Charge Delocalization of Radical Cation in PVCz

Figure 3-1 shows the transient absorption spectrum of a PVCz - p-DCNB system at 2 μs after excitation. The absorption band at ca. 430 nm was assigned to the radical anion, p-DCNB$^{\cdot-}$. The $Cz^{\cdot+}$ gives two absorption bands. One is the visible band at

ca. 750 nm[7,8] which is very broad compared with that of the monomer radical cation, $EtCz^{\cdot+}$. The other is the CR band at a wavelength longer than 1900 nm. The CR band is shifted to longer wavelengths than that of the dimer radical cation, appearing at ca. 1600 nm and at ca. 1800 nm for the fully-overlapped dimer radical cation for m-DCzPe and the partially-overlapped dimer radical cation for r-DCzPe, respectively. According to the Hückel MO theory, the CR band of the dimer radical cation is shifted to shorter wavelengths with the increasing interaction, i.e., the increasing stability of the dimer radical cation. However, this cannot be applied to PVCz, since the $Cz^{\cdot+}$ in PVCz is stabler than the dimer radical cation as described below. On the other hand, Hückel MO calculations indicate that the CR band of a radical cation should be shifted to longer wavelengths with increasing charge delocalization such as dimer, trimer, and tetramer.[9,10] The longer-wavelength shift for PVCz is considered to be due to an increasing charge delocalization.

The transient absorption spectra for the copolymers were measured to investigate the neighboring chromophore interaction on the radical cation. Figures 3-2 and 3-3 show the transient absorption spectra of $Cz^{\cdot+}$ in the copolymers of VCz with MMA (A1 - A3) and of VCz with VAc (B1 - B4) at 2 μs after excitation, respectively. As shown in Figure 3-2-(a), $Cz^{\cdot+}$ of A1 gave only the visible band at ca. 820 nm which was similar in shape to that of the monomer radical cation, $EtCz^{\cdot+}$, and the CR band in the near-infrared region was not observed. This means that A1 forms only the monomer radical cation and that the neighboring chromophore interaction is interrupted by the inert comonomer, MMA. This is expected by the fact that the fraction (F_1) of isolated VCz in the comonomer, MMA, is 0.93, suggesting that

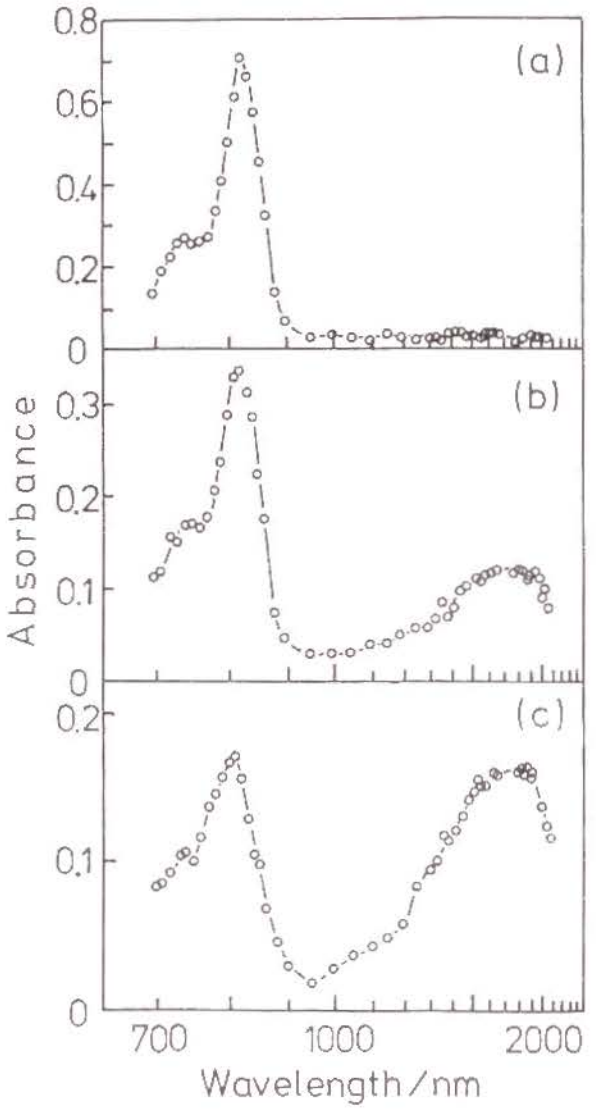

Figure 3-2. Transient absorption spectra of $Cz^{\cdot+}$ for the copolymers of VCz with MMA in DMF at 298 K at 2 μs after excitation: (a) A1; (b) A2; (c) A3. The absorbance of carbazole chromophore at 308 nm was adjusted to ca. 1.8. All the samples contain 8.0×10^{-2}M p-DCNB.

there is almost no interaction of $Cz^{\cdot+}$ with remote carbazole chromophores in a polymer chain. The other copolymers showed the CR band in the near-infrared region along with the visible band. In Figure 3-4, the peak wavelength (λ_{CR}) of the CR band and the ratio of the absorbance of the CR band to that of the radical anion, p-DCNB$^{\cdot-}$ (430 nm) (A_{CR}/A_{430}) were plotted against the probability of carbazole chromophore not to be isolated, $1-F_1$. For the copolymer with $1-F_1<0.4$, the CR bands appear at ca. 1800 nm, and the relative absorbance of the CR band increases with the increasing $1-F_1$. Since the probability (F_3) that $Cz^{\cdot+}$ is formed in the sequence having more than two VCz units is very

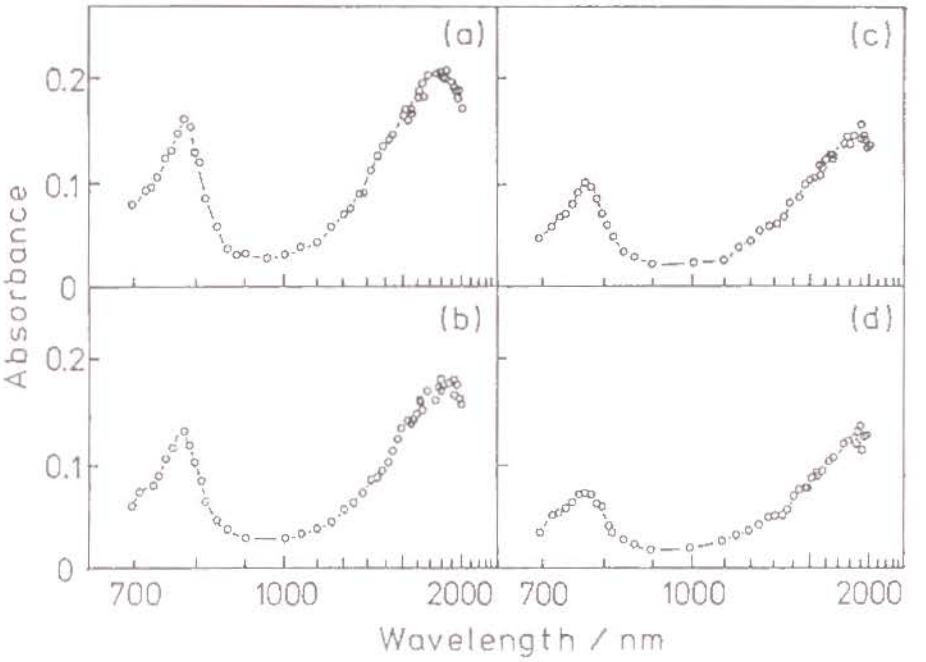

Figure 3-3. Transient absorption spectra of $Cz^{\cdot+}$ for the copolymers of VCz with VAc in DMF at 298 K at 2 μs after excitation: (a) B1; (b) B2; (c) B3; (d) B4. The absorbance of carbazole chromophore at 308 nm was adjusted to ca. 1.8. All the samples contain 8.0×10^{-2}M p-DCNB.

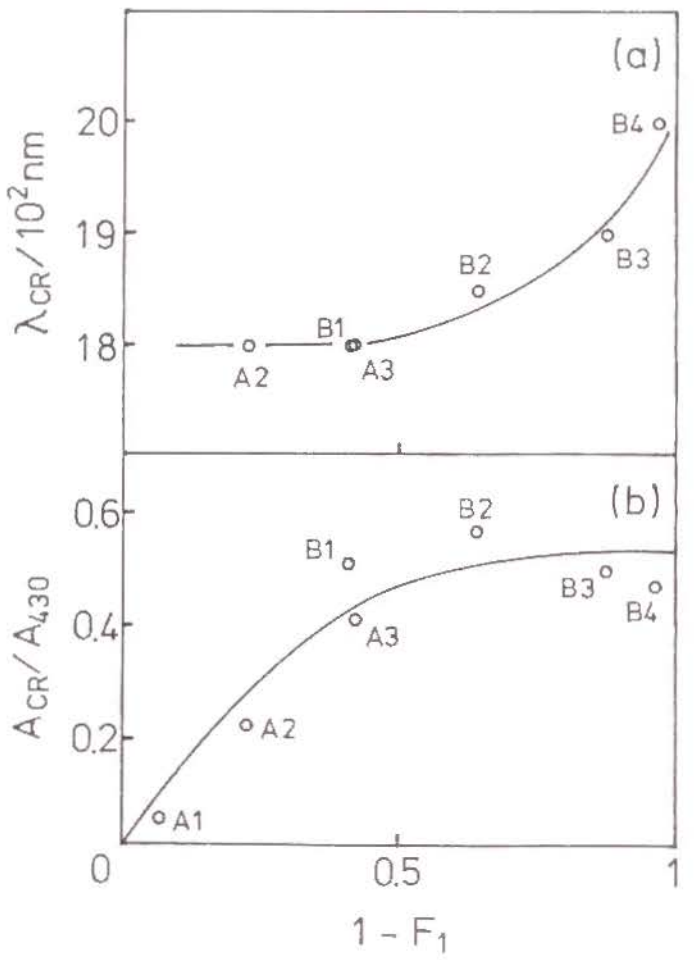

Figure 3-4. Peak wavelength of the CR band (λ_{CR}) and its relative absorbance to that at 430 nm (A_{CR}/A_{430}) are plotted against $1-F_1$.

small in the region $1-F_1<0.4$, the CR band is due to the dimer radical cation formed in the dyad sequence of VCz. With the increase of $1-F_1$, the fraction of $Cz^{+\cdot}$ formed in the dyad sequence to the monomer radical cation increases, and the absorption intensity of the CR band is enhanced. For the copolymer with $1-F_1>0.5$, the CR band is shifted to longer wavelengths with the increase of $1-F_1$. An absorption of the

solvent prevents measuring a transient absorption spectrum in the wavelength region longer than 2100 nm. Therefore, the shape and the halfwidth of the CR band were roughly evaluated. The CR band seems to become broader with longer-wavelength shifts. At least, the CR bands for B4 and PVCz are obviously broader than those for A2 and A3 which are considered to form mainly the dimer radical cation. The longer-wavelength shift and broadening of the CR band for PVCz are not due to a perturbed dimer radical cation but to increasing contribution of $Cz^{+\cdot}$ delocalized among more than two chromophores. In fact, the shift of the CR band begins at $1-F_1=0.5$, where the fraction of $Cz^{+\cdot}$ formed in the VCz sequence having more than two units is larger than that of $Cz^{+\cdot}$ formed in the dyad sequence. Furthermore, B4 with $F_3=0.9$ gave the same transient absorption spectrum as PVCz (Figure 3-3-(d)). Thus, the shift and broadening of the CR band correspond to the increase of F_3. This suggests that the $Cz^{+\cdot}$ in the polymer, PVCz is stabilized by the charge delocalization among more than two chromophores.

3-3-2. Stabilization Energy of Radical Cation in PVCz

At first, the free energy change (ΔG) dependence of the rate constant (k_{tr}) of the radical cation transfer reaction was investigated. The radical cation transfer to amine compounds D_2 (TMPD, DMOA, DMT, DMA, DPA, TPA, and DMI) was measured for EtCz and the copolymer A1. The free energy change (ΔG) in eq. 3-1 was estimated by the difference between the oxidation potential of EtCz and that of D_2.

$$\Delta G = E_{1/2}(D_2) - E_{1/2}(EtCz) \qquad (3\text{-}1)$$

Since $Cz^{+\cdot}$ in A1 is not stabilized by neighboring chromophore

interaction, the oxidation potential of carbazole chromophore in Al is assumed to be equal to that of EtCz. The decay curves of $Cz^{\cdot+}$ were measured at 790 nm for EtCz and at 820 nm for Al. As an example, the decay curve of $EtCz^{\cdot+}$ for EtCz - DPA - p-DCNB system is shown in Figure 3-5.

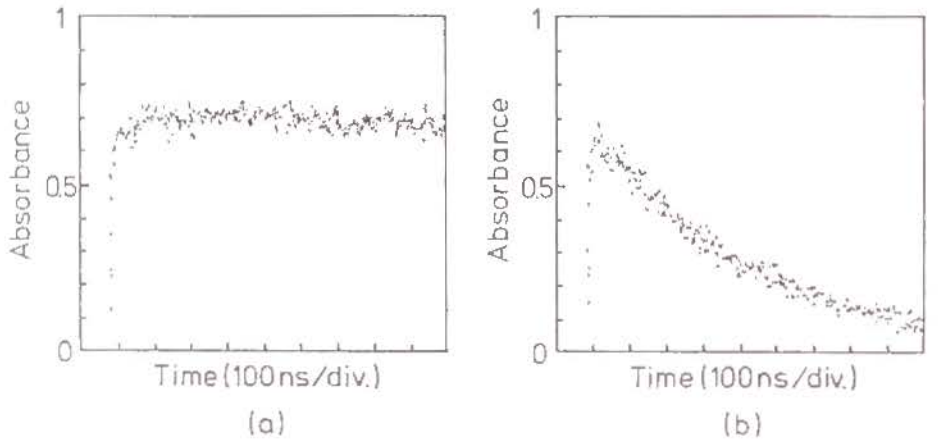

Figure 3-5. Transient absorption decays at 790 nm of EtCz radical cation in DMF at 298 K in the presence of p-DCNB (6.4×10^{-2}M): (a) without DPA; (b) with DPA (7.0×10^{-4}M).

In the absence of DPA, $EtCz^{\cdot+}$ recombines with $p\text{-}DCNB^{\cdot-}$, but the absorption scarcely decays in this time region (Figure 3-5-(a)). The addition of DPA accelerated the decay of $EtCz^{\cdot+}$ by the radical cation transfer to DPA (Figure 3-5-(b)). The rate of the radical cation transfer is much faster than that of the recombination: $k_{tr}[D_1^{\cdot+}][D_2] >> k_r[D_1^{\cdot+}][A^{\cdot-}]$. Then, k_{tr} was determined by the slope in the plot of ln A against t using eq. 7 in Appendix. Figure 3-5-(b) gave $k_{tr}=3.22\times10^9$ $M^{-1}s^{-1}$. For the other systems, k_{tr} was determined in the same way by addition of a proper concentration of D_2. Table 3-II shows the results. The second and the fourth columns are k_{tr}'s for EtCz and for

Table 3-II. Free energy change (ΔG) and rate constants (k_{tr}, k_e) of radical cation transfer to D_2 for EtCz and Al systems.

D_2	$-\Delta G$/eV	EtCz/10^9M^{-1}s^{-1}		Al/10^9M^{-1}s^{-1}	
		k_{tr}	k_e	k_{tr}	k_e
TMPD	1.04	6.25	-	3.07	-
DMOA	0.54	5.02	25	2.42	11
DMT	0.46	4.86	21	2.66	-
DMA	0.41	4.35	14	2.30	9.17
DPA	0.23	3.22	6.64	1.55	3.13
TPA	0.19	2.92	5.48	1.44	2.71
DMI	0.12	2.73	4.85	1.39	2.54

Al, respectively. In each system, k_{tr} for Al is smaller than that for EtCz. However, these values cannot be simply compared with each other, since the radical cation transfer in this intermolecular system contains the diffusion process and the electron transfer process. For the radical cation transfer to occur, first of all, $Cz^{\cdot+}$ and D_2 must be brought close together. Therefore, the radical cation transfer reaction can be considered to be a consecutive reaction that the electron transfer process follows the diffusion process. In the radical cation transfer systems studied in this experiment, the electron transfer process is a rate-limiting step except for the case of TMPD. Then, the rate constant of the radical cation transfer is given by the following equation.[11]

$$k_{tr}^{-1} = k_d^{-1} + k_e^{-1} \qquad (3\text{-}2)$$

where k_d and k_e are rate constants of the diffusion and the electron transfer processes, respectively. It is considered that the radical cation transfer to TMPD is exothermic (ΔG = -1.04 eV) enough to be diffusion-controlled. Therefore, the rate constant of the radical cation transfer to TMPD was taken as k_d; k_d = 6.25×10^9 $M^{-1}s^{-1}$ for EtCz systems and k_d = 3.07×10^9 $M^{-1}s^{-1}$ for Al systems. This is supported by the fact that the Einstein-Smoluchowski equation: $k_d = 8RT/3000\eta$ gives 6.50×10^9 $M^{-1}s^{-1}$, where η is the viscosity of a solvent, DMF. The diffusion-rate constant, k_d, for Al is almost half of that for EtCz. This is justified by the fact that the diffusion of the copolymer, Al, is negligibly small compared with that of the low molecular weight compound. The rate constants, k_e, for EtCz and for Al are listed in the third and the fifth columns in Table 3-II, respectively. In Figure 3-6, k_e's for EtCz and for Al are plotted against ΔG. Each system gave a linear relationship between the logarithm of k_e and ΔG. The linear relationship between the logarithm of the rate constant k_e and ΔG was also observed for the electron transfer quenching of an excited state of aromatic molecules by anion.[12] The relation was discussed by the Polanyi equation.[13] In the present study, the following experimental equations were obtained.

$$\log k_e = -1.83\ \Delta G + 9.44 \quad \text{for EtCz system} \qquad (3\text{-}3)$$

$$\log k_e = -1.83\ \Delta G + 9.14 \quad \text{for Al system} \qquad (3\text{-}4)$$

Each system has a similar slope in the semilogarithmic plot of k_e as a function of ΔG, but the intercept for Al is smaller than that for EtCz; k_e for Al is nearly equal to a half value of that for EtCz. As described previously, the chromophore interaction in Al is interrupted by the inert comonomer, and

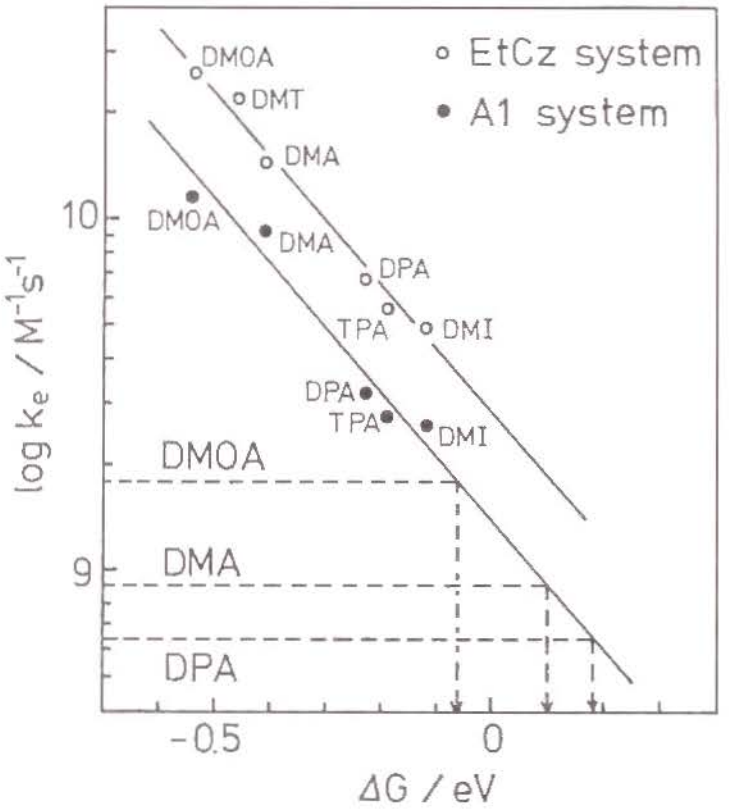

Figure 3-6. Relationship between k_e and ΔG in the radical cation transfer to D_2 for EtCz and Al systems. Open and closed circles indicate EtCz and Al systems, respectively. D_2 is shown by the abbreviation in the figure. For PVCz, ΔG of the radical cation transfer to DMOA, DMA, and DPA was estimated from k_e as shown by the dashed lines.

$Cz^{\cdot+}$ in Al is not stabilized. Therefore, a smaller value of k_e for Al is considered to be due to the steric hindrance of the polymer chain to the access of D_2, that is, the polymer chain sterically restricts the direction for D_2 to approach $Cz^{\cdot+}$ in the polymer chain, or that electron transfer in the polymer system may occur at a longer distance due to the steric hindrance of polymer chain.

Table 3-III. Apparent transfer rate constant (k_{tr}), electron transfer rate constant (k_e), free energy change (ΔG), and stabilization energy ($-\Delta H$) for PVCz system.

D_2	$k_{tr}/10^8 M^{-1}s^{-1}$	$k_e/10^8 M^{-1}s^{-1}$	ΔG/eV	$-\Delta H$/eV
DMOA	11.3	17.9	-0.06	0.48
DMA	6.98	9.03	0.10	0.51
DPA	5.28	6.38	0.19	0.42

As for the $Cz^{+\cdot}$ formed in PVCz, the radical cation transfer to DMOA, DMA, and DPA was measured. The concentration of DMOA, DMA, and DPA was 1.0×10^{-2} M. The rate constant, k_{tr}, was determined by the slope of the semilogarithmic plot of the transient absorption decay of $Cz^{+\cdot}$ at 750 nm according to eq. 7 in Appendix. Table 3-III shows the results. The rate constant, k_e, was evaluated by eq. 3-2 assuming that k_d is 3.07×10^9 $M^{-1}s^{-1}$. In the radical cation transfer from $Cz^{+\cdot}$ in PVCz to amines, not only the stabilization by charge delocalization but also polymer effects such as a steric hindrance of a main chain may affect the transfer rate constant. Therefore, by using the linear relationship between log k_e and ΔG for A1, it can be determined how ΔG increases by the stabilization through charge delocalization of $Cz^{+\cdot}$ in PVCz. In practice, the ΔG of the radical cation transfer from $Cz^{+\cdot}$ in PVCz to the radical cation acceptor was estimated as shown by the dashed line in Figure 3-6. ΔG's for DMOA, DMA, and DPA are -0.06 eV, 0.10 eV, and 0.19 eV, respectively. In the radical cation transfer to DMOA, DMA, and

DPA, the ΔG for PVCz is larger than that for A1 (-0.54 eV for DMOA, -0.41 eV for DMA, and -0.23 eV for DPA). This is due to the stabilization of $Cz^{+\cdot}$ in PVCz by the neighboring chromophore interaction, and the difference between ΔG estimated for PVCz and for A1 corresponds to the stabilization energy ($-\Delta H$) as described in the previous chapter. The evaluated stabilization energies ($-\Delta H$) are listed in Table 3-III: ca. 0.48 eV with DMOA, ca. 0.51 eV with DMA, and ca. 0.42 eV with DPA. In this way, the stabilization energy of $Cz^{+\cdot}$ in PVCz was estimated to be 0.5 $\pm$ 0.1 eV on average. In this method, the effect of the steric hindrance of the polymer chain is excluded by using the relationship between k_e and ΔG for the copolymer A1 as described above, and this value is the net stabilization energy by the neighboring chromophore interaction. The stabilization energy of $Cz^{+\cdot}$ in PVCz is larger than that of the dimer radical cations (ca. 0.1 eV for the partially-overlapped dimer radical cation and 0.3 - 0.4 eV for the fully-overlapped dimer radical cation). This is consistent with the result of the CR band for the copolymer systems. It was found that $Cz^{+\cdot}$ in the polymer is delocalized among more than two neighboring chromophores, and that it is stabler than the dimer radical cation.

3-4. Conclusion

By investigating the relationship between the CR band of the copolymers of VCz and the sequential distribution of carbazole chromophore, it was found that the $Cz^{+\cdot}$ formed in PVCz is stabilized by the charge delocalization among more than two neighboring chromophores. The CR band of the $Cz^{+\cdot}$ in PVCz was shifted to longer wavelengths than that of the dimer radical cations. This result is qualitatively consistent with the

theoretical MO prediction. The stabilization energy by the charge delocalization was estimated to be 0.5 ± 0.1 eV for PVCz by the radical cation transfer method. This stabilization energy is larger than that of the dimer radical cation (ca. 0.1 eV for the partially-overlapped dimer radical cation and 0.3 - 0.4 eV for the fully-overlapped dimer radical cation). This means that the stability of the $Cz^{+\cdot}$ increases with the charge delocalization such as a trimer radical cation.

References

1) M. Washio, S. Tagawa and Y. Tabata, Polm. J. 1981, 13, 935.

2) (a) H. Masuhara, N. Tamai, N. Mataga, F. C. De Schryver and J. Vandendriessche, J. Am. Chem. Soc. 1983, 105, 7256.

3) (a) H. Masuhara, K. Yamamoto, N. Tamai, K. Inoue and N. Mataga, J. Phys. Chem. 1984, 88, 3971. (b) H. Masuhara, Makromol. Chem., Suppl. 1985, 13, 75.

4) J. Brandrup, E. H. Immergut eds. Polymer handbook, Wiley-Interscience Pub., New York, 1974.

5) T. Alfrey, Jr. and S. L. Kapur, J. Polym. Sci. 1949, 4, 215.

6) G. E. Ham, in Copolymerization, G. E. Ham ed., High Polymers Vol. XVIII, Wiley-Interscience Pub., New York, 1964, Chap.1.

7) (a) U. Lachish, D. J. Williams and R. W. Anderson, Chem. Phys. Lett. 1979, 65, 574. (b) U. Lachish, R. W. Anderson, D. J. Williams, Macromolecules 1980, 13, 1143.

8) H. Masuhara, S. Ohwada, N. Mataga, A. Itaya, K. Okamoto and S. Kusabayashi, J. Phys. Chem. 1980, 84, 2363.

9) B. Badger and B. Brocklehurst, Nature 1968, 219, 263.

10) A. Kira and M. Imamura, J. Chem. Phys. 1979, 83, 2267.

11) R. A. Marcus, J. Chem. Phys. 1965, 43, 3477.

12) (a) H. Shizuka, M. Nakamura and T. Morita, J. Phys. Chem. 1980, 84, 989. (b) H. Shizuka and H. Obuchi, J. Phys. Chem. 1982, 86, 1297.

13) M. G. Evans and M. Polanyi, Trans. Faraday Soc. 1938, 34, 11.

CHAPTER 4

CARBAZOLE - CARBAZOLE - TEREPHTHALATE EXTERPLEX FORMATION

4-1. Introduction

A geminate ion pair formed by photo-induced electron transfer dissociates into free ions in a polar solvent, and the neighboring chromophore interaction leads to the formation of a dimer radical cation. On the other hand, the ion pair forms an exciplex in a non-polar solvent. Similarly to the case of the dimer radical cation, the charge-transfer state of the exciplex is stabilized by the neighboring chromophore interaction, forming an excited triple complex (exterplex). In 1968, Beens and Weller[1] reported electron donor (D) - electron donor (D) - electron acceptor (A) type of exterplex which consists of two naphthalene (D) and 1,4-dicyanobenzene (p-DCNB, A). Since then, many DDA type of exterplexes have been investigated.[2-8] As for the exterplex of 2-methylnaphthalene and 1,3-dinaphthylpropane with p-DCNB, Mimura and Itoh[5] studied the formation process of the exterplex by measuring time-resolved emission spectra and analyzing the emission decays. Hoyle and Guillet[6] found that a poly(N-vinylcarbazole) (PVCz) - dimethyl terephthalate (DMTP) system shows a broad emission around 520 nm in benzene, and assigned this broad emission to a carbazole - carbazole - DMTP exterplex. Furthermore, Masuhara et al.[7] reported that meso- and rac-2,4-di(N-carbazolyl)pentane (m- and

r-DCzPe) show, in the presence of 1,3-dicyanobenzene (m-DCNB), a broad exterplex emission around 510 nm and around 460 nm corresponding to their different configurations.The difference in the emission spectrum was considered to be due to the difference in the exterplex structure; it is suggested that r-DCzPe forms a DDA type of exterplex in which two carbazolyl (Cz) chromophores overlap partially (partially-overlapped exterplex), while m-DCzPe forms one in which two Cz chromophores overlap completely each other (fully-overlapped exterplex).

Previous chapters dealt with the stabilization of the carbazole radical cations for PVCz and its dimeric model compounds achieved by the neighboring chromophore interaction. In this chapter, the structure, the stability and the formation process for the Cz - Cz - DMTP exterplex were investigated by measuring the fluorescent properties of PVCz, its dimeric model compounds and the copolymers of N-vinylcarbazole in the presence of DMTP. Since the exterplex is formed by the stabilization of the charge-transfer state by the neighboring chromophore interaction, the mechanism of the stabilization is analogous to the case of the dimer radical cation. The similarity of the interaction in the exterplex to that in the dimer radical cation was discussed.

4-2. Experimental Section

4-2-1. Materials

Two kinds of PVCz having different stereoregularity were prepared, one (PVCz(c)) by BF_3OEt_2-initiated cationic polymerization in dichloromethane, the other (PVCz(r)) by AIBN-initiated radical polymerization in benzene. The monomer, N-

vinylcarbazole (VCz, Tokyo Kasei Kogyo Co.), was recrystallized from methanol and hexane several times. The weight-average molecular weight ($\bar{M}w$) was estimated to be $2x10^4$ for PVCz(c) and $8x10^5$ for PVCz(r) by means of GPC (Toyo Soda HLC 802 UR) with a G4000H and GMH column system calibrated with standard polystyrenes. The syndiotactic fraction was estimated to be ca. 0.5 for PVCz(c) and ca. 0.7 for PVCz(r) from a fluorescent spectrum.[9] As a dimeric model compound of PVCz, DCzPr, m- and r-DCzPe were synthesized. A monomeric model compound, N-ethylcarbazole (EtCz) was synthesized. These model compounds were purified by recrystallization. Styrene (St, Wako Pure Chem. Ind.) and diethyl fumarate (DEF, Wako Pure Chem. Ind.) were purified by distillation under a reduced pressure. A random copolymer of VCz with St (P(VCz-St))[10] with a VCz fraction of ca. 0.1 and an alternative copolymer of VCz with DEF (P(VCz-DEF))[11] were prepared by radical copolymerization in benzene. Poly[2-(N-carbazolyl)ethyl methacrylate] (PCzEMA) was prepared by radical polymerization of the monomer, 2-(N-carbazolyl)ethyl methacrylate.[12] The PS-calibrated GPC molecular weight ($\bar{M}w$) was found to be $7x10^4$ for P(VCz-St), $1x10^5$ for P(VCz-DEF) and $8x10^4$ for PCzEMA. Dimethyl terephthalate (DMTP, Wako Pure Chem. Ind.) was purified by recrystallization.

4-2-2. Measurements

All measurements were made in solution of degassed benzene (Dotite Spectrosol) at room temperature except the experiments of temperature dependence. The concentration of Cz chromophore was adjusted to below $3x10^{-4}$ M to avoid an intermolecular interaction. All samples contained 0.07 M DMTP as an electron acceptor.

Absorption and emission spectra were measured by a

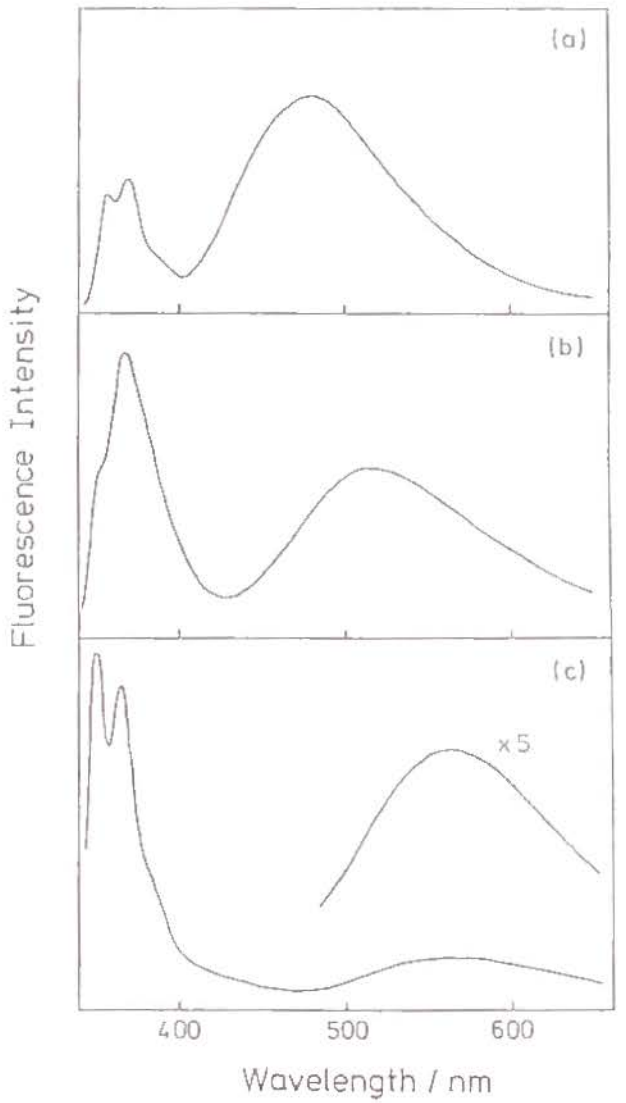

Figure 4-1. Emission spectra of the Cz monomer and dimeric model compound systems in benzene at room temperature.
(a): EtCz(3.0×10^{-4} M) - DMTP(0.1 M),
(b): r-DCzPe([Cz]=1.2×10^{-4} M) - DMTP(0.07 M),
(c): m-DCzPe([Cz]=1.0×10^{-4} M) - DMTP(0.07 M).

Shimadzu UV-200S spectrophotometer and a Hitachi 850 spectrophotofluorometer, respectively. A fluorescent lifetime was measured by a single photon counting method (PRA Inc. model 510B). The measurements of the fluorescent spectra and lifetime were carried out by selective photoexcitation of Cz chromophore.

4-3. Results

4-3-1. Emission Spectra

Figure 4-1 shows the emission spectra for the monomeric and dimeric model compound - DMTP systems. As shown in Figure 4-1-(a), EtCz - DMTP system gives a monomer emission having a vibrational structure and an exciplex emission around 480 nm. On the other hand, the dimeric model compound - DMTP systems show, as well as the monomer and the excimer emissions, a new broad emission in a wavelength region longer than the exciplex emission region. r-DCzPe system (Figure 4-1-(b)) shows a broad emission around 510 nm whose quantum yield and lifetime were measured to be 0.048 and 71 ns, respectively, while m-DCzPe system (Figure 4-1-(c)) shows a broad emission around 560 nm whose lifetime and quantum yield were measured to be 36 ns and less than 0.017, respectively. These broad emissions were assigned to Cz - Cz - DMTP exterplex emission.

Figures 4-2-(a) and (b) show the emission spectra for PVCz(c) and PVCz(r) systems, respectively. As shown by the dotted line, in the absence of DMTP, PVCz gives the second excimer emission at ca. 370 nm and the sandwich excimer emission at ca. 420 nm.[9,13] The fraction of these excimers depends on the stereoregularity; the larger the syndiotactic fraction, the larger the ratio of the second excimer emission to the sandwich

excimer one. When DMTP is added to these systems, both PVCz's give the second excimer emission at ca. 370 nm and a new broad emission around 510 nm as shown by the solid line. The latter was ascribed by Hoyle and Guillet[6] to Cz - Cz - DMTP exterplex emission. It is noteworthy that the two PVCz's show the same exterplex emission despite they are different in syndiotactic fraction.

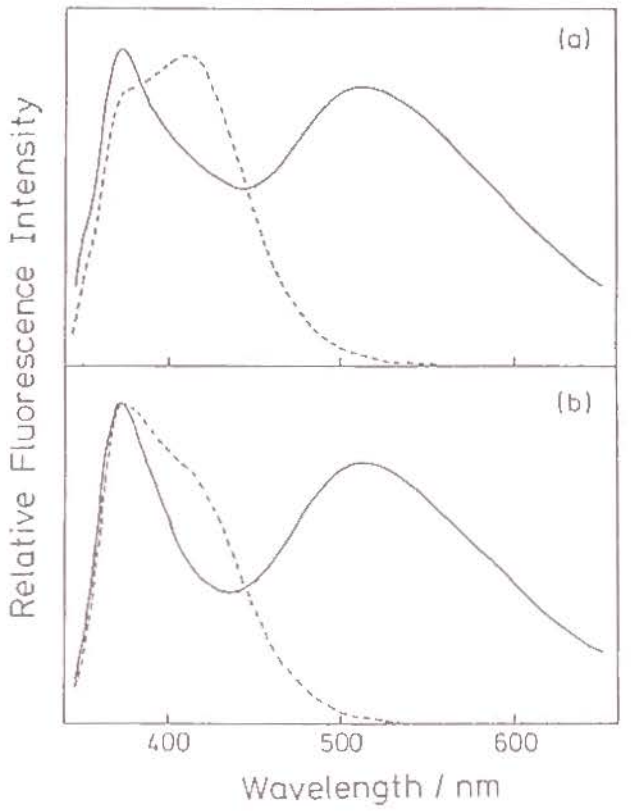

Figure 4-2. Emission spectra of PVCz systems in benzene at room temperature.
(a): PVCz(c)([Cz]=1.5×10^{-4} M) system,
(b): PVCz(r)([Cz]=1.7×10^{-4} M) system
The dotted and solid lines show the spectra in the absence of DMTP and in the presence of DMTP(0.07 M), respectively.

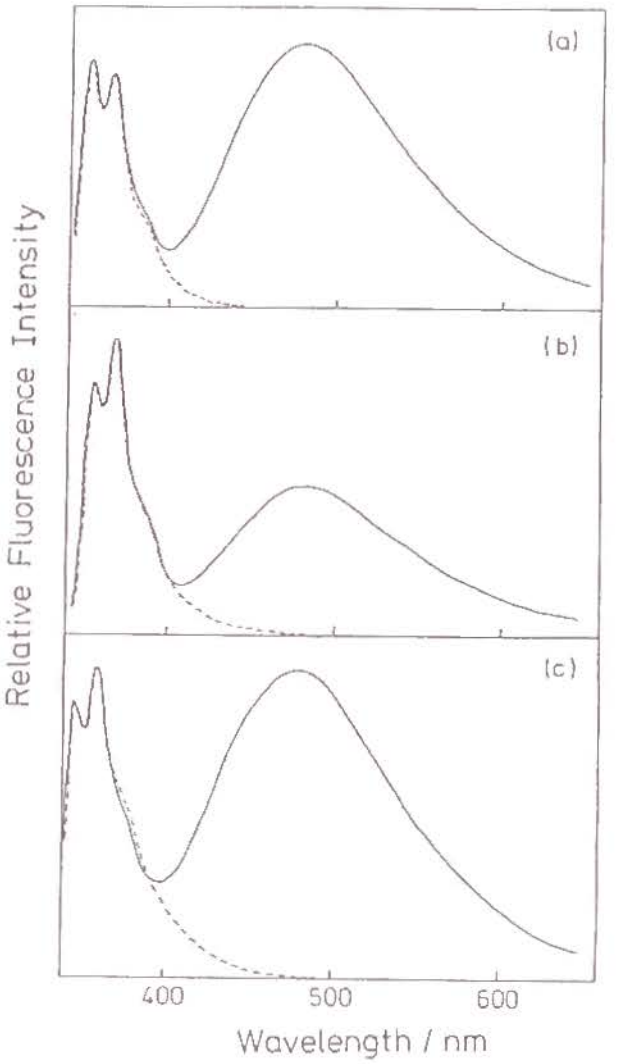

Figure 4-3. Emission spectra of the polymer systems having Cz chromophores in benzene at room temperature.
(a): PCzEMA([Cz]=1.1×10^{-4} M) system,
(b): P(VCz-St)([Cz]=2.4×10^{-4} M) system,
(c): P(VCz-DEF)([Cz]=8.5×10^{-5} M) system
The dotted and solid lines show the spectra in the absence of DMTP and in the presence of DMTP(0.07 M).

Table 4-I. Quantum yield of Cz emission (Φ_f^O) in the absence of DMTP, those of monomer emission (Φ_f) and exciplex emission (Φ_f') in the presence of DMTP and quantum efficiency of exciplex emission (q_f') in the presence of DMTP.

	Φ_f^O	Φ_f	Φ_f'	q_f'
EtCz - DMTP(0.1 M)	0.514	0.022	0.121	0.13
PCzEMA - DMTP(0.07 M)	0.473	0.022	0.088	0.09
P(VCz-St) - DMTP(0.07 M)	0.410	0.061	0.116	0.13
P(VCz-DEF) - DMTP(0.07 M)	0.128	0.014	0.054	0.06

The emission spectra of PCzEMA, P(VCz-St) and P(VCz-DEF) are shown in Figures 4-3-(a), (b) and (c), respectively. In the absence of DMTP, only the monomer emission was observed, and the excimer emission was hardly detected, as shown by the dotted line.[12,14,15] This suggests that the neighboring chromophore interaction in the excited state is suppressed because of the separation of the Cz chromophore from the main chain or as a result of copolymerization. When the Cz monomer excited state of these polymer is quenched by DMTP, a new broad emission appears around 480 nm. This is the same exciplex emission as in the EtCz - DMTP system. Table 4-1 gives the quantum yield (Φ_f^O) of the Cz monomer emission in the absence of DMTP, those of the monomer- (Φ_f) and the exciplex (Φ_f') emissions in the presence of DMTP, and the quantum efficiency of the exciplex emission (q_f') calculated with the following equation.

$$q_f' = \Phi_f' / (1 - \Phi_f / \Phi_f^O) \qquad (4-1)$$

The quantum yield Φ_f^O for P(VCz-DEF) is much smaller than that for EtCz. This is considered to be due to the intramolecular quenching by DEF, since DEF has an electron-accepting property. In the case of P(VCz-St) and PCzEMA systems, Φ_f^O and q_f' are nearly equal to those of the EtCz system.

4-3-2. Temperature Dependence of Exterplex Emission

Figures 4-4-(a) and (b) show the temperature dependence of the emission spectra for r-DCzPe and m-DCzPe systems, respectively. As the temperature rises from 15 ^oC to 75 ^oC, the quantum yields of the monomer and the excimer emissions decrease, and that of the exterplex emission increases with the peak shifted towards a shorter wavelength. The PVCz(c) system behaves differently (Figure 4-4-(c)). With increasing temperature, the yields of the monomer and the exterplex emissions decrease, and the peak wavelength of the exterplex emission is shifted towards a longer wavelength.

4-4. Discussion

4-4-1. Partially-overlapped and Fully-overlapped Exterplexes

The emission spectra for DCzPe - DMTP system indicates that DCzPe forms two kinds of exterplex in which the degree of overlapping of the Cz chromophores is different because of the steric hindrance of methyl groups in the main chain. This is analogous to the DCzPe - m-DCNB system studied by Masuhara et al..[7] That is, r-DCzPe - DMTP system forms a partially-overlapped exterplex, while m-DCzPe forms a fully-overlapped

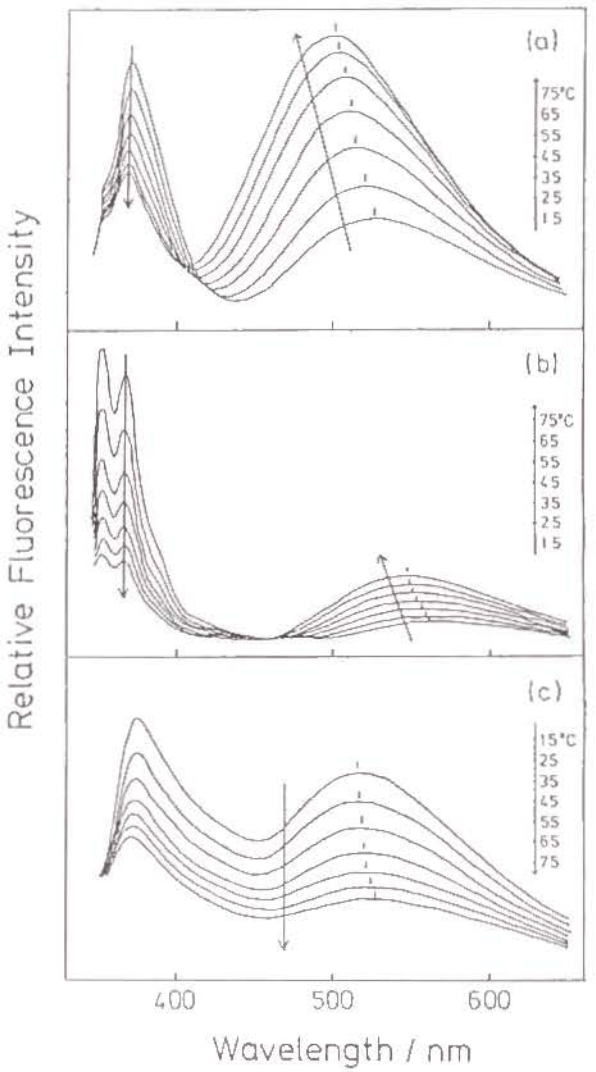

Figure 4-4. Temperature dependence of emission spectra for the PVCz and DCzPe systems in benzene.
(a): r-DCzPe([Cz]=1.4x10^{-4} M) - DMTP(0.07 M),
(b): m-DCzPe([Cz]=1.3x10^{-4} M) - DMTP(0.07 M),
(c): PVCz(c)([Cz]=1.9x10^{-4} M) - DMTP(0.07 M).
The emission spectra were measured at 15, 25, 35, 45, 55, 65, and 75 ^{o}C.

one. The partially-overlapped and fully-overlapped exterplexes show a broad emission band around 510 nm and around 560 nm, respectively. The quantum yield of the exterplex emission for the partially-overlapped type is three times as large as that for the fully-overlapped one. Furthermore, since the quenching by DMTP of the Cz monomer excited state and the excimer state is essentially a diffusion-controlled process and the quenching efficiency is higher than 80 %, the yield of the exterplex formation should be nearly equal for the two types of exterplexes. Therefore, the difference in the quantum yield of the exterplex emission is considered to be due to that in the quantum efficiency of the exterplex emission; the quantum efficiency for the fully-overlapped exterplex is lower than that of the partially-overlapped one.

Since DCzPr has no methyl group in the main chain, it can take both the fully-overlapped and the partially-overlapped conformations. Nevertheless, the DCzPr - DMTP system selectively forms a fully-overlapped exterplex like the m-DCzPe system. This suggests that the fully-overlapped exterplex is stabler than the partially-overlapped one. The exterplex is considered to be stabilized through the delocalization of the charge produced by partial electron transfer from Cz chromophore to DMTP. Thus, this stabilization corresponds to that of the dimer radical cation in a polar solvent. As for the Cz dimer radical cation as described in Chapter 2, the fully-overlapped dimer radical cation is stabler than the partially-overlapped one. The larger the degree of overlap of the Cz chromophores, the stronger the stabilization by charge delocalization between the Cz chromophores. This was found to be the case also with the exterplex.

As for the temperature dependence of the exterplex

emission for the dimeric model compound systems, the decrease of the peak wavelength with increasing temperature is due to the decreasing dielectric constant of the solvent.

4-4-2. Exterplex of PVCz - DMTP System

As we have seen, both PVCz(c) and PVCz(r) show a broad emission at the same wavelength, around 510 nm, in spite of their difference in the syndiotactic fraction. By comparing with the case of the dimeric model compound systems as described previously, this broad emission was ascribed to the partially-overlapped exterplex, which is formed in the syndiotactic dyad. Since the partially-overlapped exterplex is formed by a small conformational change, the exterplex is easier to form than the fully-overlapped one. If the equilibrium between two types of exterplexes is not attained, their fractions are determined at the stage of the formation. Furthermore, since the quantum efficiency of the fully-overlapped exterplex is smaller than the partially-overlapped one, the former contribution to the emission spectra is smaller. Presumably this explains why both PVCz(r) and PVCz(c) give the partially-overlapped exterplex emission irrespective of the syndiotactic fraction. In this way, PVCz systems mainly show the partially-overlapped exterplex emission, though the fully-overlapped exterplex is stabler thermodynamically. With increasing temperature, the fraction of the stable fully-overlapped exterplex increases; consequently, the peak wavelength of the exterplex emission is shifted to longer wavelengths.

As for P(VCz-St) and PCzEMA, the emission spectra and the quantum efficiency of the exciplex emission suggest that these polymers form the same exciplex with DMTP as EtCz. That is, the exterplex of PVCz - DMTP systems is formed by neighboring

chromophore interaction and the interaction is weakened either by separating Cz chromophore from the main chain or by copolymerization with an inert comonomer.

References

1) H. Beens and A. Weller, Chem. Phys. Lett. 1968, 2, 140.

2) G. N. Taylor, E. A. Chandross and A. H. Schiebel, J. Am. Chem. Soc. 1974, 95, 2693.

3) J. Saltiel, D. E. Townsend, B. D. Watson and P. Shannon, Ibid. 1975, 97, 5688.

4) K. H. Grellmann and U. Suckow, Chem. Phys. Lett. 1975, 32, 250.

5) (a) T. Mimura and M. Itoh, J. Am. Chem. Soc. 1976, 98, 1095. (b) T. Mimura and M. Itoh, Bull. Chem. Soc. Jpn. 1977, 50, 1739.

6) (a) C. E. Hoyle and J. E. Guillet, Macromolecules 1978, 11, 221. (b) C. E. Hoyle and J. E. Guillet, ibid. 1979, 12, 956.

7) H. Masuhara, J. Vandendriessche, K. Demeyer, N. Boens and F. C. De Schryver, ibid. 1982, 15, 1471.

8) G. F. M. Hendrik, J. van Ramesdonk and J. W. Verhoeven, J. Am. Chem. Soc. 1984, 106, 1335.

9) F. Evers, K. Kobs, R. Memming and D. R. Terrell, ibid. 1983, 105, 5988.

10) T. Alfrey, Jr. and S. L. Kapur, J. Polym. Sci. 1949, 4, 215.

11) Y. Shirota, M. Yoshimura, A. Matsumoto and H. Mikawa, Macromolecules 1974, 7, 4.

12) S. Ito, K. Yamashita, M. Yamamoto and Y. Nishijima, Chem. Phys. Lett. 1985, 117, 171.

13) A. Itaya, K. Okamaoto and S. Kusabayashi, Bull. Chem. Soc. Jpn. 1976, 49, 2082.

14) G. E. Johnson, J. Chem. Phys. 1975, 62, 4697.

15) M. Yokoyama, T. Tamamura, M. Atsumi, M. Yoshimura, Y. Shirota and H. Mikawa, Macromolecules 1975, 8, 101.

CHAPTER 5

STERIC EFFECT ON FORMATION OF DIMER RADICAL CATION AND EXTERPLEX -- POLY(3,6-DI-tert-BUTYL-N-VINYLCARBAZOLE) AND ITS DIMERIC MODEL COMPOUNDS

5-1. Introduction

Ito et al.[1] studied the fluorescent behavior of poly(3,6-di-tert-butyl-N-vinylcarbazole) (PBVCz) and 2,4-bis(3,6-di-tert-butyl-N-carbazolyl)pentanes (BCzPe), the latter being a dimeric model compound of the former. Figure 5-1 shows the molecular structure of 3,6-di-tert-butylcarbazole. A tert-butyl group introduced in a carbazole (Cz) chromophore is very bulky as the figure implies (the shaded parts), and its steric hindrance should be very large. In both systems, therefore, the neighboring chromophore interaction in an excited state was found to be suppressed:[2-4] PBVCz gave only one kind of unstable excimer whose stability was even smaller than the second excimer formed by r-DCzPe. meso Isomer of BCzPe (m-BCzPe) gave no excimer, while racemic isomer of BCzPe (r-BCzPe) gave some excimer, but the excimer fraction was smaller than in r-DCzPe.

In this chapter, for these compounds having bulky tert-butyl groups in Cz chromophore, the transient absorption spectra of radical cations were measured in a polar solvent, and the fluorescent behavior of the DDA exterplex with DMTP

was investigated in a non-polar solvent. It will be discussed how the steric hindrance effects on the formation of a dimer radical cation and an exterplex.

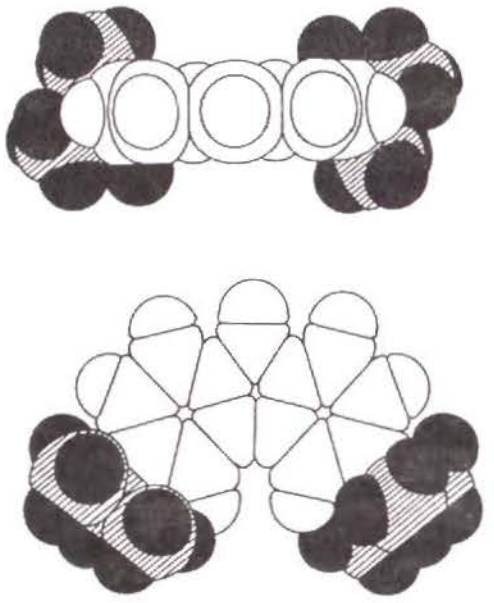

Figure 5-1. Molecular structure of 3,6-di-tert-butylcarbazole. Shaded parts show tert-butyl groups.

5-2. Experimental Section

5-2-1. Materials

3,6-Di-tert-butyl-N-vinylcarbazole (BVCz), 3,6-di-tert- butyl-N-ethylcarbazole (BEtCz), BCzPe, and BCzPr were synthesized from 3,6-di-tert-butylcarbazole (BCz) in the same way as for the corresponding carbazole compounds with no tert-butyl group. PBVCz with a molecular weight of ca. $1x10^6$ was obtained by a cationic polymerization of BVCz. The diastereoisomers, r- and m-BCzPe, were separated by liquid chromatography and were used as model compounds for syndiotactic and isotactic dyads,

respectively, in a PBVCz chain.

An electron acceptor, dimethyl terephthalate (DMTP, Wako Pure Chem. Ind.) was purified several times by recrystallization.

Acetonitrile (MeCN, Wako Pure Chem. Ind.) was distilled over P_2O_5 several times. Tetrahydrofuran (THF, Dotite Spectrosol) and toluene (Dotite Spectrosol) were used without further purification.

5-2-2. Transient Absorption Measurements

Transient absorption measurements were made by the excimer laser photolysis system. A 351-nm laser pulse of XeF excimer laser was used for excitation. Two kinds of detection systems were used; one equipped with a photomultiplier tube (Hamamatsu, R928) as a detector and the other equipped with a photovoltaic indium arsenide (InAs) diode (Hamamatsu, P838).

An electron donating chromophore, BCz, was excited selectively by the laser pulse in the presence of an electron acceptor, DMTP (0.05 M), and the transient absorption decays and spectra of the radical ions formed by a photoinduced electron transfer reaction were measured. The pulse intensity was attenuated properly by filters. The concentration of BCz chromophore was so adjusted as to give about a unit absorbance at 351 nm. THF was used as a solvent for the PBVCz system. Other systems were measured in MeCN. All samples were degassed by the freeze-pump-thaw method in a 1-cm quartz cell.

5-2-3. Fluorescent Measurements

The fluorescent properties of PBVCz and its model compounds were investigated in a non-polar solvent in the presence of DMTP (0.05 M). Fluorescent spectra were recorded with a Hitachi 850 spectrophotofluorometer. Fluorescent decay

and time-resolved fluorescent spectra were measured by a single photon counting method. The photo-excitation of BCz chromophore was made by a 322-nm pulse (fwhm ca. 75 ps) of a Spectra-Physics picosecond synchronously pumped, mode-locked, cavity-dumped dye laser (Models 2020, 342A, 375B, 344S). The concentration of BCz chromophore was so adjusted as to give about a unit absorbance at 322 nm. The PBVCz system was measured in THF. Other systems were measured in toluene. All samples were degassed by the freeze-pump-thaw method, and the measurements were carried out in a 1-cm quartz cell at 25 ^{o}C.

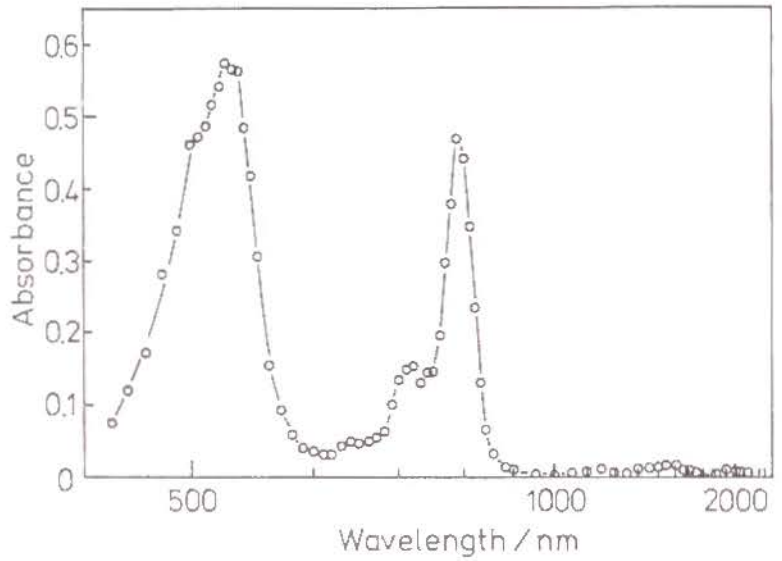

Figure 5-2. Transient absorption spectrum of BEtCz - DMTP (0.05M) system in MeCN at 25 ^{o}C at 1 μs after excitation. The absorbance of BEtCz at 351 nm is about unity.

5-3. Results and Discussion

5-3-1. Dimer Radical Cation Formation in Polar Solvent

Figure 5-2 shows the transient absorption spectrum of the BEtCz - DMTP system in MeCN at 25 ^{o}C at 1 μs after excitation.

The absorption band of the radical cation of BEtCz (BEtCz$^{+\cdot}$) appears at ca. 795 nm, and that of the radical anion of DMTP (DMTP$^{-\cdot}$) appears at ca. 530 nm.[6,7] No absorption was observed in the near-infrared region (1000 - 2000 nm). The monomer band of BEtCz$^{+\cdot}$ is similar in shape and in peak wavelength to that of the radical cation of N-ethylcarbazole (EtCz$^{+\cdot}$), as shown in Figure 2-1. Therefore, the tert-butyl group is considered to have little effect on the radical cationic state of Cz chromophore.

Figure 5-3 shows the transient absorption spectra of the dimeric model compound - DMTP systems in MeCN at 25 ^{o}C at 1 μs after excitation. Each system gives two absorption bands of the radical cation of BCz chromophore; one, the dimer band, appears in the visible wavelength region, and the other appears around 2000 nm. The former band is shifted to shorter wavelengths and is broader than that of BEtCz$^{+\cdot}$; the peak wavelengths are 760 nm for m-BCzPe (Figure 5-3-A), 750 nm for BCzPr (Figure 5-3-B) and 700 nm for r-BCzPe (Figure 5-3-C). The latter band is a CR band of the dimer radical cation formed intramolecularly. The CR band is shifted to shorter wavelengths, the peak wavelengths being >2100 nm for m-BCzPe (Figure 5-3-A), 2100 nm for BCzPr (Figure 5-3-B) and 2000 nm for r-BCzPe (Figure 5-3-C). Each dimeric model compound has no obvious absorption peak of the monomer radical cation (ca. 795 nm), despite the molar extinction coefficient (ε) of the monomer radical cation is larger than that of the dimer radical cation, as will be described later. This suggests that the contribution of the monomer radical cation can be neglected. The molar extinction coefficient (ε) of the dimer radical cation was estimated on the basis of that of DMTP$^{-\cdot}$ at 530 nm (ε = 12300)[6] by assuming that the concentration of the dimer radical cation is equal to that of

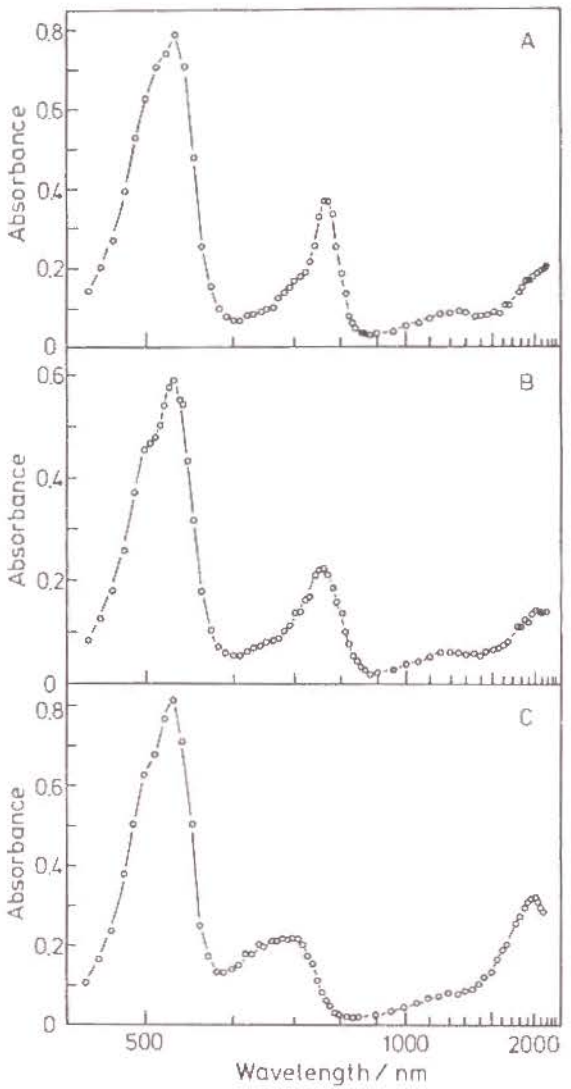

Figure 5-3. Transient absorption spectra of the dimeric model compound - DMTP (0.05M) systems in MeCN at 25 ^{o}C at 1 μs after excitation.
A: m-BCzPe, B: BCzPr, C: r-BCzPe.
The absorbance of BCz chromophore at 351 nm is about unity.

Table 5-I. Peak wavelengths (λ_{max}) and molar extinction coefficients (ε) of the visible dimer band and those of the CR band for the dimeric model compounds.

	λ_{max}/nm	ε	λ_{max}/nm	ε
BEtCz[a]	795	10500	--	--
m-BCzPe	760	6400	>2100	3700
BCzPr	750	4600	2100	3000
r-BCzPe	700	3900	2000	5400

[a] Value for the monomer radical cation.

DMTP. This assumption is justified since almost all the radical cations form the dimer radical cation. Table 5-I gives the peak wavelength (λ_{max}) and the molar extinction coefficient (ε) of the visible dimer band and the CR band.

Now, these dimer radical cations are compared with those for the dimeric model compounds having Cz chromophores without tert-butyl groups. The fully-overlapped dimer radical cation of m-DCzPe and the partially-overlapped one of r-DCzPe give the CR band around 1600 nm and 1800 nm, respectively. As described in Appendix, the CR band is more and more shifted to shorter wavelengths as the interaction increases. The CR bands of the dimer radical cation of BCz chromophore are shifted to longer wavelengths than those of the Cz chromophore. This means that the interaction in the dimer radical cation is weakened due to the steric hindrance imposed by tert-butyl groups. That is, the stabilization energy is less than 2 kcal/mol (0.1 eV), this figure

being estimated for the second dimer radical cation of r-DCzPe.

The transient absorption spectra of the visible dimer band were measured at 25 ^{o}C and 72 ^{o}C to observe the dissociation of the dimer radical cation to the monomer radical cation. These spectra were normalized by the absorbance of $DMTP^{\cdot-}$ at 530 nm.

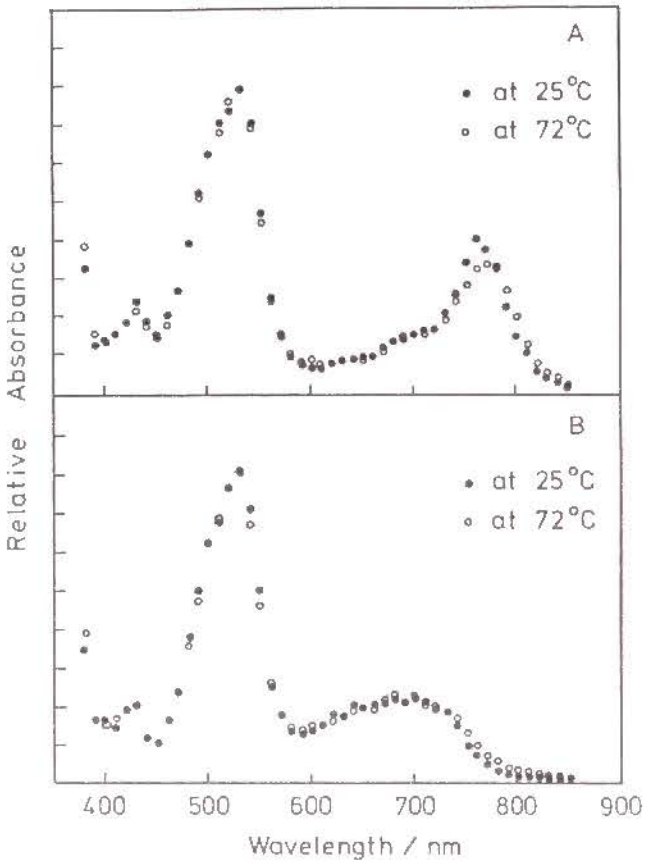

Figure 5-4. Temperature dependence of the visible dimer band of BCzPe - DMTP (0.05M) systems in MeCN at 1 μs after excitation.
A: m-BCzPe, B: r-BCzPe.
Filled and open circles indicate the spectra measured at 25 ^{o}C and 72 ^{o}C, respectively. These spectra are normalized by the absorbance of $DMTP^{\cdot-}$ at 530 nm.

Figures 5-4-A and B are for m-BCzPe and r-BCzPe, respectively. The visible dimer band gave no obvious change with increasing temperature in any system, even though the visible dimer band for m-BCzPe showed a small shift to a longer wavelength at 72 ^{o}C. Thus, the dimer radical cation scarcely dissociates into the monomer radical cation at 72 ^{o}C; the stabilization energy of the dimer radical cation is sufficiently large compared with the thermal energy.

The shift of the CR bands suggests that the interaction increases in the order: m-BCzPe$^{+\cdot}$ < BCzPr$^{+\cdot}$ < r-BCzPe$^{+\cdot}$. The increase of the interaction is accompanied by the shorter-wavelength shift and broadening (a decreasing of ε) of the visible dimer band and an increasing intensity, i.e., an increasing ε of the CR band. The difference in the interaction among the dimeric model compounds is associated to the configurational difference. In the racemic isomer of the pentane model, TT conformation is a stable one allowing an interaction between two chromophores. Then, r-BCzPe forms the dimer radical cation in the partially-overlapped conformation close to the TT conformation. This is the most stable of the three dimeric model compounds. On the other hand, m-BCzPe cannot form the dimer radical cation in the TT conformation (fully-overlapped conformation) because of the steric hindrance of tert-butyl groups in BCz chromophore. Presumably m-BCzPe also forms the partially-overlapped dimer radical cation. In order for m-BCzPe to form the partially-overlapped dimer radical cation, it must take a distorted conformation and hence this dimer radical cation is unstable as compared with that of r-BCzPe. Thus, all dimeric model compounds form the dimer radical cation assuming a partially-overlapped conformation, and the stability of the dimer radical cation is affected even by a

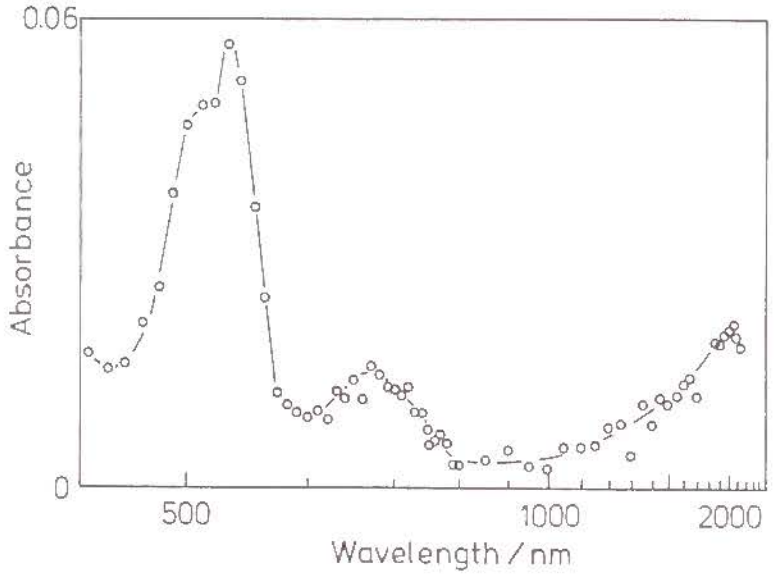

Figure 5-5. Transient absorption spectrum of PBVCz - DMTP (0.05M) system in THF at 25 ^{o}C at 1 μs after excitation. The absorbance of BCz chromophore is about unity.

small change in the dimer structure induced by the configurational difference.

Figure 5-5 shows the transient absorption spectrum of the PBVCz - DMTP system in THF at 25 ^{o}C at 1 μs after excitation. The absorbance of the spectrum was very small compared with that of the monomeric and the dimeric model compounds. This is partly due to the low quantum efficiency of ionization in THF which has a relatively low dielectric constant and partly due to S-S annihilation along the polymer chain. The radical cation formed in PBVCz was found to have two absorption bands; one is a very broad band around 700 nm and the other is the CR band around 2000 nm. This spectrum is similar to that of the r-BCzPe - DMTP system. This indicates that PBVCz forms the partially-overlapped dimer radical cation in the syndiotactic dyad, which corresponds to the racemic isomer of the pentane model. The

situation is very different from that of PVCz. The radical cation formed in PVCz is considered to interact with more than two neighboring chromophores and to be stabler than the dimer radical cation. By the introduction of tert-butyl groups to BCz chromophore, the interaction of more than two chromophores is hindered, and the dimer radical cation is formed in a polymer chain.

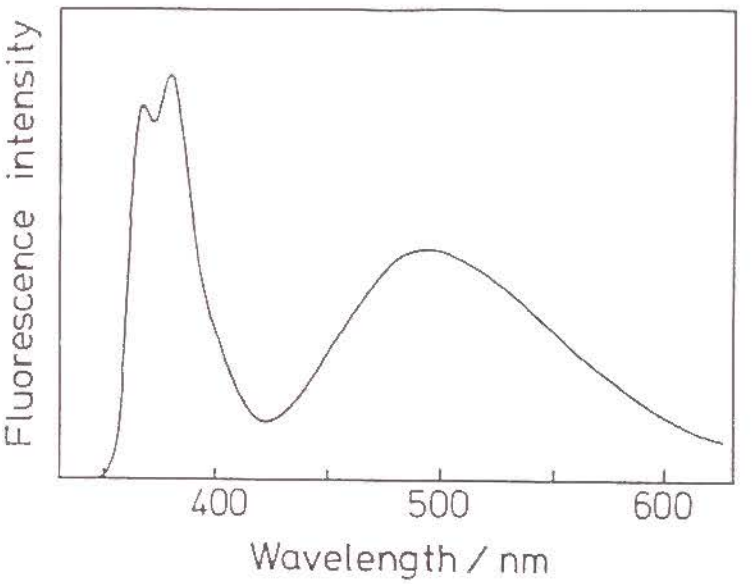

Figure 5-6. Emission spectrum of BEtCz - DMTP (0.05 M) in toluene at 25 ^{o}C. The absorbance of BEtCz at 322 nm is about unity.

5-3-2. Exterplex Formation in Non-polar Solvent

Figure 5-6 shows the emission spectrum of BEtCz - DMTP system in toluene. The exciplex emission was observed at ca. 495 nm as well as the monomer emission having a vibrational structure. This exciplex emission was somewhat shifted to longer wavelengths than that of EtCz - DMTP system at ca. 480 nm (Chapter 4). This is considered to be due to the effect of

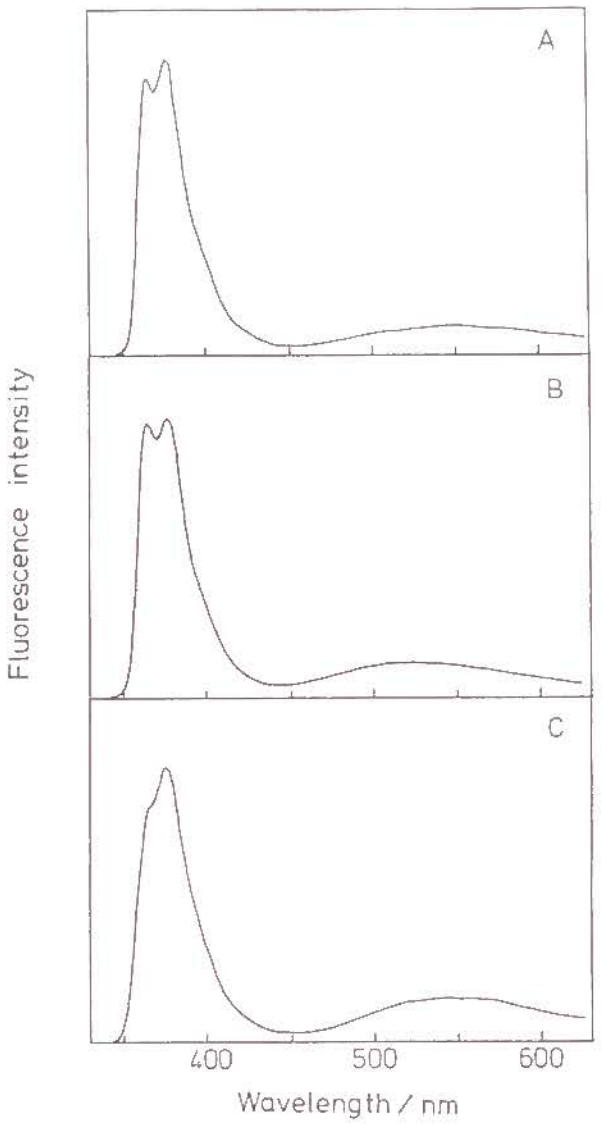

Figure 5-7. Emission spectra of the dimeric model compound - DMTP (0.05M) systems in toluene at 25 ^{o}C.
A: m-BCzPe, B: BCzPr, C: r-BCzPe.
The absorbance of BCz chromophore at 322 nm is about unity.

tert-butyl substitution. On the other hand, the dimeric model compounds show, as well as the monomer and/or the excimer emissions, a broad emission at the wavelength (ca. 540 nm) longer than the exciplex emission (Figure 5-7). This broad emission band was ascribed to the DDA exterplex which consists of two BCz chromophores and DMTP. Beens and Weller[8] estimated the stabilization energy (ΔG) of the charge-delocalization by neighboring chromophore interaction using the following equation.

$$\Delta E = \nu'_{max} - \nu''_{max} \qquad (5\text{-}1)$$

where ν'_{max} and ν''_{max} are the peak wavenumbers of DA exciplex emission and DDA exterplex emission, respectively. For all dimeric model compounds having BCz chromophores, the stabilization by the charge-delocalization was estimated to be ca. 0.21 eV. This is comparable to the stabilization energy (0.25 eV) of the partially-overlapped exterplex for r-DCzPe; that of the fully-overlapped exterplex for m-DCzPe was estimated to be ca. 0.42 eV. By the steric hindrance of tert-butyl groups, all BCz dimeric model compounds do not form the fully-overlapped exterplex but form the partially-overlapped one, which is not so stable as the partially-overlapped exterplex of r-DCzPe. It is noteworthy that m-BCzPe and BCzPr form the partially-overlapped exterplex, though they form no excimer.

By introducing tert-butyl groups, the formation scheme of exterplex becomes very simple, especially in the case of m-BCzPe and BCzPr. Scheme 5-I shows the formation process of exterplex for the m-BCzPe and BCzPr systems. Since they do not form any excimer, only the quenching of the monomer excited state by DMTP is taken into account. The monomer

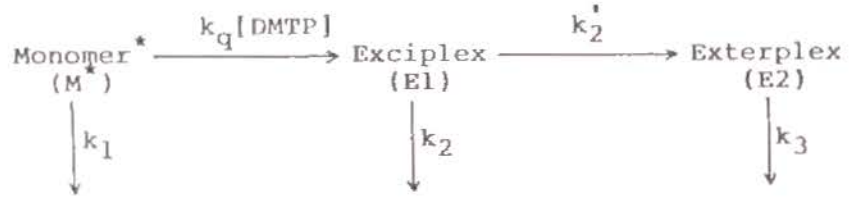

Scheme 5-I. Exterplex formation scheme for m-BCzPe and BCzPr systems.

excited state is quenched by DMTP with the rate constant, k_q, and forms the exciplex. The exciplex changes its conformation and forms the exterplex by neighboring chromophore interaction with the rate constant, k_2'. In this scheme, k_1, k_2 and k_3 are the rate constants of the deactivation processes which contain the fluorescent and radiationless transitions. The dissociation of the exciplex and the exterplex to the monomer excited state is neglected. The exciplex formation by quenching of the monomer excited state and the following exterplex formation were confirmed by the time-resolved emission spectra for the m-BCzPe system as shown in Figure 5-8. The solid line indicates the emission spectrum in the time range from 1.7 ns to 3.3 ns. Along with the monomer emission, a broad emission was observed in the longer wavelength region. To investigate what this broad band is assigned to, the monomer emission was subtracted from this spectrum by using the emission spectrum at t=0 as the monomer emission band. As shown by the broken line, the subtracted spectrum gives a broad emission band around 500 nm. This corresponds to the exciplex emission for the BEtCz - DMTP system. In the time range from 30 ns to 40 ns, the exterplex emission was observed around 540 nm as shown in the dash-dotted line in Figure 5-8. This suggests that the exciplex is mainly

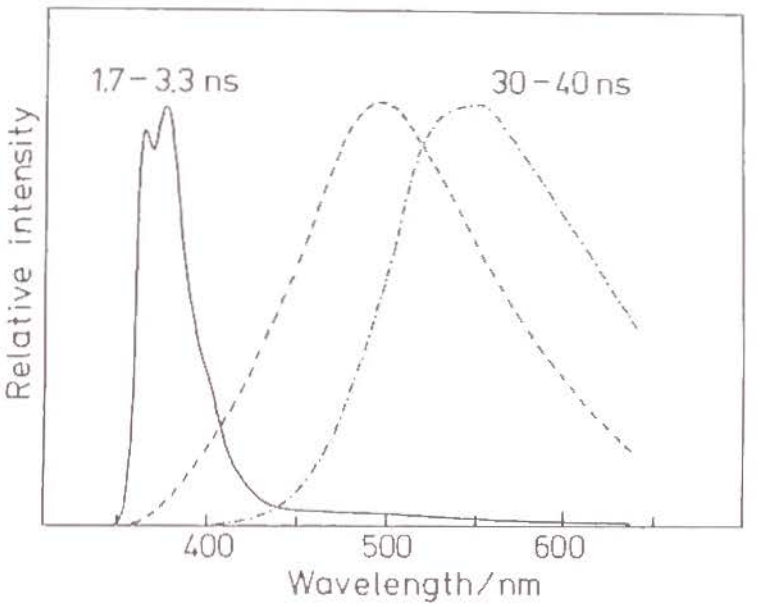

Figure 5-8. Time-resolved emission spectra of m-BCzPe - DMTP (0.05 M) system in toluene at 25 ^{o}C observed at 500 nm (a) and 640 nm (b).
The solid and dash-dotted lines show the emission spectra in the time range from 1.7 ns to 3.3 ns and from 30 ns to 40 ns, respectively. The broken line indicates the subtracted spectrum in the time range from 1.7 ns to 3.3 ns after subtracting the monomer emission.

formed in the earlier stage, and subsequently, the exterplex is formed. The time dependence of the emission spectrum for the BCzPr system was essentially the same as that for m-BCzPe.

According to this scheme, the rise and decay functions of the monomer excited state (M^*), the exciplex ($E1^*$), and the exterplex ($E2^*$) are expressed by the following equation.

$$[M^*] \propto \exp(-t/\tau_M) \qquad (5\text{-}2)$$

$$[E1^*] \propto -\exp(-t/\tau_M) + \exp(-t/\tau_{E1}) \qquad (5\text{-}3)$$

$$[E2^*] \propto T_1\exp(-t/\tau_M) - T_2\exp(-t/\tau_{E1}) + (T_2-T_1)\exp(-t/\tau_{E2}) \qquad (5\text{-}4)$$

$$T_1 = (\tau_M^{-1} - \tau_{E2}^{-1})^{-1},\ T_2 = (\tau_{E1}^{-1} - \tau_{E2}^{-1})^{-1}$$

where τ_M, τ_{E1}, and τ_{E2} are the lifetimes of the monomer excited state, the exciplex, and the exterplex, respectively.

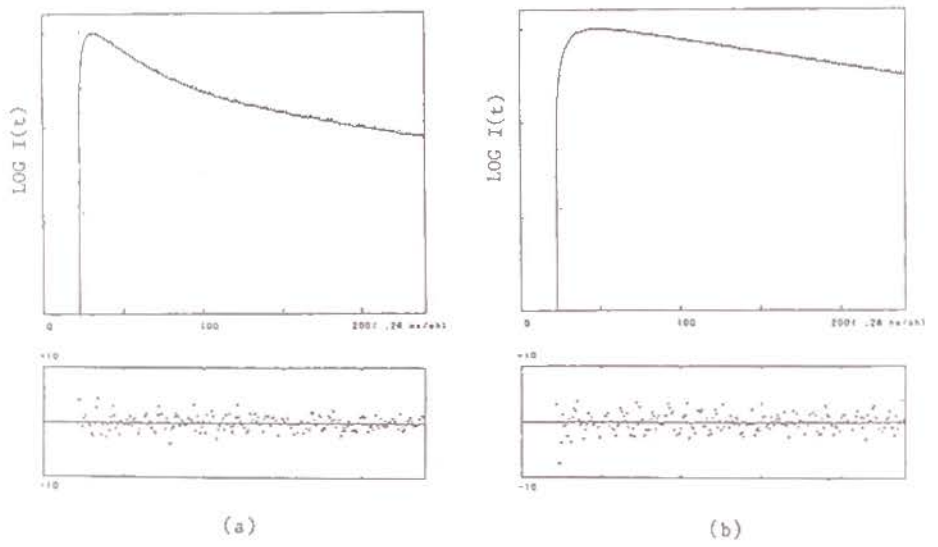

Figure 5-9. Rise and decay curves of fluorescence for m-BCzPe - DMTP (0.05 M) system in toluene at 25 ^{o}C.
The solid line indicates the simulation line by the three-exponential function.

Figures 5-9-(a) and (b) show the decay curves observed at 500 nm and at 640 nm, respectively. As a main component, the former decay curve contains the exciplex emission, and the latter, the exterplex emission. These decay curves were simulated by the three-exponential function as the sum of the exciplex (eq. 5-3) and the exterplex emission (eq. 5-4). The solid line shows a

simulation line. The best-fit three exponential functions are as follows.

$$I_{500}(t) = -0.848\exp(-t/0.96)+0.881\exp(-t/6.57) + 0.229\exp(-t/40.99) \qquad (5\text{-}5)$$

$$I_{640}(t) = -0.779\exp(-t/2.01)-0.075\exp(-t/6.57) + 0.966\exp(-t/40.99) \qquad (5\text{-}6)$$

Since the lifetime, τ_M, of the monomer excited state is nearly in the limit of measurability in this time range, the experimental error is large. Therefore, τ_M was determined by means of the decay curve at 365 nm, where the contribution of the exciplex and the exterplex emissions can be neglected. Thus, a τ_M value of ca. 1.8 ns was obtained. Then, τ_M, τ_{E1}, and τ_{E2} were evaluated to be 1.8 ns, 6.6 ns, and 41.0 ns, respectively.

For the BCzPr system, each lifetime was determined in the same way. The lifetime τ_M was determined to be 1.8 ns by the decay curve at 365 nm. Figures 5-10-(a) and (b) show the decay curves at 500 nm and at 640 nm for the BCzPr system, respectively. These decay curves were simulated by the three-exponential function, and the following functions were obtained.

$$I_{500}(t) = -0.917\exp(-t/0.90)+0.429\exp(-t/9.23) + 0.759\exp(-t/30.12) \qquad (5\text{-}7)$$

$$I_{640}(t) = -0.992\exp(-t/1.75)-0.200\exp(-t/9.23) + 1.329\exp(-t/30.12) \qquad (5\text{-}8)$$

For the BCzPr system, τ_M, τ_{E1}, and τ_{E2} were found to be 1.8 ns, 9.2 ns, and 30.1 ns, respectively.

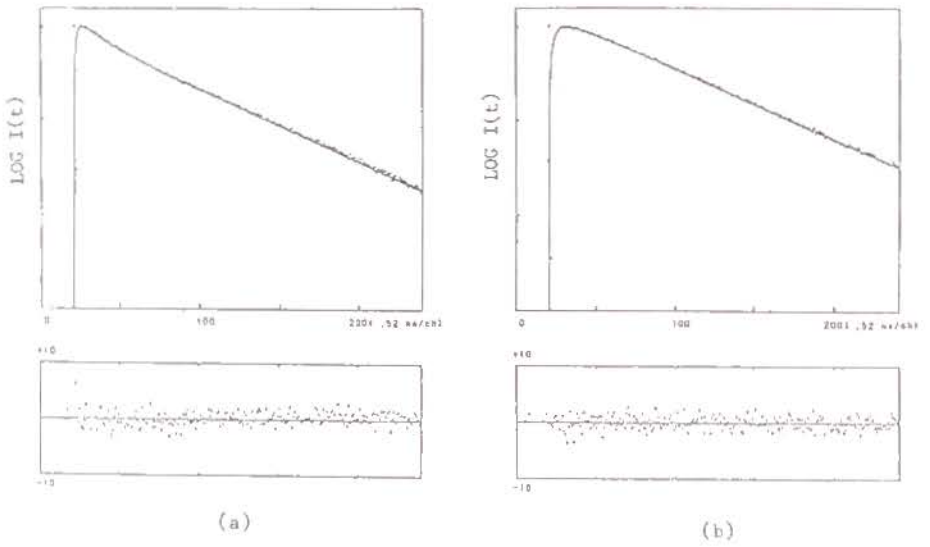

(a) (b)

Figure 5-10. Rise and decay curves of fluorescence for BCzPr - DMTP (0.05 M) system in toluene at 25 ^{o}C observed at 500 nm (a) and 640 nm (b).
The solid line indicates the simulation line by the three-exponential function.

On the other hand, this scheme cannot be applied to r-BCzPe system, since r-BCzPe forms the excimer. Therefore, Scheme 5-II was assumed. In this scheme, the equilibrium between the monomer excited state and the excimer is taken into account and is assumed to be reached much more rapidly than the other processes.[1] Since the quenchings of both the monomer excited state and the excimer by DMTP are considered to be diffusion-controlled,[9] the quenching rate constants (k_q) for both processes are assumed to be equal. The constant, k_1, k_2, k_3 and k_4 are the rate constants of deactivation processes of each excited state. In this case, the exterplex is formed in two processes; one is via the excimer and the other is via the exciplex. The rapid exterplex formation via the excimer was

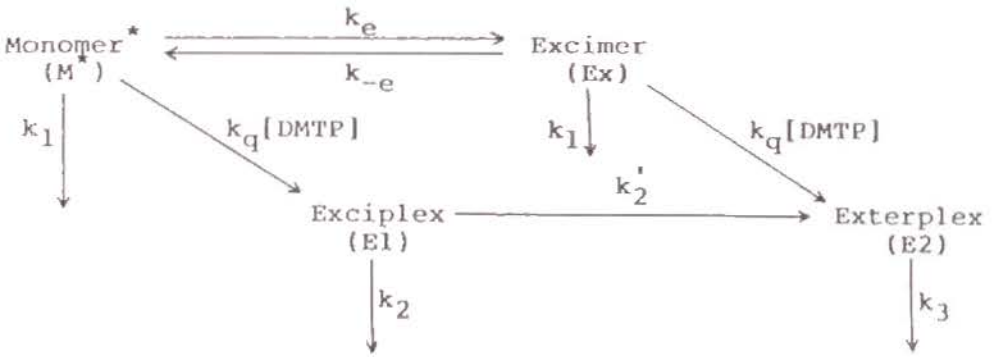

Scheme 5-II. Exterplex formation scheme for r-BCzPe system.

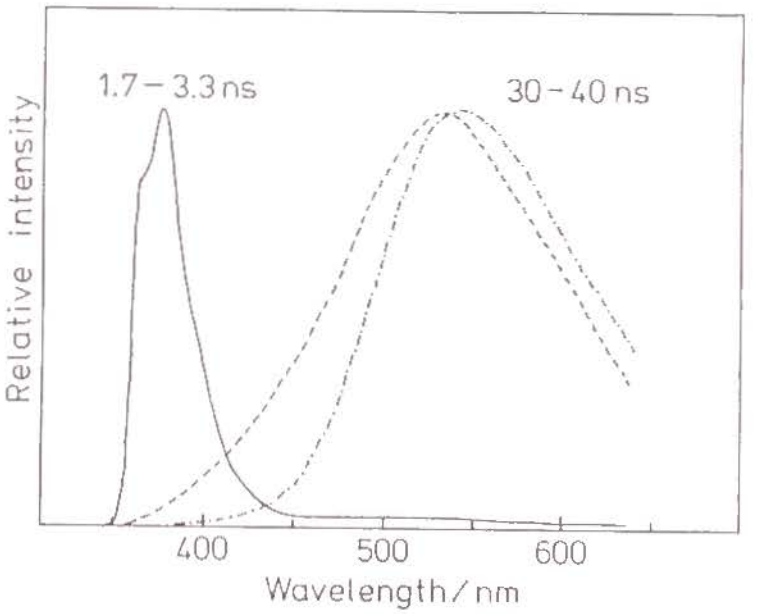

Figure 5-11. Time-resolved emission spectra of r-BCzPe - DMTP (0.05 M) system in toluene at 25 ^{o}C.
The solid and the dash-dotted lines show the emission spectra in the time range from 1.7 ns to 3.3 ns and from 30 ns to 40 ns, respectively. The broken line indicates the subtracted spectrum in the time range from 1.7 ns to 3.3 ns after subtracting the monomer and excimer emissions.

confirmed by the time-resolved emission spectra, as shown in Figure 5-11. The solid curve gives the emission spectrum in the time range from 1.7 ns to 3.3 ns. Along with the monomer and the excimer emissions, a broad emission band was observed in the longer wavelength region. The monomer and the excimer emissions were subtracted by using the emission spectrum at t=0. The subtracted spectrum is shown by the broken line. It is a broad emission around 540 nm, which was ascribed to the exterplex emission. This suggests that the exterplex is formed in the earlier stage in contrast to the cases of the m-BCzPe and BCzPr systems. In the later stage from 30 ns to 40 ns (the dash-dotted line), the relative intensity in the shorter wavelength region is decreased and that in the longer wavelength region is increased as compared with the subtracted spectrum in the time range from 1.7 ns to 3.3 ns. This indicates a slow exterplex formation process via the exciplex.

This exterplex formation scheme leads to the following rise and decay functions of the monomer excited state, the excimer, the exciplex, and the exterplex.

$$[M^*] \propto \exp(-t/\tau_M), \qquad [E^*] \propto \exp(-t/\tau_M) \tag{5-9}$$

$$[E1^*] \propto -\exp(-t/\tau_M) + \exp(-t/\tau_{E1}) \tag{5-10}$$

$$[E2^*] \propto (k_2'T_3-K^{-1})T_1\exp(-t/\tau_M) - k_2'T_2T_3\exp(-t/\tau_{E1}) + [k_2'T_3(T_2-T_1)+K^{-1}T_1]\exp(-t/\tau_{E2}) \tag{5-11}$$

$$T_1 = (\tau_M^{-1}-\tau_{E2}^{-1})^{-1},\ T_2 = (\tau_{E1}^{-1}-\tau_{E2}^{-1})^{-1},$$

$$T_3 = (\tau_M^{-1}-\tau_{E1}^{-1})^{-1},\ K = k_e/k_{-e}$$

where K is the equilibrium constant between the monomer excited state and the excimer. These equations are expressed by the

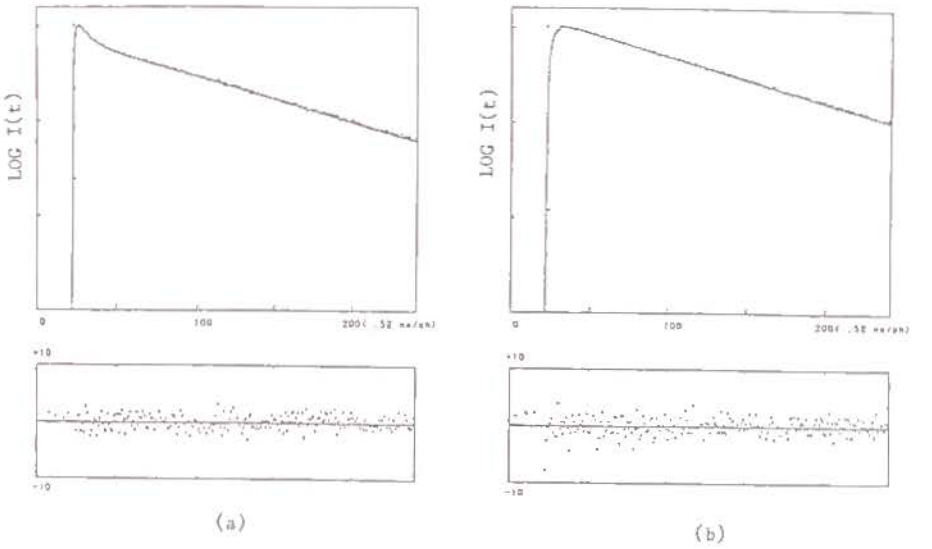

Figure 5-12. Rise and decay curves of fluorescence for r-BCzPe - DMTP (0.05 M) system in toluene at 25 ^{o}C observed at 500 nm (a) and 640 nm (b).
The solid line indicates the simulation line by the three-exponential function.

three exponential function using their lifetimes (τ_M, τ_{E1}, and τ_{E2}). Figures 5-12-(a) and (b) show the decay curves observed at 500 nm and at 640 nm, respectively. By simulating the decay curve using the three-exponential function, the following decay functions were obtained.

$$I_{500}(t) = -0.914\exp(-t/0.60)+0.590\exp(-t/3.76) +0.670\exp(-t/46.94) \tag{5-12}$$

$$I_{640}(t) = -0.963\exp(-t/1.55)-0.076\exp(-t/3.76) +1.146\exp(-t/46.94) \tag{5-13}$$

The lifetime, τ_M was determined to be 1.7 ns by analyzing the decay curve at 365 nm. In this way, τ_M, τ_{E1}, and τ_{E2} for r-

Table 5-II. Lifetimes of the monomer excited state (τ_M), the exciplex (τ_{E1}), and the exterplex (τ_{E2}), quenching rate constants (k_q), and exterplex-formation rate constants (k_2') for the dimeric model compound systems.

	τ_M/ns	τ_{E1}/ns	τ_{E2}/ns	$k_q/10^9 M^{-1}s^{-1}$	$k_2'/10^8 s^{-1}$
BEtCz	1.8	59.3	-	9.8	-
m-BCzPe	1.8	6.6	41.0	9.5	1.4
BCzPr	1.8	9.2	30.1	9.5	0.92
r-BCzPe	1.7	3.8	46.9	10.1	2.5

BCzPe were estimated to be 1.7 ns, 3.8 ns, and 46.9 ns, respectively.

The rate constant (k_q) of quenching by DMTP and the rate constant (k_2') of the exterplex formation from the exciplex were calculated by using the lifetimes according to each formation scheme. The results are listed in Table 5-II together with the lifetime data. The quenching rate constant is ca. $1x10^{10}$ $M^{-1}s^{-1}$ for all systems. The quenching process is an exothermic reaction enough to be diffusion-controlled. The rate constants k_2' decrease in the order; r-BCzPe > m-BCzPe > BCzPr. This is due to the difference between the ground state conformation and the exterplex one. r-BCzPe is considered to form the exterplex with the least conformational change of the three. The exterplex for r-BCzPe has the longest lifetime of the three. This suggests that r-BCzPe forms the most stable exterplex. These BCz dimeric model compounds do not form the fully-overlapped exterplex. Thus, r-BCzPe was found to have the most favorable configuration for forming the partially-overlapped exterplex.

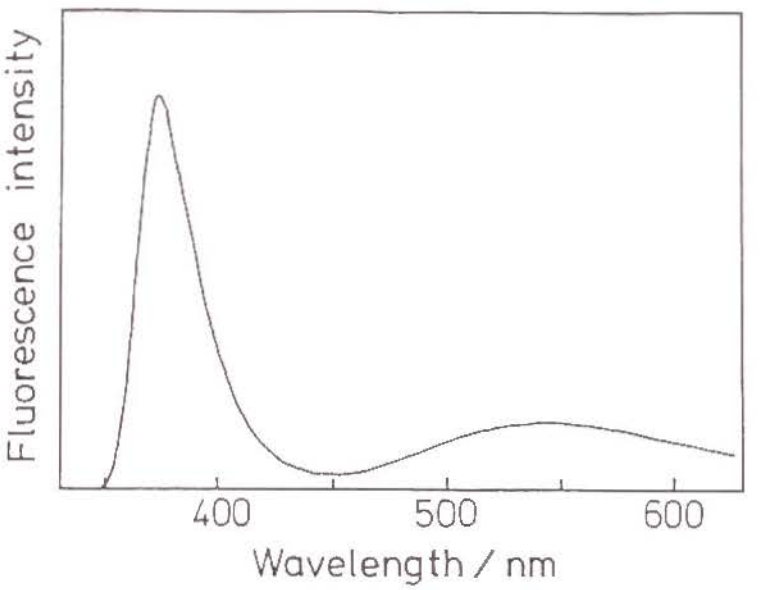

Figure 5-13. Emission spectrum of PBVCz - DMTP (0.05 M) in THF at 25 °C. The absorbance of PBVCz at 322 nm is about unity.

Figure 5-13 shows the emission spectrum of the PBVCz - DMTP system in toluene. As well as the monomer and the excimer emissions, a broad emission in the longer wavelength region was observed around 540 nm. This broad band is similar to the exterplex emission for the dimeric model compound systems described previously. PBVCz is also considered to form the partially-overlapped exterplex.

5-4. Conclusion

The dimeric model compounds having BCz chromophores form a partially-overlapped dimer radical cation in a polar solvent and a partially-overlapped exterplex in a non-polar solvent. Due to the steric hindrance of tert-butyl groups, the involved interactions somewhat are weakened compared with those involved

in the dimer radical cation and the exterplex of Cz chromophore. Among the dimeric model compounds, r-BCzPe was found to form the most stable dimer radical cation and exterplex. This suggests that r-BCzPe has the most favorable configuration for forming the partially-overlapped dimer radical cation and exterplex. The formation of the dimer radical cation and the exterplex was observed even in m-BCzPe and BCzPr which form no excimer. This means two things: the conformational requirement for the stabilization by the charge-delocalization leading to the formation of the dimer radical cation and the exterplex is not so strict as in the case of the excimer, and the stabilization energy by the charge-delocalization is larger than that of the excimer. As for the radical cation formed in PBVCz, the interaction among more than two chromophores is hindered by the steric effect in contrast to the case of PVCz, and the formation of the same partially-overlapped dimer radical cation as in r-BCzPe system was observed.

References

1) S. Ito, K. Takami and M. Yamamoto, Makromol. Chem., Rapid Commun. 1989, 10, 79.

2) A. Itaya, K. Okamoto and S. Kusabayashi, Bull. Chem. Soc. Jpn. 1976, 49, 2082.

3) (a) F. C. De Schryver, J. Vandendriessche, S. Toppet, K. Demeyer and N. Boens, Macromolecules 1982, 15, 406. (b) J. Vandendriessche, P. Palmans, S. Toppet, N. Boens, F. C. De Schryver and H. Masuhara, J. Am. Chem. Soc. 1984, 106, 8057.

4) F. Evers, K. Kobs, R. Memming and D. R. Terrell, J. Am. Chem. Soc. 1983, 105, 5988.

5) N. P. Buu-Hoi and P. Cagniant, Ber. 1944, 77, 121.

6) A. Tsuchida, M. Yamamoto and Y. Nishijima, J. Phys. Chem. 1984, 88, 5062.

7) U. Lachish, R. W. Anderson and D. J. Williams, Macromolecules 1980, 13, 1143.

8) H. Beens and A. Weller, Chem. Phys. Lett. 1968, 2, 140.

9) D. Rehm and A. Weller, Israel J. Chem. 1970, 8, 259.

PART II

STABILITY OF RADICAL IONS OF VARIOUS CHROMOPHORES

CHAPTER 6

STRUCTURE AND STABILITY OF NAPHTHALENE DIMER RADICAL CATIONS

6-1. Introduction

A number of studies have been made on the dimer radical cations of naphthalene and its derivatives.[1-10] Lewis and Singer[1] detected an intermolecular dimer radical cation of naphthalene by ESR. Badger et al.[3] observed its charge-resonance (CR) band at 77 K by warming a γ-ray irradiated glassy matrix. By theoretical consideration, Badger and Brocklehurst[4] suggested the structure of the naphthalene intermolecular dimer radical cation to be "distorted". Irie et al.,[9] who recently carried out pulse radiolysis experiments, proposed two possible structures for the dimer radical cation of 1,3-di(2-naphthyl)propane (22DNP); a fully-overlapped and a partially-overlapped conformations.[9]

In this chapter, transient absorption bands of the naphthalene dimer radical cations were measured by laser photolysis for 22DNP, 1-(1-naphthyl)-3-(2-naphthyl)propane (12DNP) and 1,3-di(1-naphthyl)propane (11DNP), and the stabilities of these dimer radical cations were discussed in relation to their conformations or the degree of overlapping of the naphthyl groups. Each dimeric model compound with two naphthyl groups, which are unsymmetrical about the bond axis with the methylene

chain, can take two sandwich conformations, as shown in Figure 6-1. Both 22DNP and 11DNP can take a partially-overlapped and a fully-overlapped conformations, while 12DNP can take two conformations of partially-overlapped type only. Thus, it was possible to photochemically characterize the partially-overlapped and fully-overlapped conformations by using the transient absorption bands for 12DNP as reference. Here, the naphthalene radical cations formed in polymers of poly(1-

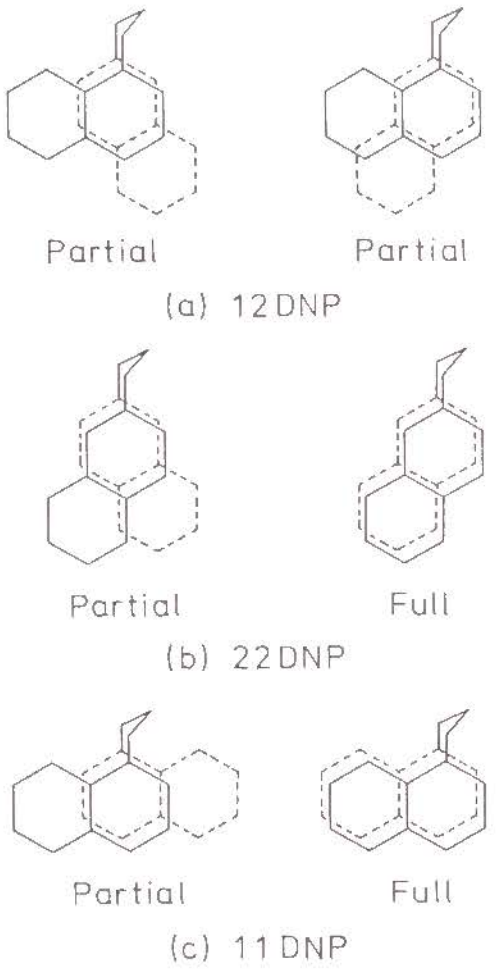

Figure 6-1. Overlapped conformations of dinaphthylpropanes: (a) 12DNP; (b) 22DNP; (c) 11DNP.

vinylnaphthalene) (P1VN) and poly(2-vinylnaphthalene) (P2VN) were studied as compared with the dimer radical cations.

6-2. Experimental Section

6-2-1. Materials

Naphthalene (Np, Wako Pure Chem. Ind.) was purified by recrystallizing it from ether three times. 1-Ethylnaphthalene (1-EN, Tokyo Kasei Kogyo Co.) and 2-ethylnaphthalene (2-EN, Tokyo Kasei Kogyo Co.) were purified by distillation under reduced pressure. 11DNP, 22DNP and 12DNP were synthesized according to the procedure of Chandross and Dempster,[11] and purified by silica-gel column chromatography and recrystallization. P1VN was prepared by radical polymerization of 1-vinylnaphthalene initiated by α,α'-azobisisobutyronitrile in benzene. P2VN was prepared by anionic polymerization of 2-vinylnaphthalene initiated by n-butyllithium in tetrahydrofuran. These polymers were purified by three-fold precipitation, and the molecular weight was determined to be 4×10^3 for P1VN and 9×10^3 for P2VN by GPC (Toyo Soda HLC 802UR) with a GMH and a G4000H columns. 1-Vinylnaphthalene and 2-vinylnaphthalene were synthesized from 1-bromonaphthalene (Wako Pure Chem. Ind.) and 2-acetonaphthone (Wako Pure Chem. Ind.), respectively.

An electron acceptor, 1,2-dicyanobenzene (o-DCNB, Wako Pure Chem. Ind.) was purified by three-fold recrystallization. Triethylamine (TEA, Wako Pure Chem. Ind.) was purified by distillation. TEA was used as a radical cation acceptor in the radical cation transfer experiments.

Acetonitrile (MeCN, Wako Pure Chem. Ind.) was purified by refluxing over P_2O_5 and subsequent distillation. Spectroscopic grade of N,N-dimethylformamide (DMF, Dotite Spectrosol) was used

without further purification.

6-2-2. Measurements

Transient absorption was measured on an excimer laser photolysis system equipped with a XeCl excimer laser (308 nm). Two detection systems were used; one was a photomultiplier system for measurements in the visible region, and the other was a photovoltaic indium arsenide (InAs) diode system for measurements in the visible and near-infrared regions. The concentration of naphthyl chromophore was adjusted so that the absorbance became ca. unity at 308 nm. An electron acceptor, o-DCNB (1.0×10^{-1} M) was added to the sample, and the solution was degassed by the freeze-pump-thaw method. DMF was used as a solvent for polymer systems, and MeCN was used for other systems. The measurements were made in a 1-cm quartz cell at 298 K. For the radical cation transfer experiments, TEA was added to the above system as a radical cation acceptor.

The absorption spectra were obtained with a UV-200S spectrophotometer (Shimadzu).

6-3. Results and Discussion

Figure 6-2-(a) shows the transient absorption spectrum for the Np - o-DCNB system at 900 ns after excitation. Np forms a dimer radical cation intermolecularly, which is in equilibrium with the monomer radical cation. In the spectrum, a visible dimer band at ca. 570 nm and a CR band at ca. 1100 nm were observed along with the monomer bands at ca. 620 nm and ca. 680 nm. The absorption below 450 nm is due to the triplet state of Np. The CR band at ca. 1100 nm corresponds to the one at 1030 - 1040 nm[3,7,8] observed at 77 K by warming the γ-ray

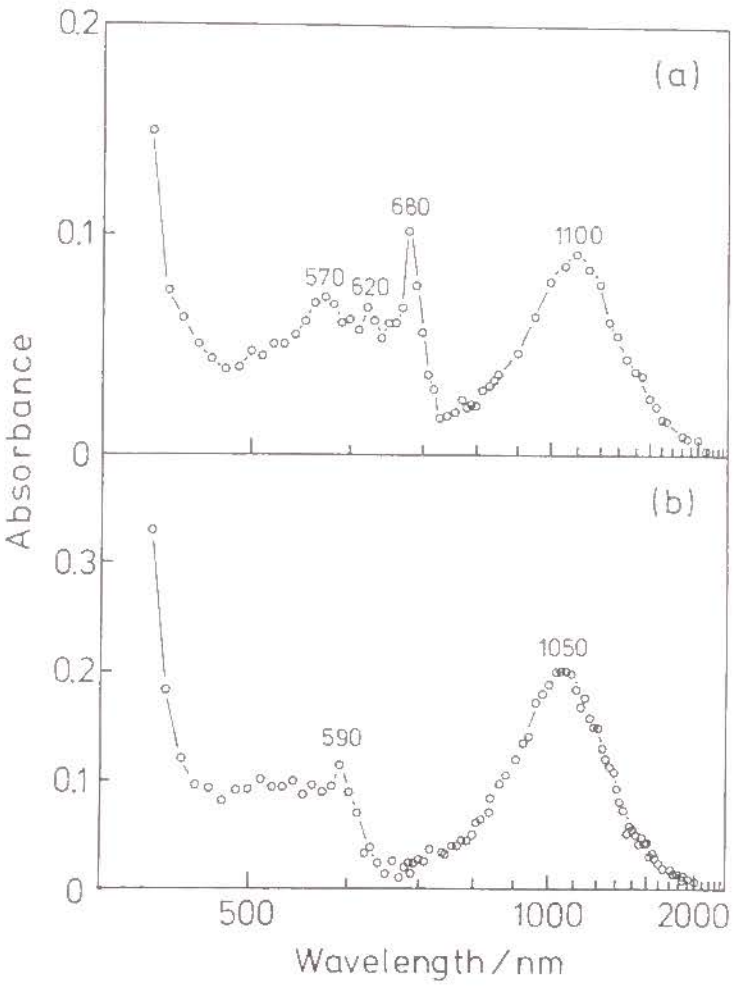

Figure 6-2. Transient absorption spectra of radical cations with o-DCNB (0.1M) at 900 ns after excitation in MeCN at 298 K: (a) Np (5.9×10^{-3}M); (b) 12DNP (1.0×10^{-3}M).

irradiated glassy matrix. The difference in the experimental conditions has caused the small shift of the peak. This means that by warming the glassy matrix, Np is allowed to diffuse enough to form a stable dimer radical cation as in solution. A comparison with the transient absorption spectrum for 12DNP as will be described later suggests that this intermolecular dimer radical cation has a partially-overlapped structure (a partially-

overlapped dimer radical cation). This is consistent with the structure proposed by Badger and Brocklehurst.[4)]

Figure 6-2-(b) shows the transient absorption spectrum of the dimer radical cation of 12DNP at 900 ns after excitation. There was no absorption band of the monomer radical cation, but only the dimer radical cation was observed. The dimer radical cation is formed intramolecularly. Two dimer bands were observed; one is a visible dimer band at ca. 590 nm, and the other is a CR band at ca. 1050 nm. These bands correspond to the dimer bands at 570 nm and 1100 nm for the intermolecular dimer radical cation of Np. The RIS model (Figure 6-1-(a)) suggests that 12DNP can take only the partially-overlapped conformation but not the fully-overlapped one. Therefore, these bands were assigned to the intramolecular partially-overlapped dimer radical cation. This suggests that Np which shows the same transient absorption spectrum as 12DNP also forms a partially-overlapped dimer radical cation intermolecularly.

Figure 6-3-(a) shows the transient absorption spectrum for the 2-EN - o-DCNB system at 900 ns after excitation. A shoulder around 570 nm, which was observed along with monomer bands at ca. 620 nm and at ca. 680 nm, was ascribed to the partially-overlapped dimer radical cation formed intermolecularly. This is confirmed by the fact that 2-EN gives the same CR band at ca. 1100 nm as Np. There was little effect of the 2-position substituent on transient absorption bands.

Figure 6-3-(b) shows the transient absorption spectrum of the dimer radical cation of 22DNP at 900 ns after excitation. Two visible dimer bands (ca. 580 nm and ca. 660 nm) appear. The former is ascribed to the intramolecular partially-overlapped dimer radical cation. 22DNP can take both the partially-

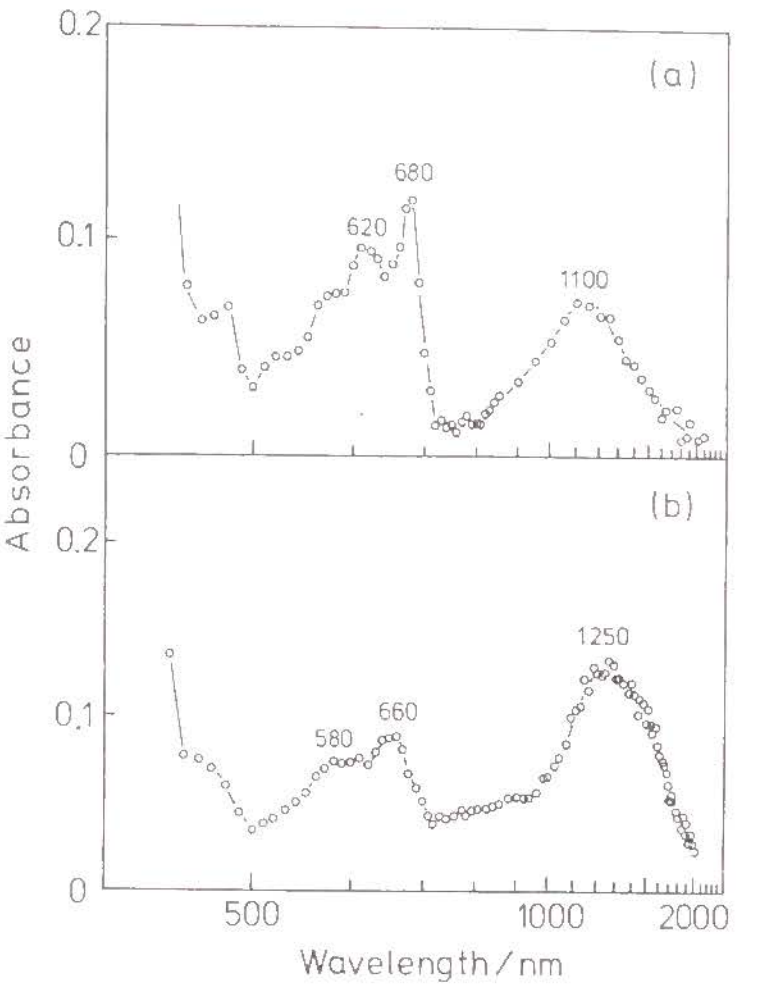

Figure 6-3. Transient absorption spectra of radical cations with o-DCNB (0.1M) at 900 ns after excitation in MeCN at 298 K: (a) 2-EN (2.9×10^{-3}M); (b) 22DNP (8.3×10^{-4}M).

overlapped and fully-overlapped conformations. At present, it is considered that the latter is due to the dimer radical cation having a fully-overlapped conformation. That is, 22DNP forms both partially-overlapped and fully-overlapped dimer radical cations. The superposed CR band of these dimer radical cations was observed at ca. 1250 nm. In the ground state, 22DNP takes the open form in which two naphthyl groups is far apart from

each other owing to a steric repulsion. If a naphthyl group is photoexcited, a naphthalene radical cation is formed by an electron transfer to o-DCNB. Though the formation of the intramolecular excimer is generally a competitive process, the electron-transfer quenching is a main process at this high concentration condition ([o-DCNB]=1.0x10^{-2} M).[16] The naphthalene radical cation with the open form, thus produced in 22DNP, interacts with the neighboring chromophore and forms the dimer radical cation. Here, there are two kinds of dimer radical cations depending on the direction of naphthyl groups approaching each other.

Transient absorption spectra of the radical cation of 22DNP were measured at 25 ^{o}C and 72 ^{o}C at 500 ns after excitation. These spectra were almost the same, and no dissociation of the dimer radical cation to the monomer radical cation was observed. This means that the stabilization energy of the dimer radical cation is sufficiently large compared with the thermal energy at 72 ^{o}C (kT = ca. 0.3 eV). Though the partially-overlapped dimer radical cation is expected to be much more stabilized than the fully-overlapped one as will be described below, 22DNP forms both types of dimer radical cations. The reason may be as follows: the conformational change of the dimer radical cation (the partially-overlapped versus fully-overlapped ones) may pass through the monomer radical cation state, but the dimer radical cation scarcely dissociates to the monomer radical cation at 25 ^{o}C owing to the sufficient stabilization energy. Then, the thermodynamic equilibrium between the two conformations is not achieved, and the fraction of these dimer radical cation is determined by the direction of naphthyl groups at the stage of initial formation.

Figure 6-4-(a) shows the transient absorption spectrum for the 1-EN - o-DCNB system at 900 ns after excitation. The monomer bands were observed at ca. 650 nm and ca. 700 nm, which are shifted to longer wavelengths than those of Np and 2-EN. This is considered to be due to a 1-substituted effect. No observable visible dimer band is detectable, while a CR band is observable at ca. 1200 nm. The CR band is also shifted to

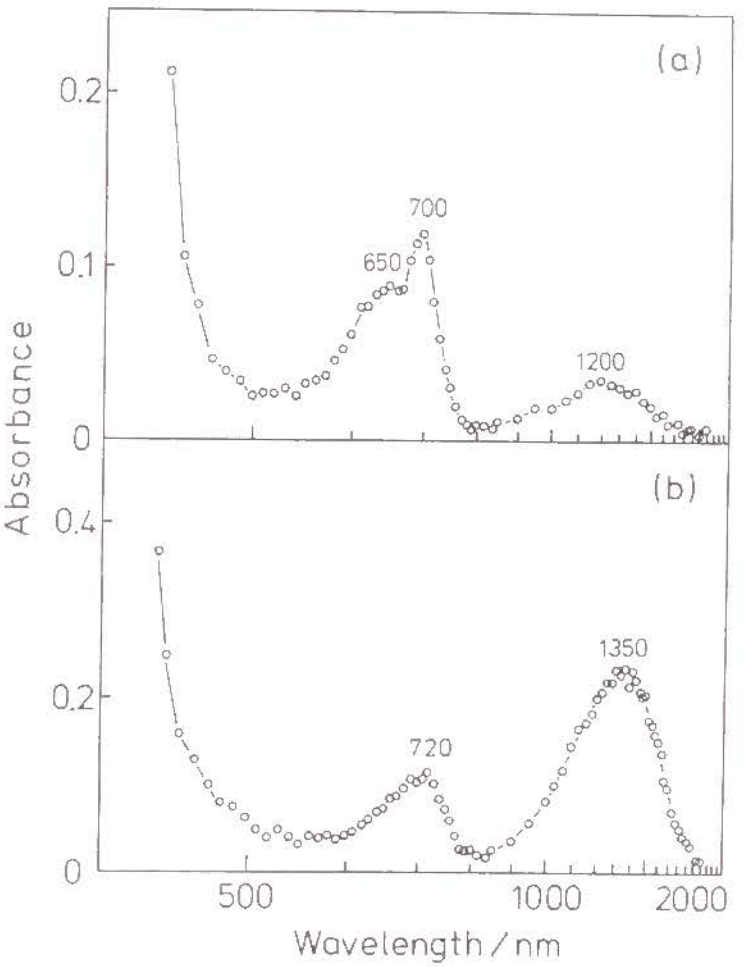

Figure 6-4. Transient absorption spectra of radical cations with o-DCNB (0.1M) at 900 ns after excitation in MeCN at 298 K: (a) 1-EN (1.6x10^{-3}M); (b) 11DNP (8.4x10^{-4}M).

longer wavelengths than those of the partially-overlapped dimer radical cations of Np and 2-EN. Because 1-EN shows the substitution effect, and the intermolecular dimer radical cations of Np and 2-EN are of partially-overlapped type, it is deduced that 1-EN may also form a partially-overlapped dimer radical cation intermolecularly.

Figure 6-4-(b) shows the transient absorption spectrum of the dimer radical cation of 11DNP at 900 ns after excitation. On the analogy of other dimeric model compounds, it is considered that 11DNP preferentially forms an intramolecular dimer radical cation. A visible dimer band and a CR band appear at ca. 720 nm and ca. 1350 nm, respectively. These bands are shifted to longer wavelengths than those for 22DNP, due to the substitution effect. The CR band is also shifted to longer wavelengths than those of the intermolecular partially-overlapped dimer radical cation of 1-EN. Like 22DNP, 11DNP also forms a partially-overlapped and a fully-overlapped dimer radical cation.

The peak wavelength (λ_{CR}) of the CR band and the stabilization energy (DH) estimated from half of the band gap are summarized in Table 6-I. The monomeric model compounds (Np, 1-EN, 2-EN) and 12DNP form the partially-overlapped dimer radical cation. The CR band of the partially-overlapped dimer radical cation except 1-EN appears at 1050 - 1100 nm with estimated stabilization energy of 0.56 - 0.59 eV. In contrast, 22DNP and 11DNP give a CR band shifted to longer wavelengths. The observed CR band is a superposition of the CR bands of the partially-overlapped and fully-overlapped dimer radical cations. Therefore, the fully-overlapped dimer radical cation should have its CR band at a wavelength longer than 1250 nm, and its stabilization energy (ΔH) should be less than 0.50 eV. This means that the partially-overlapped dimer radical cation is stabler

Table 6-I. Peak wavelength (λ_{CR}) of CR band and stabilization energy (ΔH) estimated by half of the band gap.

	λ_{CR}/nm	ΔH/eV
Np	1100	0.56
2-EN	1100	0.56
1-EN	1200	0.52
12DNP	1050	0.59
22DNP	1250	0.50
11DNP	1350	0.46

than the fully-overlapped one.

To obtain direct information on the stability of the dimer radical cation, the rate constant of radical cation transfer to TEA was measured. Figure 6-5 shows the results. The measured transient absorption decay of the dimer radical cation in the visible dimer band is shown by the dotted line. Figure 6-5-(a), (b), and (c) show the absorbances for 12DNP (590 nm), 22DNP (660 nm), and 11DNP (720 nm), respectively. For 22DNP and 11DNP, the contribution of the partially-overlapped dimer radical cation is negligible at the measured wavelengths, the absorption being predominated by the fully-overlapped dimer radical cation. In the absence of TEA, the dimer radical cation decays by recombination with the radical anion, o-DCNB$^{\cdot-}$, giving a slower decay curve (curve 1). The recombination with o-DCNB$^{\cdot-}$ is exothermic enough to allow us to assume it to be a diffusion-controlled process, so the rate constant of recombination was assumed to be the diffusion-controlled value, 1.7×10^{10} $M^{-1}s^{-1}$. When the radical cation acceptor, TEA , was added, the decay of the dimer radical

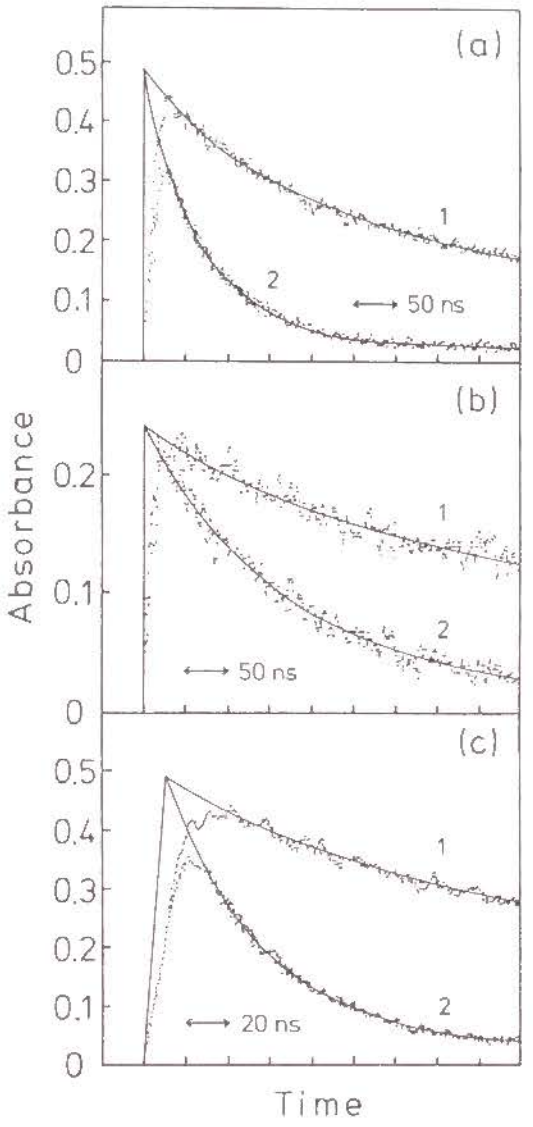

Figure 6-5. Transient absorption decay of dimer radical cation without TEA (curve 1) and with TEA (curve 2): (a) the decay curve at 590 nm for 12DNP (1.0×10^{-3}M); (b) the decay curve at 660 nm for 22DNP (8.3×10^{-4}M); (c) the decay curve at 720 nm for 11DNP (8.4×10^{-3}M).
As for the concentration of TEA, see Table 6-II. The solid line indicates the simulation line for the radical cation transfer.

Table 6-II. Molar extinction coefficient (ε) at the measured wavelength (λ) and rate constant (k_{tr}) of the radical cation transfer to TEA.

	[TEA]/10^{-3}M	λ/nm	ε	$k_{tr}/10^{9}M^{-1}s^{-1}$
12DNP	6.0	590	2000	1.8
22DNP	1.1	660	1950	3.5
11DNP	6.0	720	1750	2.9

cation was accelerated by the radical cation transfer to TEA, as shown by curve 2. These decay curves were simulated by using eq. 4 - 6 in Appendix, and the rate constant (k_{tr}) of the radical cation transfer and the molar extinction coefficient (ε) at this wavelength were determined. Curve 1 was simulated as $[D_2]=0$. Despite a sufficient amount of TEA was added, the absorbance did not vanish completely with a small absorption remaining. Because TEA^{+} has no absorption at this wavelength, this small residual absorption is considered to be due to a by-product. This contribution being minor in any case, the absorbance was subtracted from curve 2 on simulation. The simulation lines are given by the solid curves. The relevant parameter values, the concentrations of TEA and the wavelengths of measurements are listed in Table 6-II. The rate constant k_{tr} of the partially-overlapped dimer radical cation is ca. 1.8×10^{9} $M^{-1}s^{-1}$, while k_{tr} of the fully-overlapped dimer radical cation is ca. 3.5×10^{9} $M^{-1}s^{-1}$ for 22DNP and 2.9×10^{9} $M^{-1}s^{-1}$ for 11DNP. Hence, k_{tr} of the partially-overlapped dimer radical cation is smaller than that of the fully-overlapped one, the former being stabler than the latter. This is consistent with their stabilities estimated by

the CR band.

Furthermore, this result is supported by the fact that Np, 1-EN and 2-EN, which can take both the partially-overlapped and fully-overlapped conformations intermolecularly, preferentially form the partially-overlapped dimer radical cation. The instability of the fully-overlapped form is due to a large repulsion force. Badger and Brocklehurst predicted a distorted structure as a stable conformation of Np dimer radical cation.

Transient absorption spectra of the radical cations formed in P1VN and in P2VN were measured to investigate the neighboring chromophore interaction in the polymer chains. Figures 6-(a) and (b) show the spectra for P2VN and for P1VN in DMF at 900 ns after excitation, respectively. P2VN gave a visible dimer band at ca. 660 nm and a CR band at ca. 1300 nm. The CR band is red-shifted by ca. 50 nm from that of the dimeric model compound, 22DNP, and the ratio of the absorbance of the CR band to that of the visible dimer band in P2VN is larger than that in 22DNP. As for the trimer radical cation stabilized by the charge resonance among three chromophores, the CR band energy should be $2^{-1/2}$ times that of the dimer radical cation, according to the Hückel MO theory;[3] the CR band for a naphthalene trimer radical cation should appear in a longer wavelength region than 1500 nm. Therefore, the visible dimer band and the CR band are essentially the same as those for 22DNP. A similar result was obtained for P1VN. P1VN gave a visible dimer band at 700 - 750 nm and a CR band at ca. 1400 nm. These bands appear at almost the same wavelengths as those for the dimeric model compound, 11DNP. This means that in the polymer chain the dimer radical cation is formed between two neighboring chromophores and that the neighboring chromophore interaction in the polymer chain can be well described by the

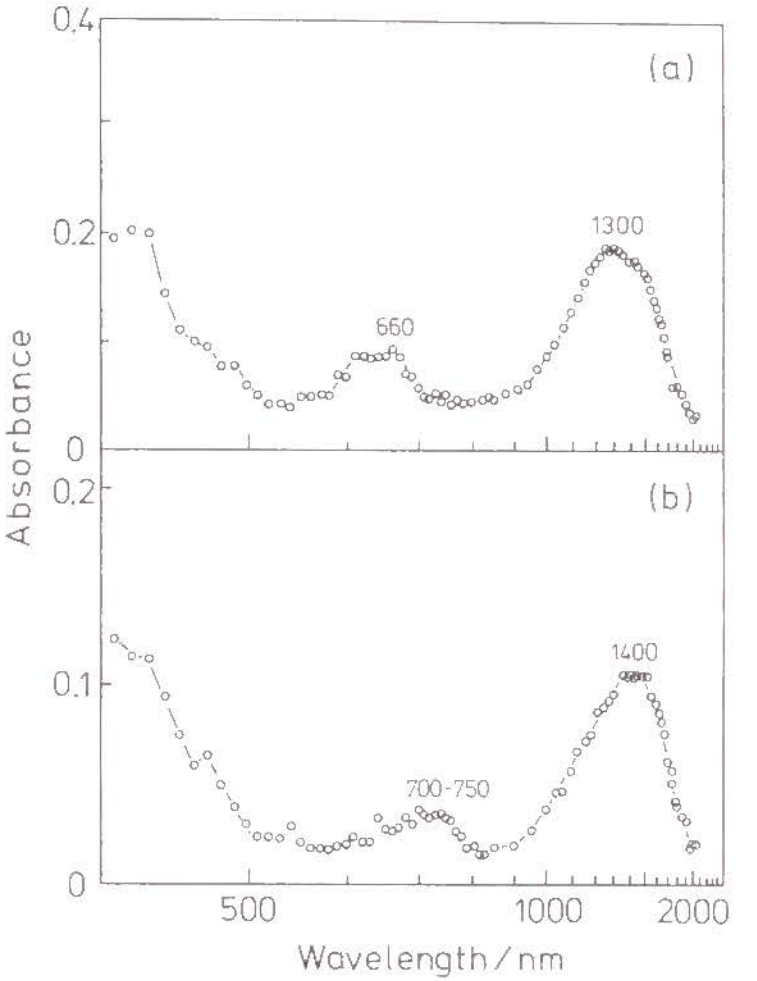

Figure 6-6. Transient absorption spectra of radical cations with o-DCNB (0.1M) at 900 ns after excitation in DMF at 298 K: (a) P2VN; (b) P1VN.
The concentration of naphthyl chromophore is 3.0×10^{-3}M for P2VN and 1.6×10^{-3}M for P1VN.

dimer model. This contrasts to the fact that poly(N-vinylcarbazole) (PVCz) shows the CR band shifted to longer wavelengths than the dimer radical cation and that the radical cation in PVCz is stabilized by the neighboring chromophore interaction among more than two chromophores.

References

1) I. C. Lewis and L. S. Singer, J. Chem. Phys. 1965, 43, 2712.

2) (a) O. W. Howarth and G. K. Fraenkel, J. Am. Chem. Soc. 1966, 88, 4514. (b) O. W. Howarth and G. K. Fraenkel, G.K. J. Chem. Phys. 1970, 52, 6258.

3) (a) B. Badger, B. Brocklehurst and R. D. Russell, Chem. Phys. Lett. 1967, 1, 122. (b) B. Badger and B. Brocklehurst, Nature 1968, 219, 263. (c) B. Badger and B. Brocklehurst, Trans. Faraday Soc. 1969, 65, 2588.

4) B. Badger and B. Brocklehurst, ibid. 1970, 66, 2939.

5) M. A. Rodgers, J. Chem. Soc., Faraday Trans. 1 1972, 68, 1278.

6) H. Yoshimi and K. Kuwata, Mol. Phys. 1972, 23, 297.

7) T. Shida and S. Iwata, J. Am. Chem. Soc. 1973, 95, 3473.

8) (a) A. Kira, S. Arai and M. Imamura, J. Phys. Chem. 1972, 76, 1119. (b) A. Kira, M. Imamura and T. Shida, ibid. 1976, 80, 1445. (c) A. Kira, T. Nakamura and M. Imamura, ibid. 1977, 81, 511. (d) A. Kira and M. Imamura, ibid. 1979, 83, 2267.

9) (a) S. Irie, H. Horii and M. Irie, Macromolecules 1980, 13, 1355. (b) S. Irie and M. Irie, ibid. 1986, 19, 2182.

10) M. S. El-Shall and M. Meot-Ner, J. Phys. Chem. 1987, 91, 1088.

11) E. A. Chandross and C. J. Dempster, J. Am. Chem. Soc. 1970, 92, 3586.

CHAPTER 7

THEORETICAL CONSIDERATION OF DIMER RADICAL CATION BY MO CALCULATION

7-1. Introduction

In the previous chapters, the structure and stability of carbazole and naphthalene dimer radical cations were studied; for the carbazole dimer radical cation, the fully-overlapped structure is stabler than the partially-overlapped one, whereas for the naphthalene dimer radical cation, the partially-overlapped one is stabler than the former. The stability of the dimer radical cation is generally considered to be determined by the balance between the stabilization by charge delocalization and the repulsion between chromophores. The larger the degree of overlapping of chromophores, the larger the stabilization by charge delocalization, but also the larger the repulsion.

Badger and Brocklehurst[1] calculated the electronic energy levels of the intermolecular naphthalene dimer radical cation for some typical arrangements by Hückel MO theory and compared the results with the absorption bands obtained experimentally. For the naphthalene dimer radical cation, they suggested a sandwich arrangement that is distorted owing to the large repulsion force between the filled π orbitals in a fully-overlapped arrangement.

In this chapter, the CR band energies of carbazole and naphthalene intramolecular dimer radical cations were calculated by CNDO/S[2] for the stable conformation predicted by Austin Model 1 (AM1).[3] The results of the calculations were compared with the experimental data presented in Chapters 2 and 6. The difference between carbazole and naphthalene dimer radical cations was discussed in terms of the electronic states associated with the CR band. Furthermore, the energy decomposition analysis of molecular interaction by Morokuma and Kitaura[4] was applied to the carbazole and naphthalene dimer radical cations, and the factor that will govern stabilization was discussed.

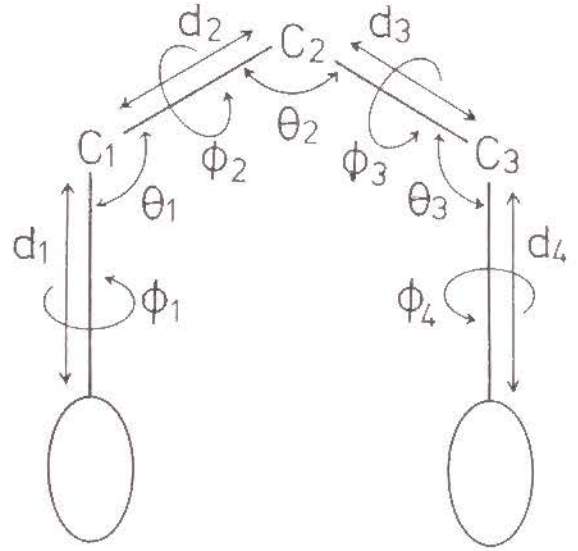

Figure 7-1. Optimized conformational parameters of a methylene chain by AM1.

7-2. Calculation Method

7-2-1. Dimer Structure and CR Band Energy

As the band energy is sensitive to the dimer structure, a stable conformation of a dimer radical cation is searched by AM1 before calculating the CR band energy. AM1 is a new parametric quantum mechanical molecular model proposed by Dewar et al.,[3] which is based on the NDDO approximation with a modified core repulsion function in MNDO.[5] By means of AM1, the conformation of a dimer radical cation was optimized by changing the structure of the methylene chain linking two chromophores. The optimum conformational parameters of the methylene bridge are shown in Figure 7-1, which include four bond lengths (d_1, d_2, d_3, and d_4), four rotational angles (ϕ_1, ϕ_2, ϕ_3, and ϕ_4), and three bond angles (θ_1, θ_2, and θ_3). The proton and/or the methyl group attached to C_1, C_2, and C_3 carbons were fixed in the stable location with a standard bond length, bond angle and rotational angle. For the structural parameters for a carbazole ring, the data obtained by X-ray analysis of carbazole derivatives were used.[6,7] For a naphthyl ring, the standard bond length, bond angle and rotational angle were used.[8] The optimization was made for meso- and rac-2,4-di(N-carbazolyl)pentanes (m- and r-DCzPe), 1,3-di(1-naphthyl)propane (11DNP), 1,3-di(2-naphthyl)propane (22DNP), and 1-(1-naphthyl)-3-(2-naphthyl)propane (12DNP). The initial conformation for m- and r-DCzPe are shown in Figure 7-2; the fully-overlapped conformation in a TT form of a methylene chain for m-DCzPe and the partially-overlapped conformation for r-DCzPe. r-DCzPe takes the partially-overlapped conformation by rotating ϕ_2 by ca. 30 degree from a TT form. In this conformation, a benzene ring of one carbazole ring is made to

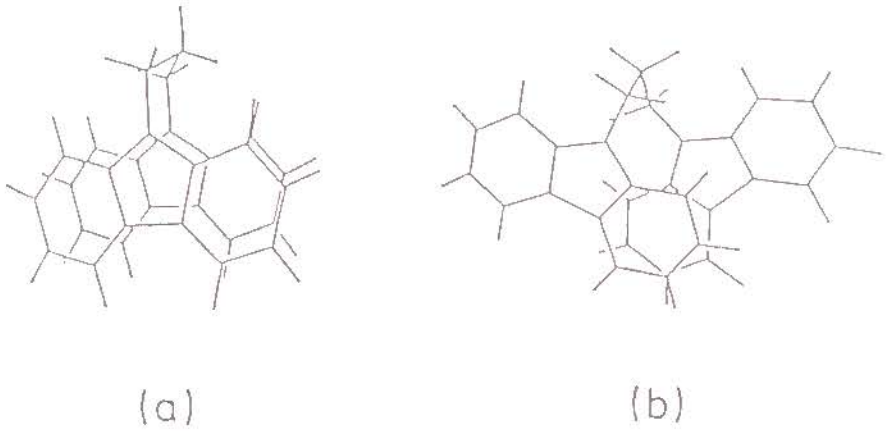

Figure 7-2. Initial conformations of m-DCzPc (a) and r-DCzPc (b) for optimization by AM1.

overlap, if partially, with a benzene ring of the other carbazole ring. As shown in Figure 7-3, each dinaphthylpropane (DNP) can take two types of overlapped conformations of naphthyl rings, for a naphthyl ring is asymmetric about a substitution axis. 12DNP gives two types of the partially-overlapped conformations, and 11DNP and 22DNP give a fully-overlapped and a partially-overlapped conformation. Therefore, calculations were made on the two initial conformations for each dimeric model compound.

CNDO/S was applied to the dimer radical cations which are in the optimized conformation determined in this way. The electronic states and energy levels of carbazole and naphthalene dimer radical cations were calculated, and the absorption band was estimated via the CI calculation.

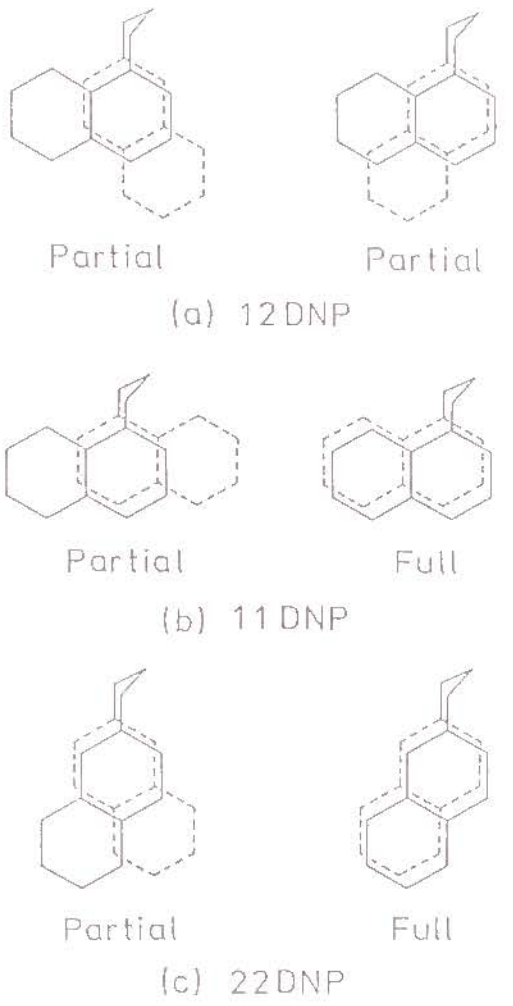

Figure 7-3. Initial conformations of 12DNP (a), 11DNP (b) and 22DNP (c) for optimization by AM1.

7-2-2. Energy Decomposition Analysis of Charge Delocalization Interaction

The energy decomposition analysis method of molecular interaction by the Ab Initio method proposed by Morokuma and Kitaura[4] was applied to a dimer radical cation. Their method is based on a Hartree-Fock supermolecule calculation. In the supermolecule method, the binding energy, BE, of a dimer radical cation is calculated with

$$BE(\underline{R}) = E(D_2^{+\cdot}, \underline{R}) - E(D^{+\cdot}) - E(D) \qquad (7\text{-}1)$$

where $E(D^{+\cdot})$ and $E(D)$ are energies of a radical cation and a neutral molecule, respectively, and $E(D_2^{+\cdot}, \underline{R})$ is the energy of a supermolecule, a dimer radical cation with a geometry $\underline{R}$. According to their method, the interaction energy, INT, is decomposed into physically meaningful energy components as follows.

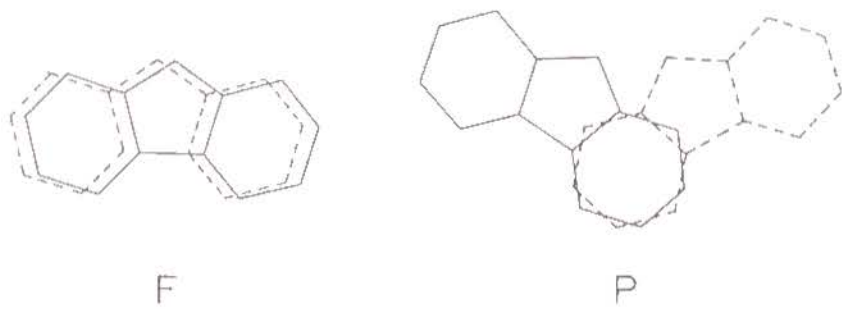

Figure 7-4. Arrangements of carbazole for energy decomposition analysis of charge delocalization interaction: a fully-overlapped arrangement (F) and a partially-overlapped ones (P).

$$INT = ES + EX + PL + CT + MIX\ (+DISP) \qquad (7\text{-}2)$$

where ES is the electrostatic or Coulombic interaction between the electron distributions of isolated molecules, EX is the exchange repulsion energy, PL is the polarization energy, CT is the charge transfer energy, MIX is the higher order coupling term among various interaction components, and DISP is the dispersion energy. In the present calculation, DISP is not included. As a basis function, STO-3G was used.

This energy decomposition analysis was carried out for carbazole and naphthalene intermolecular dimer radical cations. For carbazole, the calculation was made for the partially-overlapped and fully-overlapped arrangements shown in Figure 7-

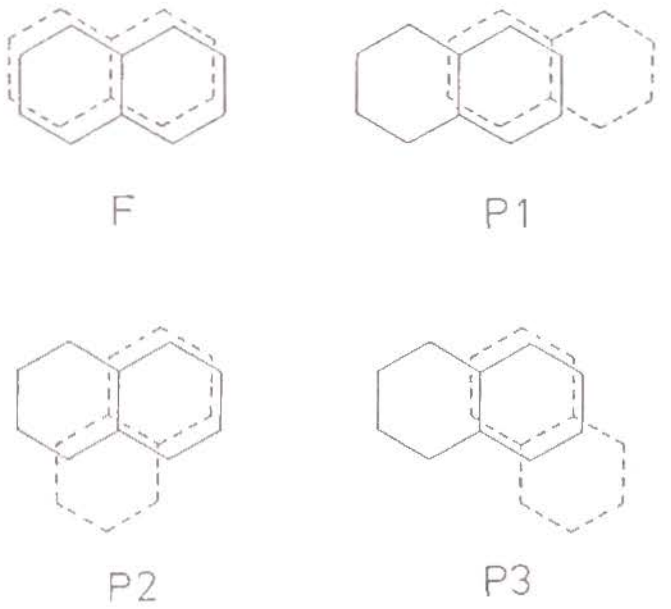

Figure 7-5. Arrangements of naphthalenes for energy decomposition analysis of charge delocalization interaction: one fully-overlapped arrangement (F) and three partially-overlapped ones (P1, P2 and P3).

4. For naphthalene, the calculation was made for the one fully-overlapped arrangement (F) and the three partially-overlapped arrangements (P1, P2, and P3) shown in Figure 7-5. In these cases, chromophores (carbazole or naphthalene) lie in two parallel planes separated by a distance d.

7-3. Results and Discussion

7-3-1. Estimation of Structure and CR Band Energy of Dimer Radical Cation

The optimized conformations of carbazole dimer radical cations for m- and r-DCzPe are shown in Figure 7-6. Both of the fully-overlapped dimer radical cation for m-DCzPe and the partially-overlapped one for r-DCzPe gave a potential minimum in the conformation when two carbazolyl rings are somewhat more separated than in the parallel arrangement of the sandwich conformation. Figure 7-7 shows the optimized conformation of the naphthalene dimer radical cation for 11DNP. Like carbazole dimer radical cations, two naphthyl rings are more separated than in the parallel arrangement. For 22DNP and 12DNP, the same results were obtained. In this way, the present semiempirical MO calculation, AM1, indicates that the carbazole and naphthalene intramolecular dimer radical cations do not take a perfect sandwich conformation but one in which two chromophores are somewhat more separated. Thus far, the conformation of carbazole dimer radical cations of DCzPe has been discussed by analogy with the structure of the excimer. However, the structure of the excimer itself has not firmly been established yet. For the dimer radical cations of 22DNP, the proposal of the fully-overlapped and partially-overlapped conformations is on the basis of trans-gauche rotations of a

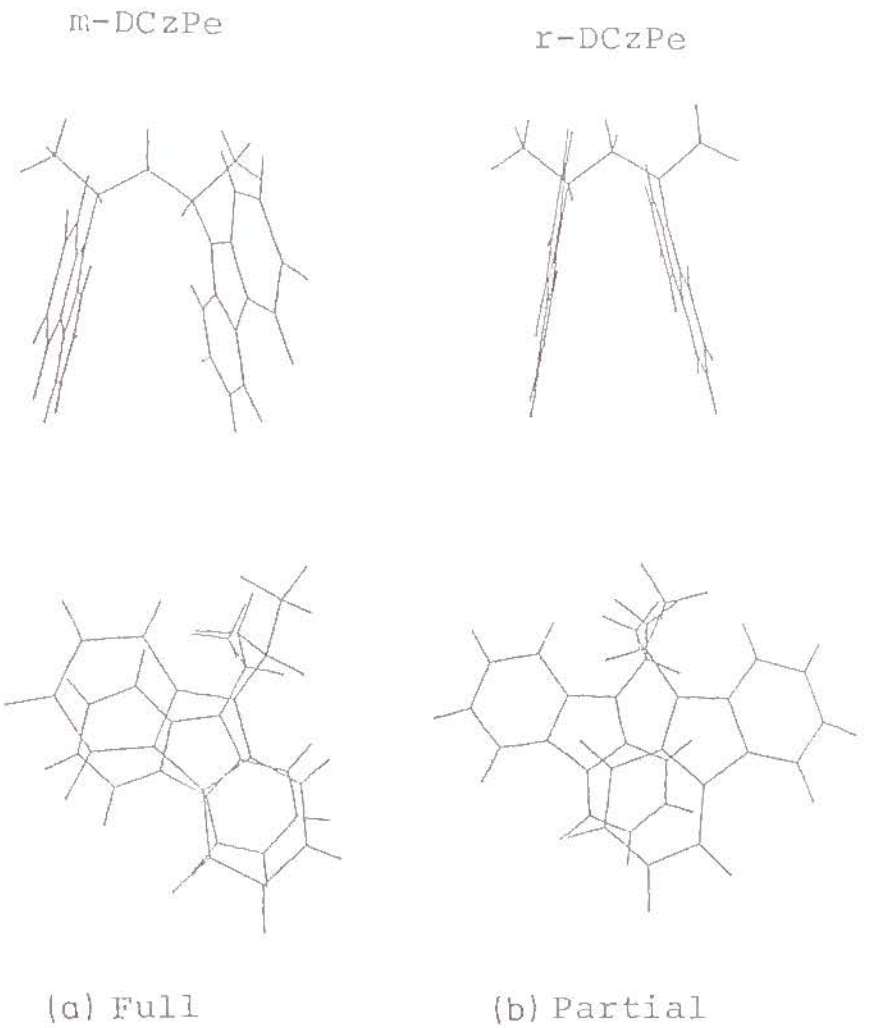

Figure 7-6. Optimized conformations of carbazole dimer radical cations for m-DCzPe (a) and r-DCzPe (b).

methylene bridge, but no theoretical ground. At the present stage, the structure of the dimer radical cation cannot be determined experimentally. In the absence of any effective experimental method to determined the structure of the dimer radical cation, the author believes that theoretical prediction is the only method to investigate the dimer structure. As will be described later, the calculated CR band with the predicted

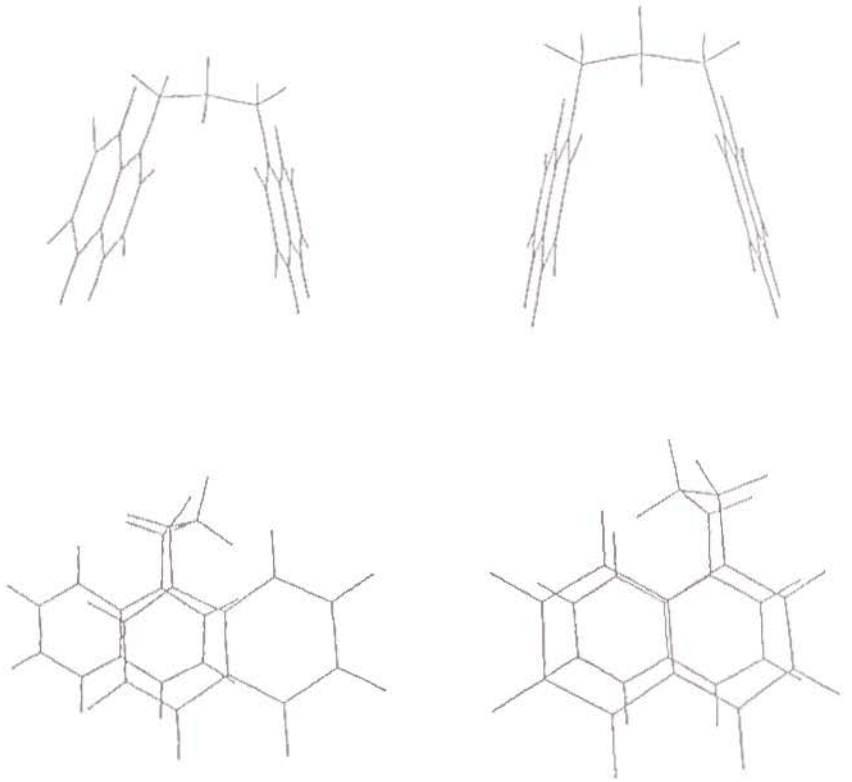

(a) Partial (b) Full

Figure 7-7. Optimized conformations of naphthalene dimer radical cations for 11DNP. (a) and (b) indicate the partially-overlapped and fully-overlapped conformations, respectively.

dimer structure qualitatively agrees with the experimental result. This may indicate the validity of the application of AM1 to the estimation of dimer structure. In this estimation, it is noted that, roughly speaking, the fully-overlapped and partially-overlapped conformations exist in a potential minimum. This means that the hitherto-expected structure of dimer radical cations is valid to some extent.

With these optimized conformations, the electronic states and energy levels of dimer radical cations were calculated by

Table 7-I. Visible and CR bands of carbazole dimer radical cations.

	Visible Band / nm		CR Band / nm	
	calculated	observed	calculated	observed
m-DCzPe	680	760	1341	1600
r-DCzPe	664	710	1441	1800

CNDO/S, and their absorption band energies were estimated by the CI calculation. The results for the carbazole dimer radical cations are compared, in Table 7-I, with the experimental data. The MO calculation could reproduce the experimentally-observed tendency of the wavelength shifts of the absorption band. That is, the fully-overlapped dimer radical cation for m-DCzPe showed the visible dimer band at a longer wavelength and the CR band at a shorter wavelength than those of the partially-overlapped dimer radical cation for r-DCzPe. For these dimer radical cations, the electron distribution of the splitted HOMO's associated with the CR band was investigated; consequently, the excitation of the CR band was suggested to be of a charge transfer type. Figure 7-8 shows the electron density differences induced by the transition of the CR band. As a whole, the electron density in one carbazole ring decreases, and that in the other carbazole ring increases; the electron of one carbazolyl ring in the lower orbital of splitted HOMO is excited to the upper orbital of the HOMO in which the electron is localized in the other carbazolyl ring. The change of the electron density on the N atom is particularly large. The N atom strongly affects the electronic state of the dimer radical

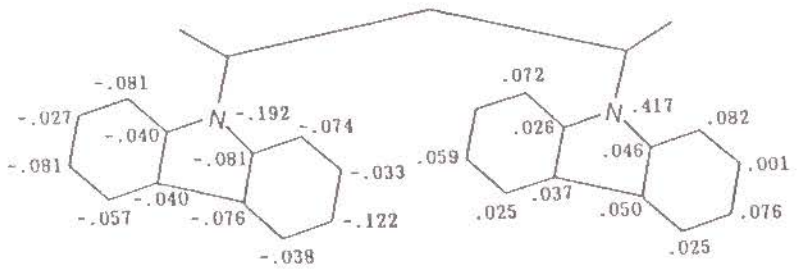

(a) Full (m-DCzPe)

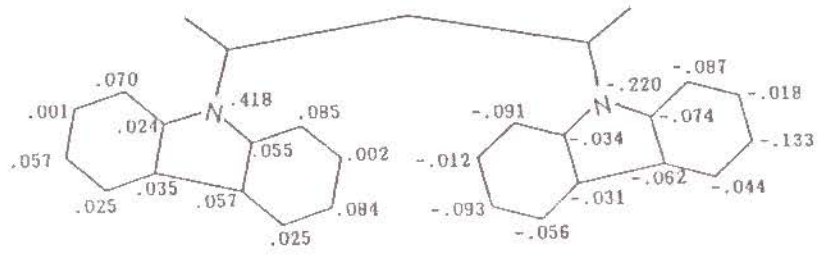

(b) Partial (r-DCzPe)

Figure 7-8. Electron density differences induced by CR band transition for m-DCzPe (a) and r-DCzPe (b).

cation.

On the other hand, as for the visible dimer bands of naphthalene dimer radical cation with differently-overlapped conformations, the calculation results were not systematic. Table 7-II shows the calculated CR bands of the two types of naphthalene dimer radical cations for each dimeric model compound along with the experimental data. The results predict the following; the partially-overlapped dimer radical cations except that of 22DNP give a CR band around 1600 nm, while the

Table 7-II. CR bands of naphthalene dimer radical cations.

	calculated/nm		observed/nm
12DNP	1662 (P)	1588 (P)	1050
11DNP	1678 (P)	2398 (F)	1350
22DNP	1920 (P)	1958 (F)	1250

* The character in the parentheses indicates the type of overlapping; F and P are a fully-overlapped and partially-overlapped types, respectively.

CR band of the fully-overlapped dimer radical cation appears at ca. 2000 nm. As described previously, the stronger the interaction, to a shorter wavelength is the CR band shifted. Therefore, these calculations show that the partially-overlapped dimer radical cation is stabler than the fully-overlapped one, consistently to the experimental results studied by the radical cation transfer method in Chapter 6.

The experimentally observed CR band for the dimer radical cation is considered to be a superposition of those of two types of dimer radical cations. For 12DNP, two kinds of partially-overlapped dimer radical cations were theoretically predicted to show a CR band commonly around 1600 nm. Therefore, the superposed CR band of the partially-overlapped dimer radical cations for 12DNP should appear around 1600 nm. Experimentally, the CR band for 12DNP was observed around 1050 nm. For 11DNP and 22DNP which form two types of dimer radical cations, the superposed CR band could not be predicted because the fraction of these dimer radical cations is unknown.

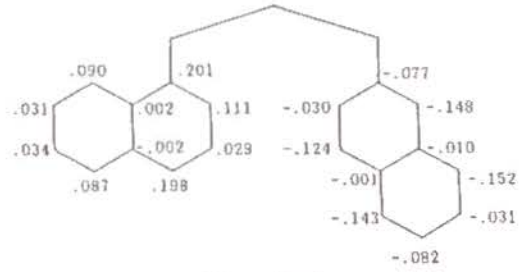

Partial

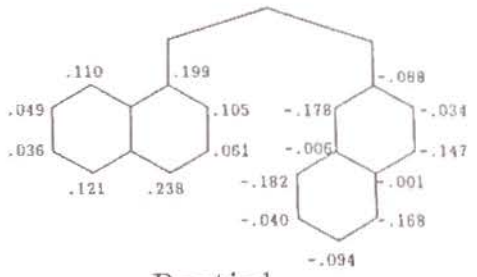

Partial

(a) 12DNP

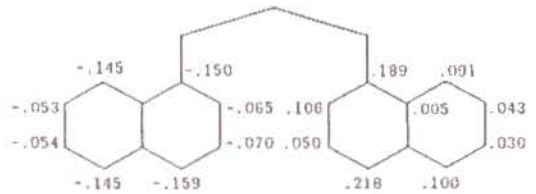

Partial

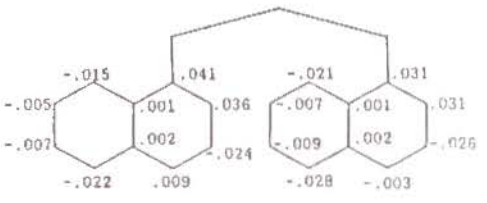

Full

(b) 11DNP

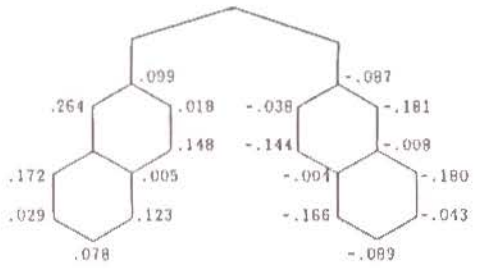

Partial

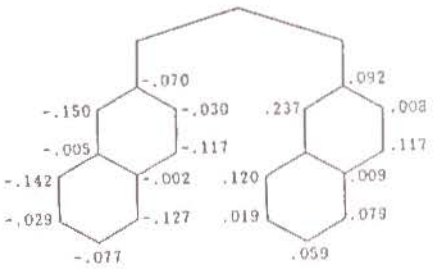

Full

(c) 22DNP

Figure 7-9. Electron density differences induced by CR band transition for 12DNP (a), 11DNP (b) and 22DNP (c).

But it should be longer than 1600 nm in wavelength. This tendency is accord with the experimental data.

Figure 7-9 shows the electron density differences induced by the CR band transition for each conformation. As a whole, the CR band transition was found to be a type of charge transfer from one naphthyl ring to the other. In contrast to carbazole dimer radical cations, the transition electron is not localized on a specific atom, but is delocalized in a naphthyl ring. The difference between carbazole and naphthalene dimer radical cations is reflected clearly in the electronic delocalization.

7-3-2. Estimate of Interaction Energy of Dimer Radical Cation

In this section, the interaction energy of dimer radical cation was decomposed into physically meaningful energy components theoretically on the basis of the Ab Initio data. The interaction energy is sensitive to dimer geometries, especially, to the overlapping and the distance between two chromophores. First of all, the dependence of the interaction energy and its energy components on the interplanar distance was examined in a sandwich and fully-overlapped arrangement. The results for N-H carbazole and naphthalene are shown in Figures 7-10 and 7-11, respectively. The isolated state in which two chromophores have no interaction, with a positive charge localized in a chromophore was taken as an energetic reference level. A positive energy indicates an unstable state, and a negative energy indicates stable state. Both carbazole and naphthalene dimer radical cations show similar dependence on the interplanar distance. With decreasing interplanar distance, EX increases, and CT and ES decrease. That is, EX is repulsive, while CT and ES are attractive. PL has little dependence on

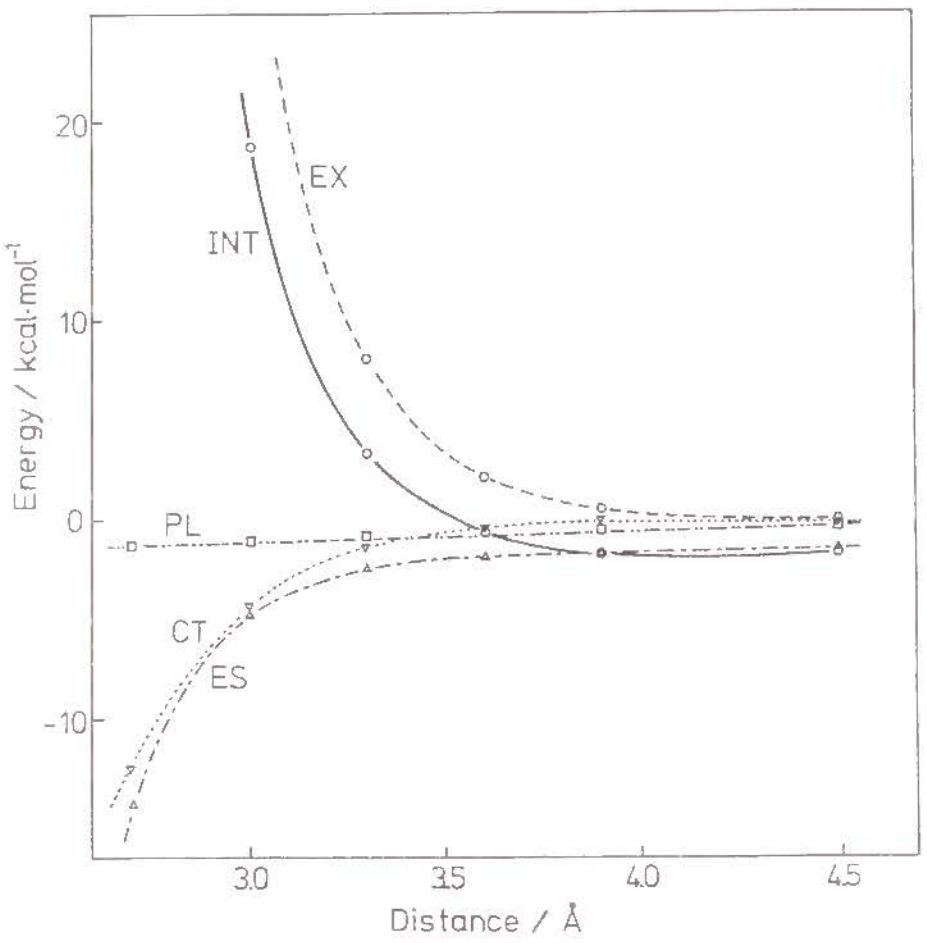

Figure 7-10. Dependence of interaction energy components on the interplanar distance for fully-overlapped dimer radical cation of N-H carbazole.

the interplanar distance. At shorter distances (< 3.5 A), EX predominates CT and ES. Therefore, the total interaction energy, INT, increases with decreasing interplanar distance, and the potential curve is repulsive. For both carbazole and naphthalene, INT becomes a minimum at ca. 4 A. This interplanar distance may be reasonable: Badger and Brocklehurst [1] used a distance of 3.0 A in the theoretical calculation of naphthalene

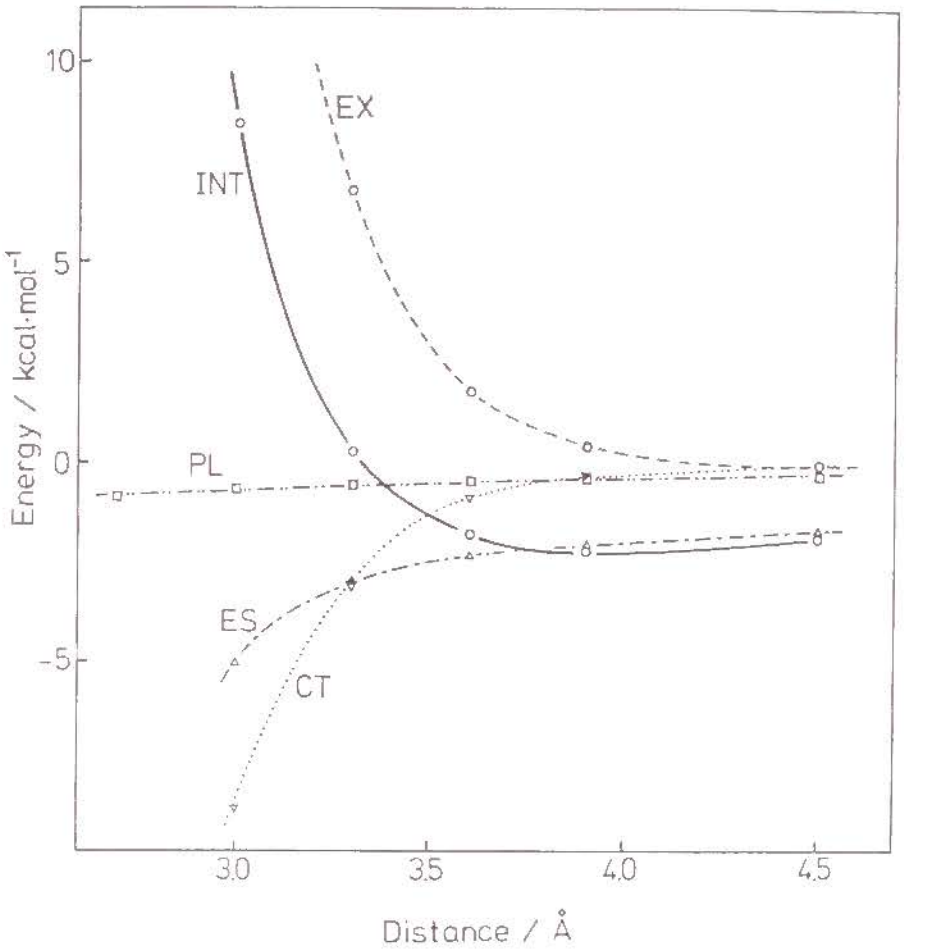

Figure 7-11. Dependence of interaction energy components on the interplanar distance for fully-overlapped dimer radical cation of naphthalene.

dimer radical cation, and in the studies of excimer, the interplanar distance is usually assumed to be 3.0 - 3.5 A.[9]

Secondly, the interaction energies of carbazole and naphthalene dimer radical cations were investigated for the fully-overlapped and partially-overlapped arrangements (Figures 7-4 and 7-5). The interplanar distance was fixed to be 3.9 A. The results are shown in Table 7-III. The total energy, INT, for

Table 7-III. Interaction energy components of carbazole and naphthalene dimer radical cations estimated by Ab Initio.

	Carbazole		Naphthalene			
	F	P	F	P1	P2	P3
INT	-1.70	-1.13	-2.14	-1.87	-1.99	-1.90
EX	0.52	0.28	0.45	0.31	0.35	0.31
ES	-1.61	-0.73	-2.00	-1.62	-1.83	-1.66
PL	-0.51	-0.63	-0.36	-0.49	-0.41	-0.47
CT	-0.11	-0.06	-0.23	-0.07	-0.10	-0.08

(kcal/mol)

* The interplanar distance is fixed to be 3.9 A.
* F indicates fully-overlapped arrangement and P, P1, P2 and P3 indicate partially-overlapped ones.
These arrangements are shown in Figures 7-4 and 7-5.

each dimer radical cation is negative, and thus each state is stable. EX is a repulsive component. ES, PL and CT are attractive components, of which ES contributes the most to the stabilization of dimer radical cation. As for carbazole dimer radical cations, the values of INT indicate that the fully-overlapped dimer radical cation is stabler than the partially-overlapped one. This is consistent with the experimental results described in Chapter 2. The large stabilization in the fully-overlapped arrangement is considered to be due to a strong interaction between N atoms. This presumably has a correlation with the theoretical result showing that a large electron-density change on N atom is induced by the CR band transition. Among the three partially-overlapped naphthalene

dimer radical cations (P1, P2 and P3), the calculated interaction energies are almost the same. INT indicates that the fully-overlapped dimer radical cation is stabler than the partially-overlapped one. This is inconsistent with the experimental results described in Chapter 6. The difference of INT between two type of naphthalene dimer radical cations is ca. 0.2 kcal/mol, the value being even smaller for carbazole (ca. 0.6 kcal/mol). It is considered that the difference of 0.2 kcal/mol may be within the calculation error by the following reason. In the partially-overlapped conformation, the repulsion is smaller than that in the fully-overlapped one. Nevertheless, the same interplanar distance was assumed. Therefore, INT for the partially-overlapped dimer radical cations may be underestimated.

7-4. Conclusion

By means of AM1, the structures of the dimer radical cations of DCzPe and DNP were estimated. The results show that the fully-overlapped and partially-overlapped conformations are in potential minima, even though two chromophores are somewhat more separated than in the parallel arrangement. This may, to some extent, justify the hitherto-assumed dimer geometries. In these optimized conformations, the CR band was calculated by CNDO/S, and the experimentally observed relationship between the CR band shift and the chromophore overlapping (full and partial overlapping) were reproduced successfully. The analysis of the electronic states indicated that the excitation of the CR band is of a charge transfer type. For carbazole, a particularly large change of electron density on the N atom was predicted to be induced by the CR band transition.

The energy decomposition analysis was applied to the intermolecular dimer radical cations of N-H carbazole and naphthalene, and the interaction energy components were calculated by Ab Initio calculations. In this analysis, the contribution of ES to the stabilization of the dimer radical cation was found to be very large. As for carbazole, the fully-overlapped dimer radical cation was predicted to be stabler than the partially-overlapped one, in agreement with the experiments.

The agreement between theory and experiment was better for carbazole than for naphthalene. Perhaps, the N atom in carbazole may be playing an important role in this problem.

References

1) B. Badger, and B. Brocklehurst, Trans. Faraday Soc. 1970, 66, 2939.

2) (a) J. D. Bene and H. H. Jaffe, J. Chem. Phys. 1968, 48, 1807. (b) J. D. Bene and H. H. Jaffe, ibid. 1970, 50, 1126.

3) M. J. S. Dewar, E. G. Zoebisch, E. F. Healy and J. J. P. Stewart, J. Am. Chem. Soc. 1985, 107, 3902.

4) K. Morokuma and K. Kitaura, in Chemical Applications of Atomic and Molecular Electrostatic Potentials, P. Politzer and D. G. Truhlar, eds., Plenum Press, New York, 1981, p.215.

5) M. J. S. Dewar and W. Thiel, J. Am. Chem. Soc. 1977, 99, 4899.

6) M. Kurahashi, M. Fukuyo and A. Shimada, Bull. Chem. Soc. Jpn. 1969, 42, 2174.

7) E. G. Popova and L. A. Chetkina, J. Struct. Chem. 1979, 20, 564.

8) J. A. Pople and D. L. Beveridge, Approximate Molecular Orbital Theory, McGraw-Hill, New York, 1970, Chapter 4.

9) J. B. Birks, Prog. Reaction Kinetics 1970, 5, 181.

CHAPTER 8

STABILITY OF TEREPHTHALATE RADICAL ANION FORMED IN POLY(VINYL METHYL TEREPHTHALATE)

8-1. Introduction

A large number of studies have been reported regarding dimer radical cations and DDA type excited triple complexes (exterplex) which consist of two electron donor (D) and an electron acceptor (A). In contrast, there have been only a few reports regarding the formation of aromatic dimer radical anions[1-3] and DAA exterplexes[4,5] formed by charge delocalization of a radical anion with a neutral electron-accepting chromophore. Shida et al.,[2] who studied dianthracene in γ-irradiated rigid methyltetrahydrofuran solutions at 77 K, observed the charge-resonance band of anthracene dimer radical anion in the near-infrared region. Hirata et al.[4] reported the formation of DAA exterplex of benzonitrile - amine systems. Tsuchida et al.[6] investigated, by the radical anion transfer method, the stabilization of the radical anion formed in poly(vinyl methyl terephthalate) (PVMTP) or in its dimeric model compounds with two terephthalate (TP) groups linked by a methylene chain. For both PVMTP and the dimeric model compounds, the radical anion transfer to 1,4-dicyanobenzene (p-DCNB) or to 1,2,4,5-tetracyanobenzene (TCNB) was found to be highly suppressed as compared with the case of a monomer model

compound, dimethyl terephthalate (DMTP). Furthermore, the degree of suppression in PVMTP was much higher than that in the dimeric model compounds. In fact, no radical anion transfer to p-DCNB was observed in the PVMTP system. This is considered to be due to the stabilization of the radical anion by interactions with the neighboring chromophores.

In this chapter, by nanosecond laser photolysis the radical anion transfer to p-DCNB was measured for copolymers of vinyl methyl terephthalate (VMTP) with vinyl acetate (VAc), and the relation between the sequence of TP chromophores and the stabilization was discussed to elucidate the nature of the radical anion formed in PVMTP. Furthermore, the fluorescent behavior of PVMTP and its model compounds in the presence of an electron donor, N-ethylcarbazole (EtCz), was studied, and the possibility of DAA exterplex formation was considered.

8-2. Experimental Section

8-2-1. Polymers

VMTP was synthesized by the ester exchange reaction of vinyl acetate with terephthalic acid monomethyl ester (Tokyo Kasei Kogyo Co.).[7] The crude sample was purified by passing through a silica-gel column with dichloromethane as eluent and subsequently recrystallized from hexane. PVMTP was prepared by radical polymerization in benzene with AIBN as initiator. The weight-average molecular weight ($\bar{M}w$) was estimated to be 1×10^5 by GPC (Toyo Soda HLC 802UR) with a G4000H and a GMH columns. VAc (Wako Pure Chem. Ind.) was purified by distillation. Four copolymers of VMTP and VAc were prepared by radical copolymerization initiated by AIBN in a benzene solution at 60 ^{o}C. The conversion was always below 30 mol%. The copolymer

samples were purified by precipitation three times from a benzene solution into hexane. The molecular weight ($\bar{M}w$) of these copolymers was estimated by GPC. The mole fraction of terephthalate units (f_{TP}) was determined by UV absorption on the basis of the known molar extinction coefficient of DMTP in dichloromethane ($\varepsilon = 1.87 \times 10^3$ $M^{-1}cm^{-1}$ at 286 nm). Copolymerization data are shown in Table 8-1. The copolymer are designated as P1, P2, P3 and P4 in the order of increasing f_{TP}. The monomer reactivity ratios, r_1 and r_2, were determined by the Fineman-Ross method[8] to be 0.26 and 0.64, respectively.

Table 8-1. Characterization of copolymers of VMTP with VAc.

Copolymer	F[1]	f_{TP}[2]	$M_w/10^4$ [3]
P1	0.20	0.18	1.9
P2	0.52	0.31	2.9
P3	1.2	0.49	3.4
P4	3.5	0.62	3.4

1) Monomer feed ratio of the copolymerization. ($F = [VMTP]_0 / [VAc]_0$)
2) Mole fraction of TP unit in the copolymer determined by UV absorption.
3) Molecular weights determined by GPC (polystyrene equivalent).

8-2-2. Other Chemicals

EtCz was synthesized by N-alkylation of carbazole and purified by recrystallization. DMTP (Wako Pure Chem. Ind.) and p-DCNB (Wako Pure Chem. Ind.) were purified several times by recrystallization. Dimeric model compounds, 1,3-bis[p-

(methoxycarbonyl)benzoyloxy]propane (1,3-MTP) and rac-2,4-bis[p-(methoxycarbonyl)benzoyloxy]pentane (2,4-MTP) were synthesized and purified as reported previously.[6] Dichloromethane (Dotite Spectrosol) and benzene (Dotite Spectrosol) were used without further purification. Benzonitrile (Wako Pure Chem. Ind.) was fractionally distilled.

8-2-3. Measurements

The transient absorption measurements were made in benzonitrile for the copolymers and the dimeric model compounds in the presence of an electron donor, EtCz. The absorption spectra and decays of the radical ions ($EtCz^{+\cdot}$, $TP^{-\cdot}$ and $p\text{-}DCNB^{-\cdot}$) produced by photoinduced electron transfer were measured by nanosecond laser photolysis. Selective photoexcitation of EtCz was made by a second harmonic pulse (347 nm) of a Q-switched giant pulse ruby laser for the copolymer systems and by an excimer laser pulse of XeF (308 nm) for the model compound systems. All samples for the laser photolysis were degassed by the freeze-pump-thaw method. In the measurement of the laser photolysis, the absorbance of EtCz was adjusted to about unity at an excitation wavelength, and the TP chromophore concentration was adjusted to 1.0×10^{-1} M for the copolymers and to 5.0×10^{-2} M for the model compounds. For radical anion transfer experiments, 1.0×10^{-2} M of p-DCNB for the copolymers and 2.0×10^{-3} M of p-DCNB for the model compounds were added to the above systems.

The reduction potentials of DMTP and p-DCNB were measured by cyclic voltammetry with a reference electrode (Ag/0.01 N Ag^{+} in acetonitrile) and were determined to be -2.11 V and -1.97 V, respectively.

The fluorescent properties of the EtCz exciplex of PVMTP

and its model compounds were studied in degassed benzene. The emission spectra and lifetimes of the exciplex were measured by a Hitachi 850 spectrophotofluorometer and a single photon counting method (PRA Inc. model 510B), respectively, under the condition of selective photoexcitation of EtCz. In the measurements of the exciplex, the concentration of EtCz was adjusted to below 3×10^{-4} M to avoid an intermolecular interaction, and the TP chromophore concentration was adjusted to 2.0×10^{-1} M for PVMTP and 1.0×10^{-1} M for the model compounds.

The UV absorption spectra were recorded on a Shimadzu UV-200S spectrophotometer.

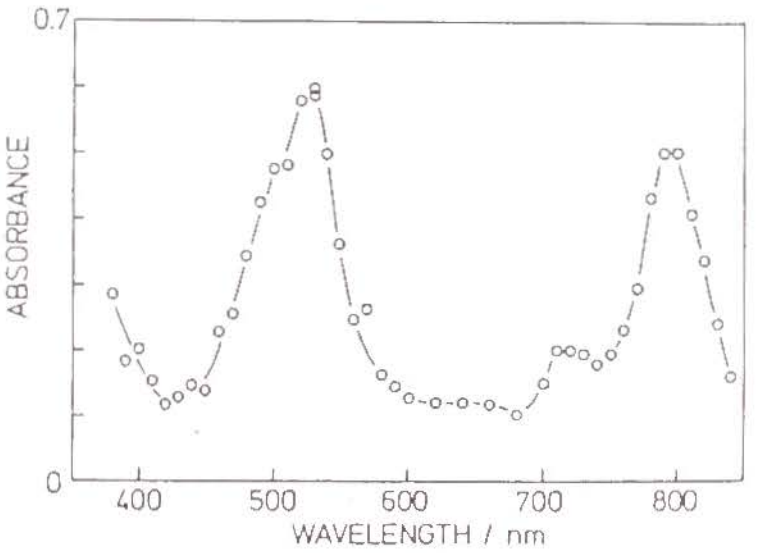

Figure 8-1. Transient absorption spectrum of EtCz - P1 system in benzonitrile measured by nanosecond laser photolysis at 298 K at 1 μs after excitation.
The absorbance of EtCz at 347 nm is about unity. The concentration of TP chromophore in the copolymer is 1.0×10^{-1} M.

8-3. Results and Discussion

8-3-1. Transient Absorption Spectra of $TP^{\cdot-}$ in the Copolymers

Figure 8-1 shows the transient absorption spectrum of the EtCz - P1 system in benzonitrile. This spectrum is almost the same as that of the monomer model compound, EtCz - DMTP system. The absorption bands around 780 nm and 530 nm were assigned to $EtCz^{\cdot+}$ and $TP^{\cdot-}$ in the copolymer, respectively. Other copolymer systems gave similar transient absorption

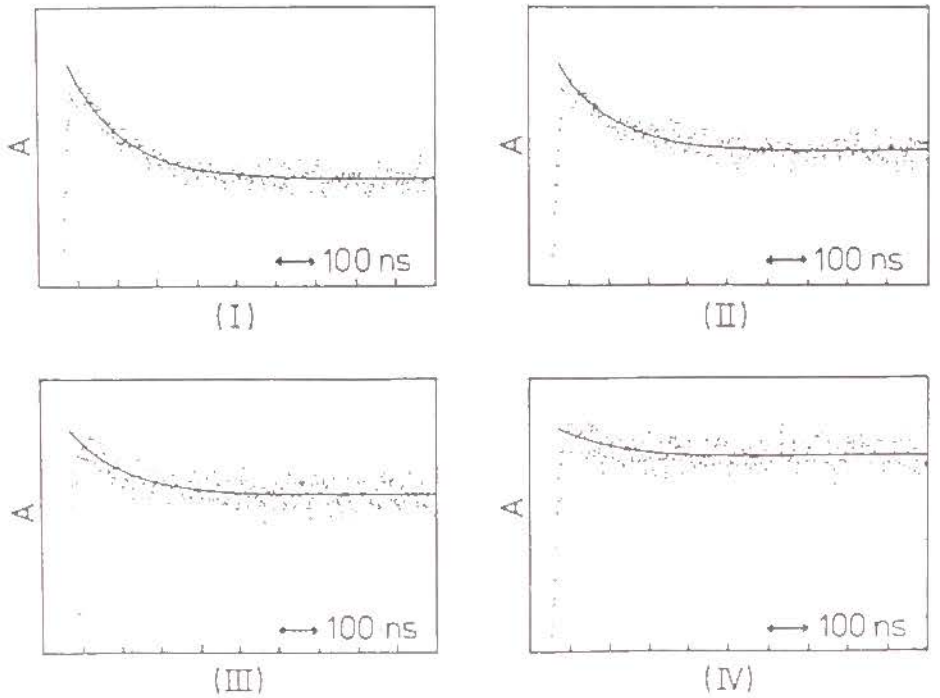

Figure 8-2. Transient absorbance decay measured at 530 nm in benzonitrile.
(I): EtCz - P1 - p-DCNB system, (II): EtCz - P2 - p-DCNB system, (III): EtCz - P3 - p-DCNB system, (IV): EtCz - P4 - p-DCNB system.
The absorbance of EtCz is about unity. The concentrations of TP chromophore in the copolymers and p-DCNB in each system are 1.0×10^{-1} M and 1.0×10^{-2} M, respectively.

spectra as that shown in Figure 8-1. The molar extinction coefficient of $TP^{\cdot-}$ for each copolymer at 530 nm was determined to be ca. 1.3×10^4 $M^{-1}cm^{-1}$ on the basis of that of $EtCz^{\cdot+}$ at 780 nm ($\varepsilon = 9.4 \times 10^3$ $M^{-1}cm^{-1}$). The molar extinction coefficient of $TP^{\cdot-}$ in the copolymer was independent of f_{TP}. This value is almost the same as that of $DMTP^{\cdot-}$ ($\varepsilon = 1.2 \times 10^4$ $M^{-1}cm^{-1}$). The fact that no change was observed in the transient absorption spectra means weak interactions between the neighboring chromophores.

8-3-2. Radical Anion Transfer from $TP^{\cdot-}$ to p-DCNB

Figure 8-2 shows the decay at 530 nm which was mainly assigned to $TP^{\cdot-}$ in the copolymer. In the absence of p-DCNB, $TP^{\cdot-}$ decreases by the recombination with $EtCz^{\cdot+}$, but its absorption hardly decays in this time region (< 1 μs). On the contrary, when an electron acceptor, p-DCNB, which has a lower reduction potential than the TP chromophore, is added, the decrease of $TP^{\cdot-}$ is accelerated, as shown in Figure 8-2. This is due to the radical anion transfer from $TP^{\cdot-}$ in the copolymer to p-DCNB. The decay consists of a fast decay component in the short time region (< ca. 200 ns) and a slow decay component following the fast decay. As f_{TP} increases from 0.18 to 0.62, the fast decay component decreases.

These decay curves were simulated by using the scheme shown in Figure 8-3. A fraction f_{tr} of $TP^{\cdot-}$ in the copolymer transfers an electron to p-DCNB with a rate constant k_{tr}, while the remaining fraction $1-f_{tr}$ do not, being stabilized by the neighboring interaction. The concentration of $TP^{\cdot-}$ ($[TP^{\cdot-}]$) at time t is expressed by eq. 8-1, as the decrease of $TP^{\cdot-}$ by the recombination with $EtCz^{\cdot+}$ is negligible in this time region (< 1 μs).

$$[TP^{\cdot}] = [TP^{\cdot}]_0(f_{tr}\exp(-k_{tr}[p\text{-}DCNB]t) + (1-f_{tr})) \quad (8\text{-}1)$$

where $[TP^{\cdot}]_0$ and [p-DCNB] are the concentration of $TP^{\cdot}$ and p-DCNB at t = 0, respectively. The first term in the parentheses corresponds to the fast decay component in the observed decay curve and represents the decrease of $TP^{\cdot}$ via the radical anion transfer. The second term corresponds to the slow decay component where $TP^{\cdot}$ does not decrease in this time region.

The observed decay curves at 530 nm were simulated using eq. 8-1. Since the absorbances of $EtCz^{\cdot+}$ and $p\text{-}DCNB^{\cdot-}$ overlap slightly on that of $TP^{\cdot}$, the contribution of these radical ions was subtracted on simulation. The initial concentration $[TP^{\cdot}]_0$ was also determined from the absorbance at t = 0 at 530 nm with the overlap contribution of $EtCz^{\cdot+}$ and $p\text{-}DCNB^{\cdot-}$ suitably taken

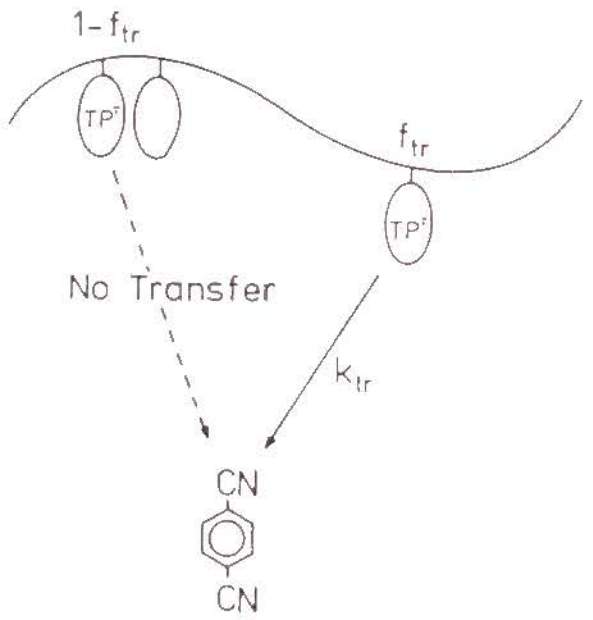

Figure 8-3. Scheme of radical anion transfer from $TP^{\cdot}$ in copolymers to p-DCNB.

into account. The formation of $p\text{-}DCNB^{\cdot-}$ through direct quenching of an excited EtCz was also taken into account. The results are summarized in Table 8-II, and the simulation lines are given by the solid line in Figure 8-2. The rate constant k_{tr} was found to be 7.7 x 10^8 $M^{-1}s^{-1}$ for each system. The fraction of electron-transferable TP, f_{tr}, decreases in the order, P1 (f_{tr} = 0.83) > P2 (f_{tr} = 0.64) > P3 (f_{tr} = 0.48) > P4 (f_{tr} = 0.21) with increasing f_{TP}.

Table 8-II. Simulation parameters of decay curves at 530 nm.

Copolymer	f_{tr}	$k_{tr}/10^8$ $M^{-1}s^{-1}$
P1	0.83	7.7
P2	0.64	7.7
P3	0.48	7.7
P4	0.21	7.7

8-3-3. Stability of $TP^{\cdot}$ in the Copolymers

In this system, the degree of interactions between the neighboring chromophores depends on the sequence distribution of VMTP in the copolymer. The fraction f_i of isolated TP groups in the copolymer, i.e., the fraction of the triad sequence VAc - VMTP - VAc was calculated from r_1 and the feed ratio (F = [VMTP]/[VAc]) using eq. 8-2.[9]

$$f_i = (1+r_1F)^{-2} \quad (8\text{-}2)$$

The calculated values of f_i for P1, P2, P3 and P4 are 0.90, 0.78,

0.58 and 0.27, respectively. Figure 8-4 shows the relation between the transferable fraction f_{tr} and f_i. The value of f_{tr} is somewhat smaller than f_i for each copolymer. This is presumably due to underestimation of the initial absorbance of $TP^{\cdot-}$, since the radical anion transfer also occurs in the excitation pulse width of 14 ns, which is out of the time-resolution in this system. It may be concluded that the transferable fraction f_{tr} is roughly proportional to f_i. This means that the radical anion $TP^{\cdot-}$ formed in the sequence VAc - VMTP - VAc is electron-transferable, while the $TP^{\cdot-}$s formed in sequences with adjacent VMTP's cannot transfer any electrons to p-DCNB. In fact, for the $TP^{\cdot-}$ formed in the homopolymer PVMTP, no radical anion transfer to p-DCNB occurs at all. It is

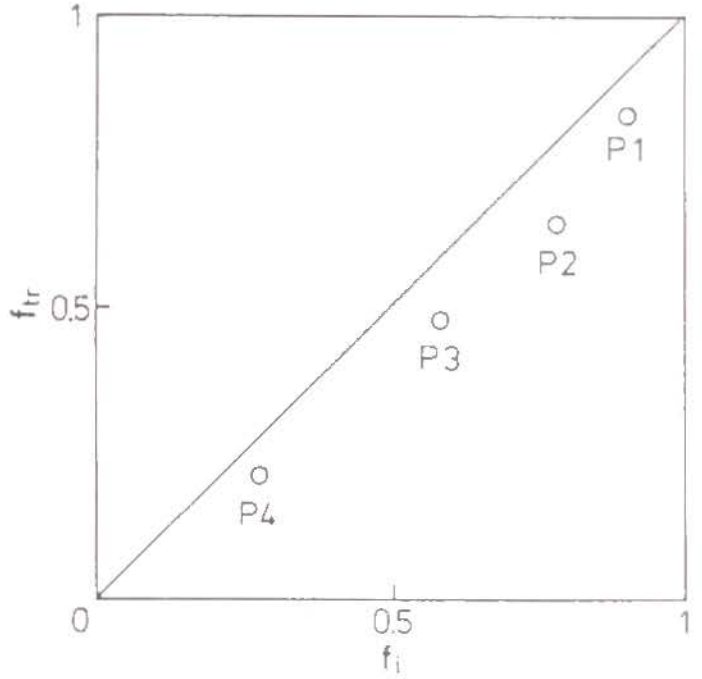

Figure 8-4. Transferable fraction f_{tr} versus isolated fraction f_i.

stabilized by interactions among more than one adjacent TP chromophores.

8-3-4. Comparison with Radical Anion of Dimeric model Compounds

In order to compare the dyad sequence of VMTP in the copolymer with the dimeric model compounds, the radical anion transfer to p-DCNB was measured for the $TP^{\cdot-}$ of the dimeric model compounds and DMTP, and k_{tr} was determined more exactly by observing the initial transient absorption decay of $TP^{\cdot-}$ at 530 nm in the time region (< 1 μs) where the recombination process could be neglected. The measured rate constants were: 1.2×10^9 $M^{-1}s^{-1}$ for DMTP, 1.0×10^9 $M^{-1}s^{-1}$ for 2,4-MTP, and 7.2×10^8 $M^{-1}s^{-1}$ for 1,3-MTP. The radical anions of the dimeric model compounds transfer an electron to p-DCNB more slowly than that of DMTP due to the stabilization exerted by the interactions between the neighboring chromophores. Furthermore, the stability of 1,3-MTP is stronger than that of 2,4-MTP, which can be explained by the difference in the conformation between the dimeric model compounds, i.e., 1,3-MTP is easier to take a sandwich like conformation than 2,4-MTP.

On the other hand, the radical anion $TP^{\cdot-}$ formed in the copolymer sequence VAc - VMTP - VMTP - VAc does not transfer its electron to p-DCNB as described above. This suggests that the $TP^{\cdot-}$ in the sequence VAc - VMTP - VMTP - VAc in the copolymer is stabler than the dimeric model compound. This enhanced stabilization observed in the polymer system seems to be caused partly by a stronger neighboring interaction and partly by a steric effect of the polymer chain hindering p-DCNB molecules from approaching. Such steric hindrance of a polymer chain were seen in the radical cation transfer for PVCz systems as described in Chapter 3. Due to the steric effect, the chance

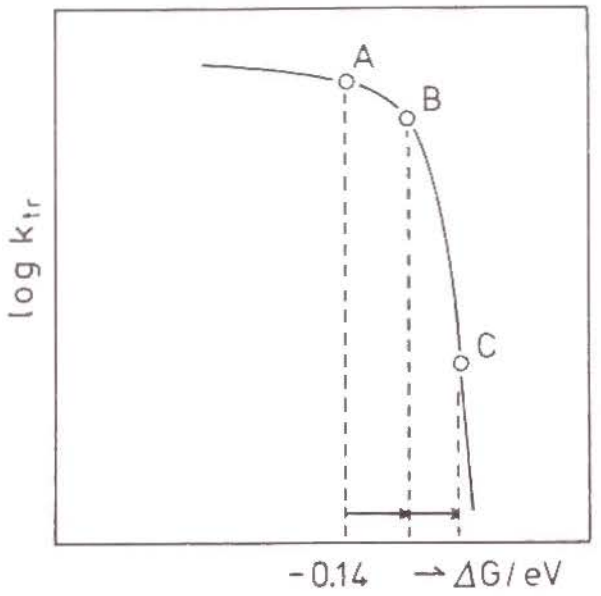

Figure 8-5. Relation between k_{tr} and free energy change in the radical anion transfer from TP$^{\cdot-}$ to p-DCNB.

of electron transfer in the polymer system would be smaller than in low-molecular-weight compounds, and hence the transfer rate constant is smaller in the former system than in the latter. Figure 8-5 schematically shows the above situation. The relation between k_{tr} and the free energy change ΔG for the electron transfer is shown by the solid curve: k_{tr} decreases slowly at first with increasing ΔG in the exothermic region and drops rapidly at and above ca. ΔG = 0.[10] For monomer model compound systems, the free energy change ΔG of the radical anion transfer to p-DCNB is estimated to be ca. -0.14 eV from the difference of the reduction potentials of DMTP ($E_{1/2}$ = -2.11 V) and p-DCNB ($E_{1/2}$ = -1.97 V). This case is represented by point A in the figure. For the dimeric model compound, k_{tr} becomes smaller than that of the monomer model compound due to the interactions between the neighboring chromophores. This dimer

system is represented by point B. The radical anion in a dyad TP in the copolymer is further stabilized by the neighboring chromophore interactions and the steric hindrance. This makes ΔG larger (point C). Around ΔG = 0, even a slight increase in ΔG causes a large decrease in k_{tr}. As for the homopolymer, radical anion transfer was not observed in our experimental resolution; therefore, TP$^{\cdot-}$ in the homopolymer is estimated to be stabler than DMTP$^{\cdot-}$ by at least 0.1 eV.

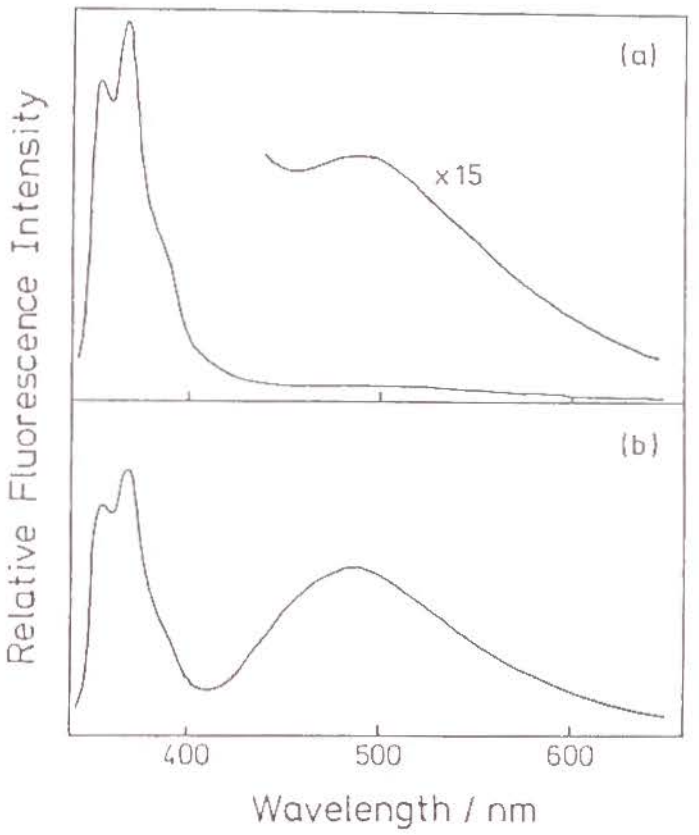

Figure 8-6. Emission spectra of the PVMTP and 2,4-MTP systems in benzene at room temperature.
(a): EtCz(3.0×10^{-4} M) - PVMTP([TP]=0.2 M),
(b): EtCz(2.8×10^{-4} M) - 2,4-DMTP([TP]=0.1 M).

Table 8-III. Quantum yield (Φ_f) of monomer emission, and peak wavelength (λ), lifetime (τ_e), quantum yield (Φ_f') and quantum efficiency (q_f') of exciplex emission.

	Φ_f	λ/nm	τ_e/ns	Φ_f'	q_f'
EtCz - DMTP(0.1 M)	0.022	480	52.0	0.121	0.13
EtCz - 2,4-MTP([TP]=0.1 M)	0.041	485	45.2	0.090	0.10
EtCz - PVMTP([TP]=0.2 M)	0.164	490	21.6	0.036	0.05

8-3-5. Cz - TP Exciplex Quenching by Neighboring TP Chromophore

Figures 8-6-(a) and (b) show the emission spectra of EtCz - PVMTP and 2,4-MTP systems, respectively. Each system has a monomer emission with a vibrational structure in the shorter wavelength region and a broad exciplex emission in a longer wavelength region. Table 8-III gives the quantum yield (Φ_f) of the monomer emission, the peak wavelength (λ), the lifetime (τ_e), the quantum yield (Φ_f') and the quantum efficiency (q_f') of the exciplex emission. The quantum efficiency, q_f', was calculated with the following equation.

$$q_f' = \Phi_f' / (1 - \Phi_f / \Phi_f^{O}) \qquad (8\text{-}3)$$

where Φ_f^{O} is the emission quantum yield of EtCz in the absence of the electron acceptor. The table shows that Φ_f increases in the order DMTP < 2,4-MTP < PVMTP, and Φ_f' decreases in the order DMTP > 2,4-MTP > PVMTP. This is due to decreasing diffusion rate of the electron acceptor, i.e., decreasing quenching efficiency, since the quenching process is diffusion-controlled in each systems, as will be described later.

Therefore, the fluorescent characteristics of the exciplex need be compared in terms of the quantum efficiency q_f' of the exciplex emission. The peak wavelength λ of the exciplex emission is a little sifted towards longer wavelengths in the order DMTP < 2,4-MTP < PVMTP. However, no new emission ascribable to a new excited complex such as DAA exterplex could be observed. Thus, even if a new excited complex may be formed, its stabilization energy must be very small. The quantum efficiency q_f' of the exciplex emission decreases in the order of the DMTP system (0.13), the 2,4-MTP system (0.10) and the PVMTP system (0.05). This corresponds to the decrease in the exciplex lifetime in the same order. Though the emission from a new excited complex could not be observed, it is evident that Cz - TP exciplex is quenched by neighboring chromophore interactions. The interaction between the TP chromophores in PVMTP must be weak as compared with the neighboring chromophore interaction in PVCz which forms DDA exterplex. This is similar to the case of the radical anion. The stabilization by charge delocalization between TP chromophores is considered to be small.

Figures 8-7-(a), (b) and (c) show the temperature dependence of Φ_f and Φ_f' of EtCz - DMTP, 2,4-MTP and PVMTP systems, respectively. In each system, Φ_f decreases and the quenching efficiency increases with increasing temperature. On the contrary, Φ_f' increases with increasing temperature and at higher temperatures, a decrease of Φ_f' was observed in the DMTP and 2,4-MTP systems. The temperature at which $\Phi_f'$is maximum is ca. 50 ^{O}C for DMTP system and ca. 65 ^{O}C for 2,4-MTP system. For PVMTP system, no such decrease of Φ_f' was observed at least in the temperature range below 75 ^{O}C. The strength of the neighboring chromophore interaction seems to play an important

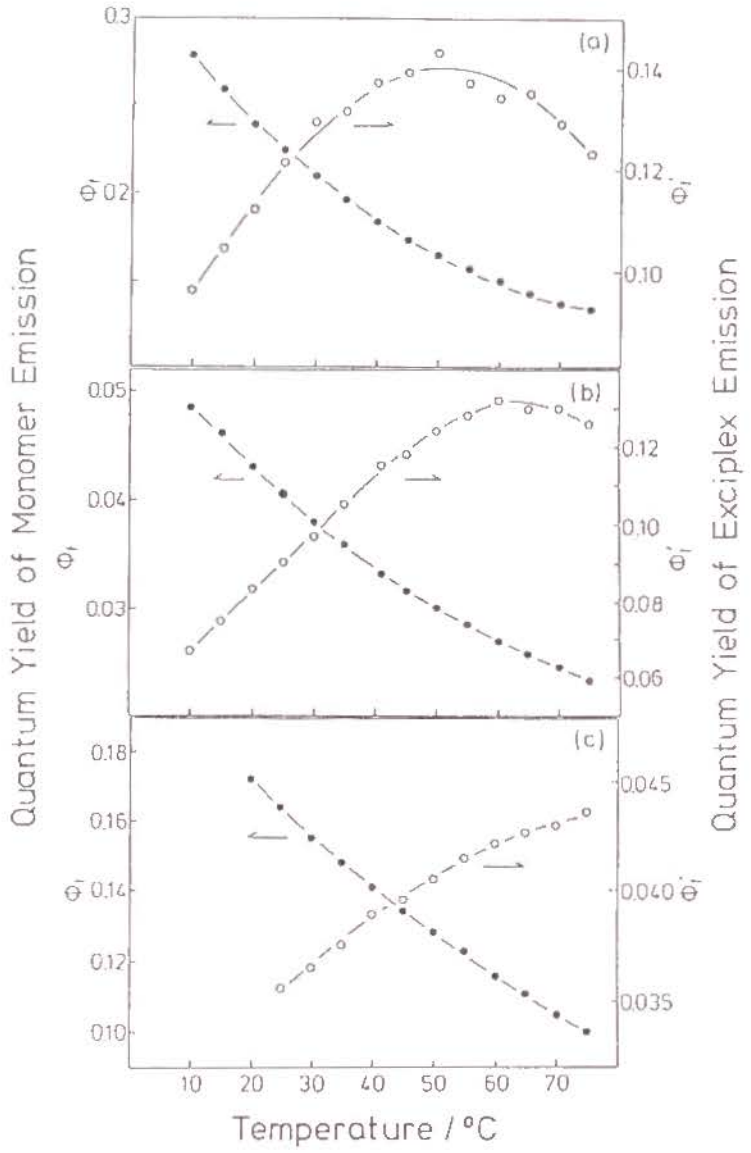

Figure 8-7. Temperature dependences of the quantum yield Φ_f, Φ_f' of monomer and exciplex emission for PVMTP and its model compound systems.
(a): EtCz(2.9×10^{-4} M) - DMTP(0.07 M),
(b): EtCz(2.9×10^{-4} M) - 2,4-MTP([TP]=0.1 M),
(c): EtCz(2.9×10^{-4} M) - PVMTP([TP]=0.2 M).

role in this problem. The stronger the interaction, the more difficult for the exciplex to dissociate thermally.

An assumed scheme for the formation of the exciplex is shown in Figure 8-8, in which k_n and k_f are the rate constants of the radiationless transition and the fluorescent transition of the monomer excited state, respectively, and k_n' and k_f' are those of the exciplex state. The constant, k_q, is the quenching rate constant. According to the scheme, the activation energy E of the quenching process was estimated by using the following equation.

$$\ln(\Phi_f^{-1} - \Phi_f^{0\,-1}) = \ln(k_q[TP] / k_f) - E/kT \quad (8\text{-}4)$$

The results are listed in Table 8-IV. In each system, the activation energy is close to that of the viscosity of the solvent, benzene, 2,6 kcal/mol. This suggests that the quenching of the EtCz excited state by the TP chromophore is diffusion-controlled in all the systems.

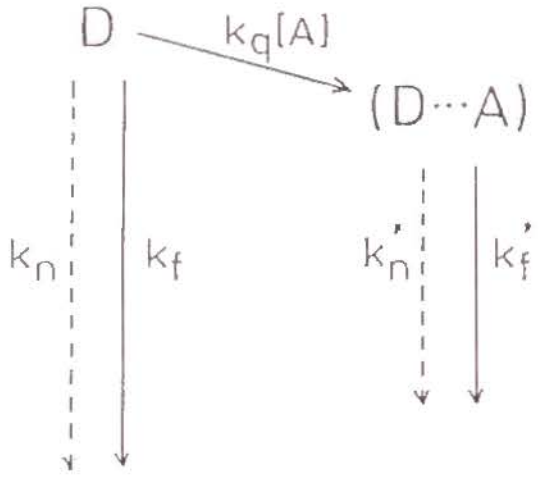

Figure 8-8. Scheme for exciplex formation.

Table 8-IV. Activation energies (E) of quenching process.

	E/kcal mol^{-1}
EtCz - DMTP	2.4
EtCz - 2,4-MTP	2.4
EtCz - PVMTP	2.6
Viscosity of Benzene	-2.6

8-4. Conclusion

In the polar solvent benzonitrile, the radical anion $TP^{\cdot-}$ formed in the copolymer of VMTP and VAc is stabilized depending on the location of the VMTP. A $TP^{\cdot-}$ isolated by VAc units in the copolymer transfers an electron to p-DCNB with a rate constant of 7.7×10^8 $M^{-1}s^{-1}$, whereas $TP^{\cdot-}$ formed in the VMTP sequences does not transfer an electron to p-DCNB; nor does the radical anion $TP^{\cdot-}$ in the homopolymer PVMTP. This is partly due to the neighboring interactions and partly due to the steric hindrance of the polymer chain. The steric hindrance is considered to be one of the reasons why the $TP^{\cdot-}$ formed in the dimer sequence in the copolymer is stabler than that formed in the dimeric model compound.

In the non-polar solvent benzene, PVMTP and its dimeric model compound form the exciplex with EtCz. Even though an obvious emission ascribable to a new excited complex such as DAA exterplex could not be observed, the exciplex was found to

be quenched by neighboring chromophore interaction.

Thus, the radical anion in PVMTP and the charge-transfer state of the exciplex of PVMTP with EtCz interact with the neighboring TP chromophore, but the stabilization is small as compared with the case of radical cations and DDA exterplexes.

References

1) E. D. Sprague, K. Takeda and F. Williams, Chem. Phys. Lett. 1971, 10, 299.

2) T. Shida and S. Iwata, J. Chem. Phys. 1972, 56, 2858.

3) S. Arai, A. Kira and M. Imamura, J. Phys. Chem. 1977, 81, 110.

4) Y. Hirata, M. Takimoto, N. Mataga, Y. Sakata and S. Misumi, Chem. Phys. Lett. 1982, 92, 76.

5) A. M. Swinnen, F. Ruttens, M. Van der Auweraer and F. C. De Schryver, ibid. 1985, 116, 217.

6) (a) A. Tsuchida, M. Yamamoto, and Y. Nishijima, J. Phys. Chem. 1984, 88, 5062. (b) A. Tsuchida, N. Masuda, M. Yamamoto, and Y. Nishijima, Macromolecules 1986, 19, 1299.

7) R.L. Adilman, J. Am. Chem. Soc. 1949, 71, 1057.

8) M. Fineman and S.D. Ross, J. Polym. Sci. 1950, 5, 259.

9) G.E. Ham, "Copolymerization," G.E. Ham, Ed., High Polymers Vol. XVIII; Interscience Publishers, John Wiley & Sons, Inc., New York, 1964, Chapter 1.

10) D. Rehm and A. Weller, Israel J. Chem. 1970, 8, 259.

APPENDIX

EXPERIMENTAL METHODS
TO ESTIMATE THE STABILITY OF RADICAL CATIONS

1. Introduction

In this thesis, a CR band and a radical cation transfer to a stronger electron donor were measured to investigate the stabilization, by neighboring chromophore interactions, of radical cations. The CR band corresponds to the transition between two levels of HOMO split by neighboring chromophore interactions, and its band gap reflects the strength of the interactions. The radical cation transfer method is one to estimate the stability of radical cation on the basis of the free energy change dependence of the rate constant of the radical cation transfer. These transient absorption measurements of radical cations were made by a laser photolysis technique. Two laser photolysis systems were used; one is a ruby laser photolysis system equipped with Q-switched ruby laser,[1] and the other is an excimer laser photolysis system equipped with excimer laser.

The laser photolysis technique is a method to measure the absorption of the transient species produced by a laser pulse. The formation and decay of transient species can be directly observed. The method for measuring transient absorption was established as a flash photolysis technique by Norrish and

Porter in 1949,[2] and was applied for the studies of aromatic molecules in the triplet state.[3] Afterward, the development of a laser technique brought about improvements in time-resolution and made it possible to observe transient phenomena in nanosecond and picosecond time ranges.[4-7]

In this appendix, the relationship between the peak shift of the CR band and the stability of the radical cation is described along with the principle of the radical cation transfer method. Here, the laser photolysis apparatus used for the transient absorption measurements is described.

2. Method to Estimate the Stability of Radical Cation

(A) Charge-resonance Band

As for the dimer radical cation, the CR band reflects the neighboring chromophore interaction directly. Figure 1 shows the energy level diagram of the dimer radical cation.[8] The interaction between a radical cation and a neutral chromophore makes the orbitals split into two energy levels. The CR band corresponds to the transition between two levels of split HOMO. The visible dimer band is due to the absorption from split HOMO to split LUMO as shown with an arrow in Figure 1. The stronger the chromophore interaction, the larger the width of the splitting. Then, the stronger interaction leads to the shorter-wavelength shift of the CR band. The stabilization energy (ΔH) of the dimer radical cation is approximately equal to a half of the energy gap (ΔE) of the CR band. The CR band is a measure of the strength of the chromophore interaction, i.e., the stability of the dimer radical cation.

However, for the charge delocalization in the polymer having pendant chromophores, the CR band of a radical cation

should be shifted to longer wavelengths with increasing charge delocalization such as dimer, trimer, and tetramer, according to the Hückel MO calculation.[9,10]

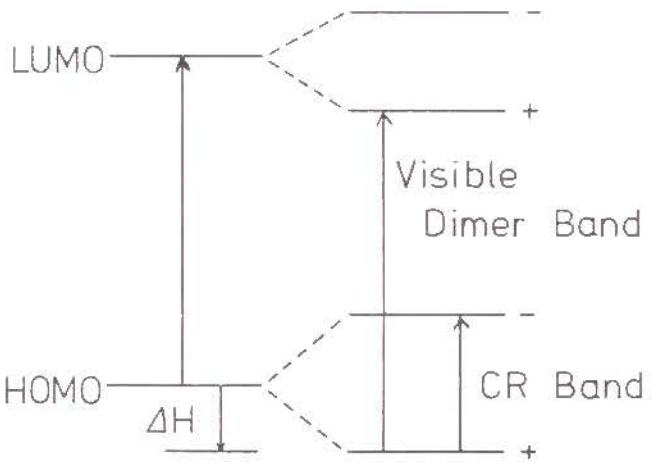

Figure 1. Schematic diagram of energy levels of dimer radical cation.

(B) Radical Cation Transfer Method

When an electron donor (D_1) is photoexcited in the presence of a sufficient concentration of an electron acceptor (A) in a polar solvent, an electron transfer from an excited singlet donor (D_1^*) to A produces a radical cation ($D_1^{\cdot+}$) and a radical anion ($A^{\cdot-}$). This process is much faster than the succeeding processes. If the second electron donor (D_2, radical cation acceptor), which is a stronger electron donor than D_1, is added to this system, radical cation transfer from $D_1^{\cdot+}$ to D_2 (an electron transfer from D_2 to $D_1^{\cdot+}$) occurs (eq. 1), and this process can be observed directly by the transient absorption of $D_1^{\cdot+}$ and $D_2^{\cdot+}$.

$$D_1^{+\cdot} + D_2 \xrightarrow{k_{tr}} D_1 + D_2^{+\cdot} \qquad (1)$$

$$D_1^{+\cdot} + A^{-\cdot} \xrightarrow{k_{r1}} D_1 + A \qquad (2)$$

$$D_2^{+\cdot} + A^{-\cdot} \xrightarrow{k_{r2}} D_2 + A \qquad (3)$$

This process competes with the recombination of $D_1^{+\cdot}$ with $A^{-\cdot}$ (eq. 2), but it is possible to make the radical cation transfer the main process by adjusting the concentration of D_2 properly. $D_2^{+\cdot}$ produced by the radical cation transfer also decays by recombination with $A^{-\cdot}$ (eq. 3). The processes in eqs. 1 - 3 lead to the following rate equations.

$$d[D_1^{+\cdot}]/dt = - k_{tr}[D_1^{+\cdot}][D_2] - k_{r1}[D_1^{+\cdot}][A^{-\cdot}] \qquad (4)$$

$$d[D_2^{+\cdot}]/dt = k_{tr}[D_1^{+\cdot}][D_2] - k_{r2}[D_2^{+\cdot}][A^{-\cdot}] \qquad (5)$$

$$d[A^{-\cdot}]/dt = - k_{r1}[D_1^{+\cdot}][A^{-\cdot}] - k_{r2}[D_2^{+\cdot}][A^{-\cdot}] \qquad (6)$$

where k_{tr} is the rate constant of the radical cation transfer, and k_{r1} and k_{r2} are the rate constants of the recombination of $D_1^{+\cdot}$ with $A^{-\cdot}$ and of $D_2^{+\cdot}$ with $A^{-\cdot}$, respectively. Hence if the transient decays for $D_1^{+\cdot}$, $D_2^{+\cdot}$, and $A^{-\cdot}$ are measured by the laser photolysis method and simulated by eqs. 4 - 6, the rate constant k_{tr} is determined.

In a simple case, k_{tr} can be estimated by the transient absorption decay at the peak wavelength of $D_1^{+\cdot}$: if the rate of the radical cation transfer from $D_1^{+\cdot}$ to D_2 is much faster than that of the recombination of $D_1^{+\cdot}$ with $A^{-\cdot}$ ($k_{tr}[D_2] \gg k_{r1}[A^{-\cdot}]$), eq. 4 can be solved to give eq. 7 by neglecting the second term.

$$\ln [OD(D_1^{+\cdot})] = k_{tr}[D_2]t + C \qquad (7)$$

where C is a constant. Consequently, k_{tr} can be determined by the slope in $\ln [OD(D_1^{+\cdot})]$ vs. time plot.

To make it possible to measure the rate constants of radical cation transfer satisfactorily, a set of D_1-D_2-A systems must satisfy the following conditions. First, D_1 is photoexcited selectively by a laser pulse, and the electron transfer from D_1^* to A is sufficiently fast. Secondly, the transient absorption bands of $D_1^{+\cdot}$, $D_2^{+\cdot}$ and $A^{-\cdot}$ are separated enough to be analyzed.

The stability of the dimer radical cation is estimated from the value k_{tr} as shown in Figure 2. The rate constant of the electron transfer, k_{tr} depends on the free energy change (ΔG)

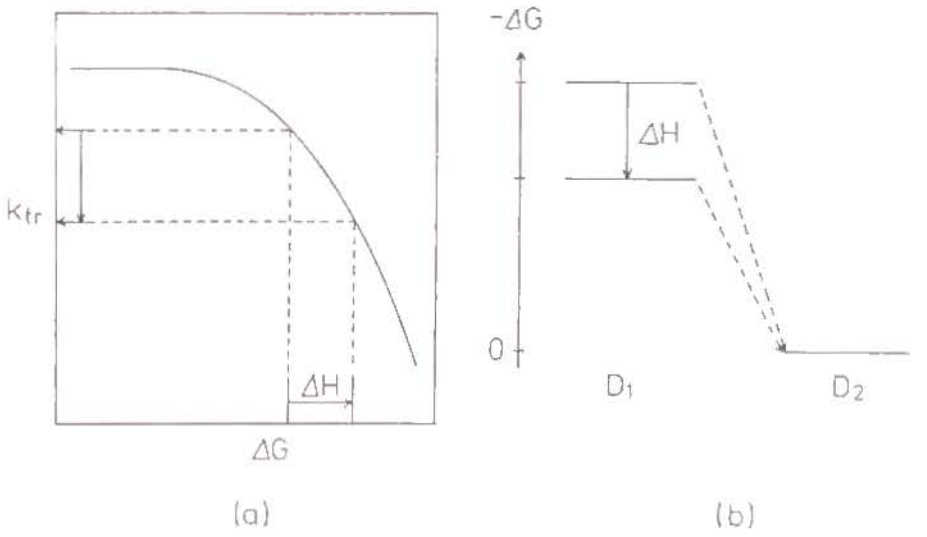

Figure 2. Estimate of the stability of dimer radical cation by the radical cation transfer method: (a) relation between k_{tr} and ΔG; (b) relation between ΔH and increment of ΔG induced by stabilization.

as shown in Figure 2-(a).[11,12] k_{tr} increases with the decreasing ΔG (an up-hill region), and the transfer process is diffusion-controlled in a sufficiently exothermic region. If the dimer radical cation is stabilized by ΔH as shown in Figure 2-(b), the exothermic quantity of the radical cation transfer decreases (ΔG increases). If ΔG is brought in the up-hill region by using D_2 having a proper oxidation potential, an increase of ΔG by the stabilization causes a decrease of k_{tr}. The stabilization of the dimer radical cation can be estimated by the decreasing k_{tr}.

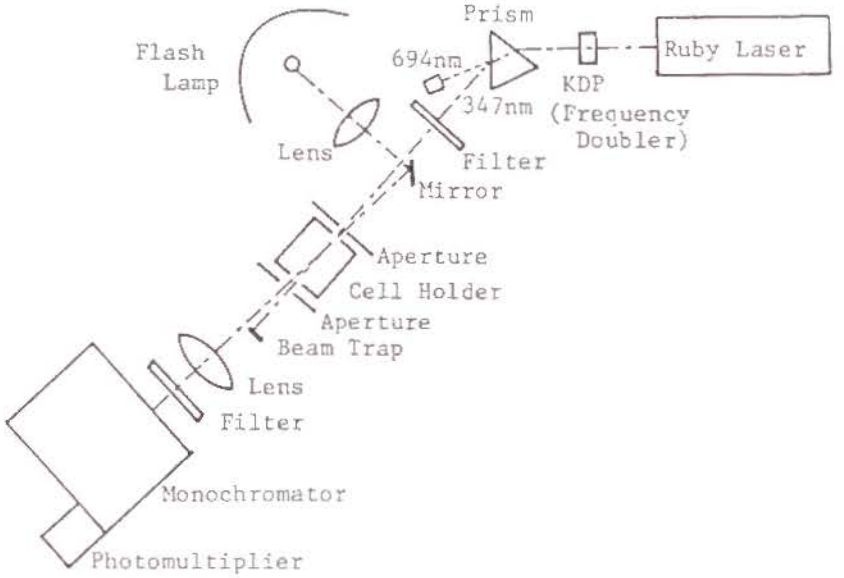

Figure 3. Schematic diagram of the ruby laser photolysis system.

3. Laser Photolysis Apparatus

Figure 3 shows the schematic diagram of a ruby laser photolysis system. The sample is excited by the second-harmonic pulse (347 nm) of Q-switched giant pulse ruby laser (NEC SLG2009), which has ca. 14 ns pulse duration. The second-harmonic pulse is

generated through the frequency-doubler, KDP crystal, and is separated by a prism from the fundamental ruby laser pulse (694 nm). The intensity of the excitation pulse is attenuated properly by filters. The monitoring system to measure the absorption of transient species consists of a monitor flash lamp (EG&G FX-33C-1.5), a monochromator and a photomultiplier tube (Hamamatsu, R928). The signal of the photomultiplier tube is recorded by a storage oscilloscope (Iwatsu, TS-8123). This monitoring system has a wavelength-sensitivity from 350 nm to 850 nm and a rise time of ca. 5 ns.

Figure 4 shows the schematic diagram of an excimer laser photolysis system. The sample is excited by an attenuated pulse

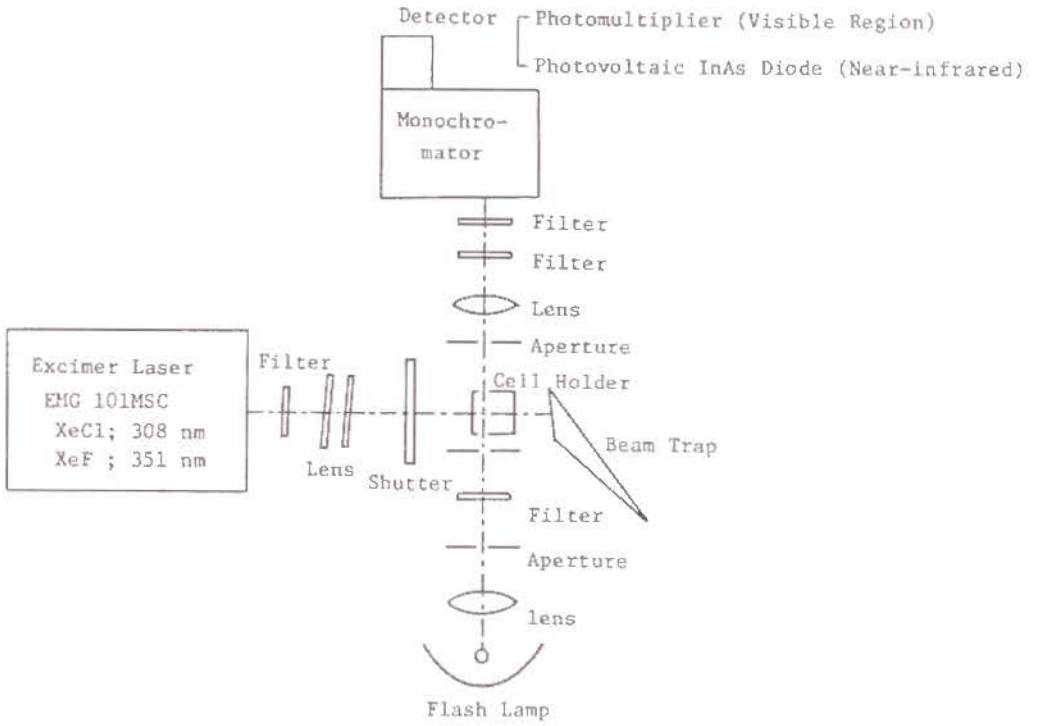

Figure 4. Schematic diagram of the excimer laser photolysis system.

of an excimer laser (Lambda Physik EMG101MSC). The emission wavelength of the excimer laser can be changed by selecting an appropriate gas. In this study, a 308-nm pulse (pulse energy ca. 100 mJ, fwhm ca. 17 ns) operating with XeCl and 351-nm pulse (pulse energy ca. 60 mJ, fwhm ca. 17 ns) operating with XeF are used. The monitoring beam is arranged at a right angle to the laser beam. The monitoring system consists of Xe flash lamp, a monochromator and a detector. As a detector, either a photomultiplier tube or a near-infrared sensitive photodiode was used depending on experiments. For the measurement of UV and visible region, a photomultiplier tube (Hamamatsu, R928) was used. As described previously, the photomultiplier-monitoring system has a wavelength-sensitivity from 350 nm to 850 nm and a rise time of ca. 5 ns. The photodiode is a photovoltaic indium arsenide (InAs) diode with a sensitive area of 0.03 cm^2 (Hamamatsu, P838).[13] The photodiode-detection system is suited for measurements in the near-infrared region. The output of the diode was directly amplified and was recorded by an oscilloscope (Iwatsu, TS-8123). This detection system has a wavelength-sensitivity from 600 nm to 2200 nm and a response time of ca. 500 ns.

References

1) (a) A. Tsuchida, "Studies on Photoinduced Charge Transfer and Its Related Photochemical Reactions," Doctoral Thesis, Kyoto University, 1982, Chapter 2. (b) A. Tsuchida, M. Yamamoto and Y. Nishijima, J. Phys. Chem. 1984, 88, 5062.

2) R. G. W. Norrish and G. Porter, Nature 1949, 164, 658.

3) (a) G. Porter and M. W. Windsor, J. Chem. Phys. 1953, 2088. (b) G. Porter and M. W. Windsor, Disc. Faraday Soc. 1954, 17, 178. (c) G. Porter and M. W. Windsor, Proc. R. Soc., Ser. A 1958, 245, 238.

4) J. R. Novak and M. W. Windsor, J. Chem. Phys. 1967, 47, 3075.

5) (a) D. Magde and M. W. Windsor, Chem. Phys. Lett. 1974, 27, 31. (b) D. Magde, B. A. Bushaw and M. W. Windsor, Ibid. 1974, 28, 263.

6) P. M. Rentzepis and R. P. Jones, J. Chem. Phys. 1973, 59, 766.

7) (a) N. Nakashima and N. Mataga, Chem. Phys. Lett. 1975, 35, 487. (b) N. Nakashima, M. Murakawa and N. Mataga, Bull. Chem. Soc. Jpn. 1976, 49, 854.

8) M. Itoh, in Kagakuhanno no Denshiron, S. Nagakura ed., Kyoritsu Shuppan, Tokyo, Japan, 1986, Chapter 7.

9) B. Badger and B. Brocklehurst, Nature 1968, 219, 263.

10) A. Kira. and M. Imamura, J. Phys. Chem. 1979, 83, 2267.

11) (a) R. A. Marcus, J. Chem. Phys. 1956, 24, 966. (b) R. A. Marcus, Ann. Rev. Phys. Chem. 1964, 15, 155.

12) (a) D. Rehm and A. Weller, Ber. Bunsenges. Physik. Chem. 1969, 73, 834. (b) D. Rehm and A. Weller, Israel J. 1970, 8, 259.

13) L. M. Dorfman, in Investigation of Rates and Mechanisms of Reactions, G. G. Hammes ed., Wiley- Interscience, New York, 1974, Chapter 11.

SUMMARY

In **Chapter 1**, a general introduction of this thesis was given. Previous studies on radical cations of dimer and higher-order aggregates of chromophores and excited triple complexes were briefly reviewed in order to make clear the backgrounds of and the connection with the individual subjects to be deal with in this thesis. In addition, outline of this thesis was described.

In **Chapter 2**, the stability of the dimer radical cations of meso- and rac-2,4-di(N-carbazolyl)pentanes (m- and r-DCzPe) and 1,3-di(N-carbazolyl)propane (DCzPr) was studied. m-DCzPe and DCzPr form a fully-overlapped dimer radical cation, whereas r-DCzPe forms a partially-overlapped one. The CR bands of these dimer radical cations were measured by laser photolysis in a near-infrared region; band peaks appeared around 1600 nm for m-DCzPe and DCzPr, and around 1800 nm for r-DCzPe. This suggests that the fully-overlapped dimer radical cation is stabler than the partially-overlapped one. By the radical cation transfer method, the stabilization energies of these dimer radical cations were estimated to be 0.3 - 0.4 eV for the fully-overlapped one and ca. 0.1 eV for the partially-overlapped one.

In **Chapter 3**, the stability of the carbazole radical cation formed in poly(N-vinylcarbazole) (PVCz) was studied in comparison with copolymers of N-vinylcarbazole (VCz) with methyl methacrylate and vinyl acetate. The CR bands of the radical cations in these polymers were measured by laser photolysis to investigate the degree of the charge delocalization in the polymers. For copolymers with a fraction of VCz (f_{VCz}) less

than 0.4, the CR band appeared at ca. 1800 nm. For copolymers with $f_{VCz}>0.5$, the CR band was shifted to longer wavelengths with increasing f_{VCz}. A copolymer with $f_{VCz}=0.83$ showed the same transient absorption spectrum as PVCz. In view of the sequential distribution of the copolymers, the charge formed in PVCz was understood to be delocalized among more than two chromophores. By the radical cation transfer method, the stabilization energy of the carbazole radical cation in PVCz was estimated to be 0.5 ± 0.1 eV. This value is larger than that of the carbazole dimer radical cation, which was described in Chapter 2. Thus, it was established that the stabilization by the charge delocalization among more than two chromophores is stronger than that of the dimer radical cation.

In **Chapter 4**, the emission properties of PVCz and its model compounds in the presence of dimethyl terephthalate (DMTP) were examined in benzene solution, and the effects of neighboring chromophores on the exciplex in polymer systems were discussed. The interaction between the neighboring carbazole chromophores leads to the formation of two kinds of exterplexes (excited triple complexes) corresponding to the dimer radical cations as described in Chapter 2; one is a partially-overlapped exterplex and the other is a fully-overlapped one. The partially-overlapped and fully-overlapped exterplexes showed the exterplex emission around 510 nm and 560 nm, respectively. The latter was found to be stabler than the former. As for PVCz-DMTP system, the partially-overlapped exterplex dominates at room temperature, presumably because of its easy formation with a small conformational change. The fraction of the stabler fully-overlapped exterplex increased with increasing temperature: the increase of fraction caused longer wavelength shifts in the exterplex emission.

In **Chapter 5**, the steric effects of bulky tert-butyl group on the formation of the dimer radical cation and the exterplex were investigated. Regarding poly(3,6-di-tert-butyl-N-vinylcarbazole) (PBVCz) and its dimeric model compounds, the transient absorption spectra of radical cations in a polar solvent were measured by laser photolysis, and the emission properties in a non-polar solvent were measured in the presence of DMTP by fluorescence spectroscopy. Though the neighboring chromophore interaction was weakened as compared with the case of a carbazole chromophore, all these compounds formed a partially-overlapped dimer radical cation in a polar solvent and a partially-overlapped exterplex in a non-polar solvent. This sharply contrasts to the fact that the meso isomer of 2,4-bis(3,6-di-tert-butyl-N-carbazolyl)pentane and 1,3-bis(3,6-di-tert-butyl-N-carbazolyl)propane do not form any intramolecular excimer. This means that the conformational requirement for the formation of the dimer radical cation and the exterplex is rather loose and that the stabilization energy is larger than that of the excimer. PBVCz also forms the partially-overlapped dimer radical cation in contrast to the case of PVCz.

In **Chapter 6**, the CR band of the dimer radical cation for poly(vinylnaphthalene)s and three isomers of dinaphthylpropane were measured by laser photolysis. 1-(1-Naphthyl)-3-(2-naphthyl)propane forms an intramolecular partially-overlapped dimer radical cation and shows a CR band at ca. 1050 nm. In contrast, 1,3-di(2-naphthyl)propane (22DNP) and 1,3-di(1-naphthyl)propane (11DNP) intramolecularly form both a partially-overlapped and a fully-overlapped dimer radical cations; these CR bands are superposed with each other and were observed as a single band at ca. 1250 nm for 22DNP and at ca. 1350 nm for 11DNP. Therefore, the fully-overlapped dimer radical cation

should have the CR band at a wavelength longer than 1250 nm. This suggests that the partially-overlapped dimer radical cation is stabler than the fully-overlapped one. This was confirmed by measuring the rate constant of radical cation transfer to triethylamine; owing to the stabilization, the rate constant of radical cation transfer for the partially-overlapped dimer radical cation was smaller than that for the fully-overlapped one. Poly(vinylnaphthalene)s formed a partially-overlapped dimer radical cation and gave the same transient absorption spectrum of the radical cation as the dimeric model compound. The stabilization of the radical cation by charge resonance among more than two chromophores was not detectable.

In **Chapter 7**, MO calculation was carried out for carbazole and naphthalene dimer radical cations, and the difference in the stability between the carbazole and naphthalene dimer radical cations was discussed in connection with the dimer structure or the degree of the overlapping of chromophores. First, the fully-overlapped and partially-overlapped conformations having minimum potential energies were determined by AM1 for these dimer radical cations. The results suggest that all dimer radical cations take the conformation in which two chromophores are further apart from each other than in parallel arrangement formed by a methylene bridge. Next, the excitation energy of the dimer radical cation in these conformations was estimated by CNDO/S. The calculated results for the CR bands reproduced the experimental data qualitatively. An analysis of the orbitals related to the CR band indicates that the excitation of the CR band is a charge-transfer type for the carbazole and naphthalene dimer radical cations. For the carbazole, the character of N atom was found to be reflected strongly on the stabilization of the dimer radical cation. Finally, the energy

decomposition analysis by Ab Initio calculations was applied. It was found that an electrostatic or Coulombic interaction between the electron distributions of the isolated chromophores makes a most significant contribution to the stabilization of the dimer radical cation.

In **Chapter 8**, the stability of the terephthalate radical anion ($TP^{\cdot}$) in a polymer chain was investigated by the radical anion transfer method using nanosecond laser photolysis. The radical anion $TP^{\cdot}$ formed in a homopolymer, poly(vinyl methyl terephthalate) (PVMTP) does not transfer an electron to 1,4-dicyanobenzene (DCNB), but the monomer model compound, dimethyl terephthalate (DMTP) does transfer, despite the two systems have the same transient absorption spectrum. As for the $TP^{\cdot}$ in copolymers of vinyl methyl terephthalate (VMTP) with vinyl acetate, the radical anion transfer rate to DCNB has two components, a fast and a slow component: the fast component has a rate constant of $7.7 \times 10^8\ M^{-1}s^{-1}$, while the slow component scarcely decays in the measurement time range (<1 μs). The fraction of the slow component increases with the VMTP fraction. These results show that the neighboring interaction of TP residues in the polymer chain stabilizes the radical anion of the TP residue. The radical anion $TP^{\cdot}$ formed in the polymer is stabilized partly by the neighboring interaction and partly by the steric hindrance of the polymer chain towards the approaching DCNB.

The emission properties of the exciplex with N-ethylcarbazole (EtCz) were investigated for PVMTP and its model compounds. Though no emission corresponding to the DAA type exterplex was observable, the lifetime of the exciplex emission was shorter, and the quantum efficiency of the exciplex emission was smaller than those of the EtCz-DMTP system. Hence, it is

evident that the exciplex is quenched by the interaction with an adjacent TP chromophore. The results for PVMTP may be interpreted due to a weak interaction between neighboring TP chromophores.

In Appendix, experimental methods to evaluate the charge-delocalized stabilization of radical cations were described. A dimer radical cation shows a characteristic CR band. Theoretically, this CR band is associated with the transition between two split HOMO's of the chromophore caused by the neighboring chromophore interaction. It can be a measure for the magnitude of the neighboring chromophore interaction or the stability of the dimer radical cation. When a radical cation is stabilized by forming a dimer radical cation, the radical cation transfer to a second electron donor is suppressed. The stabler the radical cation, the smaller the transfer rate. On the basis of this rule, the stability of radical cations was estimated. A laser photolysis apparatus for radical ion observation was introduced.

LIST OF PUBLICATIONS

Chapter 2.

1. "Estimate of the Stabilization Energy of Cation Radicals Formed in Poly(N-vinylcarbazole) and Its Dimer Model Compounds by an Ion Radical Transfer Method"
   Macromolecules 1988, 21, 665.
2. "Near-infrared Charge Resonance Band of Intramolecular Carbazole Dimer Radical Cations Studied by Nanosecond Laser Photolysis"
   Chem. Phys. Lett. 1989, 154, 559.

Chapter 3.

3. "Stabilization of Carbazole Radical Cation Formed in Poly(N-vinylcarbazole) by Charge Delocalization"
   Macromolecules 1990, 23, 4019.

Chapter 4 and 8.

4. "Exciplex Formation of Polymers Having Carbazole or Terephthalate Chromophore --- Neighboring Chromophore Interaction ---"
   J. Chem. Soc. Jpn. 1989, 1304.

Chapter 5.

5. "Steric Effect on Dimer Radical Cation Formation of Poly(3,6-di-tert-butyl-9-vinylcarbazole) and Its Dimeric Model Compounds Studied by Laser Photolysis"
   Polym. J. 1990, 22, 319.
6. "Exterplex Formation of Poly(3,6-di-tert-butyl-9-vinylcarbazole) and Its Dimeric Model Compounds"
   to be submitted in Bull. Chem. Soc. Jpn..

Chapter 6.

7. "Structure and Stability of Naphthalene Dimer Radical Cations Studied by Charge Resonance Band Measurement and Cation Radical Transfer Method"
   to be submitted in J. Am. Chem. Soc..
8. "Conformations of Naphthalene Dimer Cation Radicals Studied by Laser Photolysis"
   J. Phys. Chem. 1989, 93, 1244.

Chapter 7.

9. "Application of Semiempirical MO Calculation for Carbazole and Naphthalene Dimer Radical Cations"
   to be submitted in J. Phys. Chem..
10. "Energy Decomposition Analysis of Carbazole and Naphthalene Dimer Radical Cations by Ab Initio Calculations"
    to be prepared.

Chapter 8.

11. A part of this work; "Stabilization of an Anion Radical Formed in Poly(vinyl methyl terephthalate) Studied by Anion Radical Transfer Method"
    Polym. J. 1988, 20, 837.

Others

12. "The Behavior of the Intra- and Intermolecular Pyrene Dimer Cation Radical as Studied by Nanosecond Laser Photolysis in Near-IR Region"
    J. Chem. Soc. Jpn. 1989, 1285.
13. "Excimer Formation in Sterically Hindered Poly(vinylcarbazole) and Its Dimer Model Compounds"
    Macromolecules 1990, 23, 2666.

ACKNOWLEDGMENTS

The present thesis is a collection of the studies which the author carried out at the Department of Polymer Chemistry, Kyoto University, from 1982 to 1989.

The author wishes to express his sincere gratitude to Dr. Yasunori Nishijima, President of Kyoto University, and Professor Masahide Yamamoto for their continuous guidance and encouragement throughout the course of this work.

Grateful acknowledgment is due to Professor Takeaki Miyamoto and Associate Professor Takeshi Fukuda, Institute for Chemical Research, Kyoto University, for their kind comments and detailed criticism on the manuscript in writing this thesis.

The author is sincerely grateful to Drs. Akira Tsuchida and Shinzaburo Ito for their invaluable guidance and discussions.

The author is indebted to the late Dr. Tokuji Fujimoto and Associate Professor Yoshihiko Onogi, Mukogawa Women's University, for their useful suggestions and comments.

The author wishes to thank Mr. Masataka Ohoka and Dr. Kazuo Ashikaga for their helpful comments and discussions, and Mrs. Kyoko Kato for her encouragement.

The author would like to express his appreciation to Professor Tadamasa Shida and Dr. Takamasa Momose, Department of Chemistry, Kyoto University, for the MO calculations.

Thanks are also expressed to Associate Professor Yoshio Wada, Kyoto Institute of Technology, for the measurement of the excimer laser photolysis, and to Professor Kunio Okamoto and Associate Professor Koichi Komatsu, Department of Hydrocarbon Chemistry, Kyoto University, for the measurement of oxidation

and reduction potentials.

The author wishes to express his thanks to his colleagues in the laboratory for their kind help.

Finally, much gratitude is also due to his wife, Yuri Tsujii, and his parents, Hiroji Tsujii and Kiyoko Tsujii for their continuous encouragement.

September 1990

Yoshinobu Tsujii